UNIVERSITY FOR DEVELOPMENT STUDIES

MONITORING THE IMPACT OF UREA DEEP PLACEMENT ON RICE (O*ryza sativa* l.) GROWTH AND GRAIN YIELD USING UNMANNED AERIAL SYSTEMS TECHNOLOGY (DRONES)

TWUMASI DUODUAA AMA

2020

UNIVERSITY FOR DEVELOPMENT STUDIES, TAMALE

MONITORING THE IMPACT OF UREA DEEP PLACEMENT ON RICE (*ORYZA SATIVA* l.) GROWTH AND GRAIN YIELD USING UNMANNED AERIAL SYSTEMS TECHNOLOGY (DRONES)

BY

TWUMASI DUODUAA AMA

(BSc AGRICULTURE TECHNOLOGY)

UDS/MCS/0011/17

DISSERTATION SUBMITTED TO THE DEPARTMENT OF AGRONOMY, FACULTY OF AGRICULTURE, UNIVERSITY FOR DEVELOPMENT STUDIES, IN PARTIAL FULFILLMENT OF THE REQUIREMENTS FOR THE AWARD OF MASTER OF PHILOSOPHY DEGREE IN CROP SCIENCE (AGRONOMY OPTION)

JUNE, 2020

DECLARATION

I hereby declare that this thesis is my original work and that no part of it has been presented for another degree in this university or elsewhere. Work of others which served as useful information has been duly acknowledged by references to the authors.

Twumasi Duoduaa Ama ..... ……..

(Student) Signature Date

Supervisors'

We, hereby declare that the preparation and presentation of the thesis was supervised in accordance with guidelines on supervision of thesis laid down by the University for Development Studies.

Dr. Vincent K. Avornyo …… ……..

(Principal Supervisor) Signature Date

Dr. Raphael Adu-Gyamfi ……. ……

(Co-Supervisor) Signature Date

Prof. Andrew Manu …… ……..

(Co-Supervisor) Signature Date

ABSTRACT

Unmanned aerial systems (UAS)-based remote sensing technology is used in precision agriculture due to its ability to monitor individual crop growth, health etc. which was previously unlikely on a wide scale. In this study, UAS technology was used in three zones of the Tono Irrigation Scheme (TIS) in the Upper East region of Ghana to assess the effect of urea deep placement (UDP) compared to non-UDP Nitrogen (N) management systems on rice grain yields. The goal of the study was to capture multispectral images on a fixed wing (eBee) platform at the midseason rice crop stage and develop vegetation indices (VI's) to study in-field variations in rice yields as a function of N management system. These images were processed through the eMotion 3 software and transferred into Pix4D to create high resolution seamless orthomosaics. Four different vegetation indices (NDVI, NDRE, OSAVI, and GNDVI) were produced. Normal difference vegetation index (NDVI) was used to identify high, medium and low crop health zones. End of season rice grain yields in the health zones were in the order high > medium > low. Rice grain yields had the highest correlation with OSAVI (r = 0.50). Two approaches were used to assess the impact of non-UDP compared to UDP. In the plot scale evaluation, estimated grain yields in non-UDP and UDP fields were 6.14 MT/ha and 6.74 MT/ha, respectively and were statistically different. Variability was high in non-UDP fields compared to UDP fields. In the geospatial approach based on Jenks classified OSAVI maps, similar relationships were obtained. Results showed that UAS technology can be efficient in estimating end of season rice grain yields and their variability in fields based on mid-season multispectral data.

ACKNOWLEDGEMENT

This project was part of a collaborative study involving USAID/IFDC Agriculture Technology Transfer Project, Iowa State University and University for Development Studies. Thanks to IFDC for sponsoring this research.

Special thanks go to Professor Andrew Manu of Iowa state university for his selfless support, contribution to this work. A big thank you to my supervisors, Dr Vincent K. Avornyo and Dr Raphael Adu-Gyamfi for their immerse support, advice and contributions towards this thesis.

Thanks also go to the department of Agronomy for the opportunity to undertake this program.

I am indebted to the department laboratory technician Mr. Baba Alhassan and the staff at ICOUR for their immense contribution during the field work component of this research. To the farmers whose fields were used for this study I also say thank you.

Next, I am grateful to my family for their support throughout this graduate program.

To my colleagues in the department, I say you have been awesome and I am going to miss you all.

DEDICATION

I dedicate this work to my family for all the support they gave me throughout this graduate program.

TABLE OF CONTENTS

LIST OF FIGURES

LIST OF TABLES

CHAPTER ONE

1.0 INTRODUCTION

1.1 Background

Rice is regarded as the second most important staple grain food in Ghana, next to maize (Danso-Abbeam *et al*., 2014). The per capita consumption of rice in Ghana was estimated at 35 kg/year in 2016/2017, while annual consumption in 2017/2018, was estimated at 1.0 million MT. Government of Ghana sources indicate that annual per capita rice consumption is expected to reach 40 kg by 2020 (Bannor, 2015). The growth in rice consumption in Ghana has also been attributed to the change in consumer behavior, population growth and urbanization (Tomlins *et al*., 2007). Rapid increase in rice consumption was recorded from 1960 to 2018 with rice importation exceeding local production over these years (Figure 1.1).

Rice production in Sub-Saharan Africa (SSA) faces a variety of challenges that contribute to low yields such as inadequate fertilizer input and poor soils (Tsujimoto *et al*., 2019). As a result, SSA spends about $1.5 billion annually on rice imports (Moldenauer *et al*., 2005). According to Nwanze *et al*. (2006), 20 million farmers grow rice in SSA with about 100 million as consumers. Rice accounts for almost 15% of the Gross Domestic Product of Ghana, making it important to its economy and agriculture. However, Ghana depends mostly on rice import to complement the shortage in local rice production and uses about an average of $450 million annually to augment local demand (MOFA, 2010). This import bill invariably consumes a substantial portion of the country's foreign

exchange (Ragasa *et al*., 2013) and causes severe and unfair competition on the part of local producers; most of whom see negative returns in the process.

Production systems in SSA include irrigated lowlands, rain-fed lowlands and rain-fed uplands, with low importance of deep-water and mangrove-swamp rice (Tanaka *et al*., 2017). According to Ragasa *et al*. (2013), the Northern (37%), Upper East (27%) and Volta (15%) regions are the leading domestic rice producing regions in Ghana. The rice production zone accounts for about 45% of the total cereal planted area in Ghana, although it occupies roughly 4 percent of the total crop harvested area (MoFA, 2009). This serves as an important provider of rural employment (Danquah and Egyir, 2014). Increasing domestic rice production further remains an important challenge for SSA. Assessing the current dynamics of farm yields is important for identifying low-yield areas or areas where yield improvement is possible (Tanaka *et al*., 2017). A study by Seck *et al*. (2013) shows that, the annual growth rate of rice production in the SSA rose from 3.2% before the rice crisis (2000–2007) to 8.4% after the rice crisis (2007–2012). Over the period 2007–2012, 71% of the increase in the production of paddy rice can be explained by yield increases and 29% by area expansion, while before the rice crisis (2000–2007), only 24% of the increase in production could be attributed to yield increases, with 76% attributable to increases in the harvested region.

Although productivity of Ghanaian paddies has improved in recent years, the deficit between consumption and local production still persists. Some of the factors accounting for the 70% deficit in rice output in Ghana include low yield, high production cost (the cost of credit, farm inputs, improved seed) and inefficient

processing facilities as well as result low demand for locally produced rice (Balasubramanian *et al*., 2007). Research work by Olaf and Emmanuel (2009), and Aker *et al*. (2010), showed that application of some policy measures can bridge the gap between domestic production and foreign imports. With projected rapid population growth, urbanization and infrastructural development in the near future (Adu-Gyamfi, 2012), much pressure will be exerted on available land for alternative uses at the expense of crop production. According to (Tiamiyu *et al*., 2015) and Al-hassan, (2012), technical efficiency will be a key factor in improving productivity. Technical efficiency tests to what degree performance can be increased without the increased use of inputs under a given production technology. The efficiency of the use of nitrogen fertilizers (NUE) in rice cultivation is extremely poor. The plant 's recovery of broadcast applied N is generally between 30 and 50% (Savant and Stangel, 1990). The low NUE may be due to volatilization of the ammonia, denitrification, leaching, and surface runoff. The N loss as volatilization of ammonia from a flooded rice field can be as high as 50% of the N applied (Dong *et al*., 2012; Rochette *et al*., 2013). Deep placement of fertilizers, especially urea (UDP), in lowland rice fields has been proven as an effective management practice for transplanted rice, which increases productivity and reduces fertilizer usage (Savant and Stangel, 1990; Gregory *et al*., 2010; Bandaogo *et al*., 2015).

UDP technology is designed to improve the efficiency of nitrogen usage in rice production, which is expected to increase the rice yield. Two key components form the UDP technology. First, it is a fertilizer ‘briquette’ that weighs about 3 grams

produced by compacting urea fertilizer (Azumah *et al*., 2017). The second step is the application of this technology, by placing the briquette below the root zone. The briquettes are centered among four rice plants at a spacing of 20 cm x 20 cm and at a depth of about 7 cm to 10 cm. It is applied within two weeks after transplanting the rice. Placement can be done by hand or by mechanical process. The briquette slowly releases nitrogen, satisfying the requirements of the crop throughout the growing season (Rahman and Barmon, 2015).

Deep urea placement increases NUE by as much as 50 to 70%, increases grain yield by 15 to 20% and reduces fertilizer N use by 30 to 40% (Savant and Stangel, 1990; Alam *et al*., 2013). In addition to having a positive agronomic effect, deep nutrient placement also has an environmental advantage by reducing the nutrient load in runoff water and reducing both volatilization and denitrification losses (Savant and Stangel, 1990). Urea deep placement (UDP) has proven to be a viable management strategy that could assist in the closing of the yield gap in rice production in Ghana. In spite of the benefits of the UDP technology, rice farmers in northern Ghana are yet to fully embrace the technology as farmers still broadcast N fertilizer, sulfate of ammonia and urea (Non-UDP). Broadcasting of urea causes volatilization of nutrients due to exposure and increases nutrient load in runoff water, especially when there are heavy rains after application which results in financial loss to the farmer. The runoff water can find its way and leave nitrate residues in river bodies causing diseases such as blue baby syndrome.

Recently, in Ghana, projects like the Agriculture Technology Transfer (ATT) Project of IFDC, the Alliance for a Green Revolution in Africa (AGRA) and the

Rice Sector Support Project (RSSP) have embarked on a scaling up campaign of the UDP technology that is expected to transform rice production in northern Ghana. This largescale endeavor requires the necessary technological tool that can provide cost-effective, up-to-the-minute data that are critical for monitoring and evaluation.

This study addresses the infield variability within and between the UDP fertilizer management practice and the non UDP using unmanned aerial system (UAS) remote sensing techniques to deliver useful data for management decision making in the future.

Remote sensing (RS) is the method of collecting information about objects without the object being directly in contact. Remote sensing techniques are suitable for assessing crop status based on the relation between optical properties of plants (and canopy) and bio-physiological parameters (Stroppiana *et al.*, 2015). Remote sensing based on unmanned aerial vehicle (UAV) allows user-controlled image acquisition and bridges the gap in scale and resolution between ground observations and images acquired from conventional manned aircraft and satellite sensors. It presents a cost-effective method which allows the image characteristics to be adapted to the size of the objects observed, to the processes monitored and to the speed of change within a landscape.

Remote sensing based on UAV gives the best spatial and temporal resolutions possible for answering research questions or applications (Cress *et al.*, 2011), and has great potential to help in crop management, in particular, in the study of crop performance and subsequent yield variability within the field. During the last two

decades , numerous researchers have demonstrated the appropriateness of RS for precision viticulture purposes (Hall *et al*., 2002). This technique was used to determine the spatial variability of the water status of the vineyards (Acevedo-Opazo *et al*. , 2008; Baluja *et al*., 2012), the content of chlorophyll (Martin *et al*., 2007), the content of grapes and phenols (Lamb *et al*., 2004), as well as the quality of grapes (Martin *et al*., 2007).

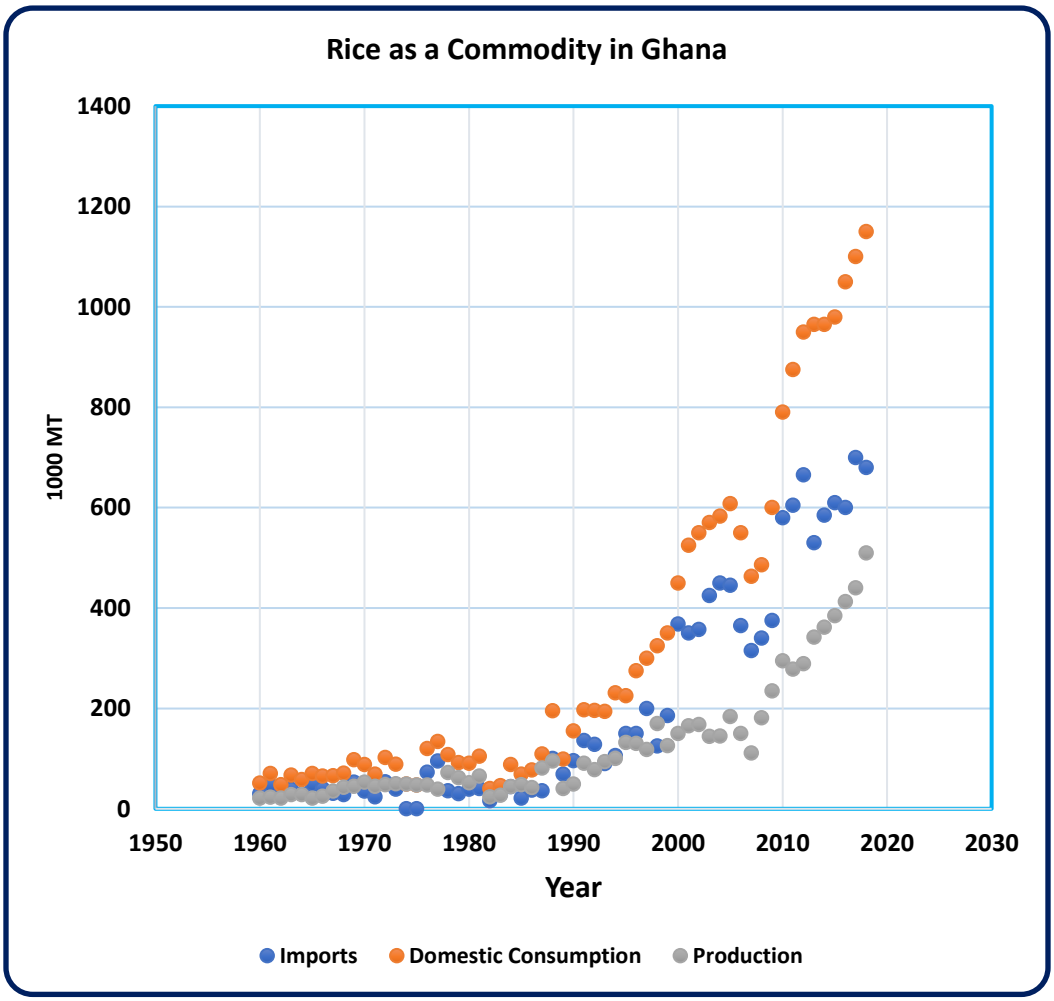

Figure 1. 1: Rice production, imports and domestic consumption in Ghana (1960-2018) (Source: Gain Report - United States Foreign Agricultural Service. 2018).

1.2 Problem statement

With increasing area under cultivation, monitoring rice growth and on-farm performance on the ground, especially on a broad landscape level, can be difficult. Using boots on the ground approach always begs the question "where are my targets?". Decisions on farm management have historically been made on the basis that the fields are uniform and that farmers measure crop growth by visual inspection on the ground. The human eye however is limited to a small portion of the total electromagnetic spectrum i.e. around 400 to 700 nm. Not only are crop scouting and sampling measurements difficult and time-consuming, in the best possible way, it offers just the status of a sample of the crops on the farm plot. Due to these factors, parts of the field are mostly left unattended and causes yield losses at the end of the season.

1.3 Justification

One important goal of agricultural production is to achieve maximum crop yield at minimum cost. Early identification and problem management by tracking crop growth and yield can help improve yield (Dahikar and Rode, 2014). Production forecasting is essential for the state, national and even international agricultural and economic departments. Precise and timely crop performance and quality information is vital for policy makers, farmers, hedgers and investors (Xijie LV, 2013). Due to clear limitations of the human eye to monitor crop growth on a large scale, different ways of monitoring crop growth appear, such as those based on satellite RS images. Imagery from remote sensing platforms such as those from

UAS have been used to locate individual plant patches, gaps, unhealthy regions, etc. on the land surface over a large scale, something that has previously been impossible. Data acquired sequentially over time on agricultural lands help in identification and mapping of crops and also in assessing crop vigor at a varied range of spatial scales (Atzberger, 2013). Remote sensing can be used to assess automatic and continuous measurements, which are easily enforced with data transmission systems such that the user has virtual real time access to data obtained from a remote device, mobile etc. (Fernández, 2014).

Use of remote sensing of canopy reflectance in sampling a plant population is vital instead of individual plants to quickly assess the spatial heterogeneity of a crop field (Wang *et al*., 2008). With the use of Unmanned Aerial Systems (UAS), data are acquired in real time and with efficient data manipulation system, remedial solutions to crop production problems can be implemented within a short timeframe (Sarkar *et al*., 2018).

1.4 Objectives

1.4.1 Main objective

This study was carried out to evaluate the use of UAS technology, coupled with extensive field survey, to do a comparative assessment of UDP and non-UDP technologies under farmer management.

1.4.2 Specific objectives

Specific objectives of this study are to:

- To capture and produce multispectral images at the midseason stage of the rice crop and use them to develop vegetation indices.
- To determine and compare crop health under UDP and non-UDP treatments.
- To access the relationship between in-field variation in rice yields and N-management system.

CHAPTER TWO

2.0 LITERATURE REVIEW

2.1 Yield variability problem in African agriculture

A critical challenge facing mankind in the 21st Century is that of feeding the world which is projected to reach 10 billion by 2050 (Wahab *et al*., 2018). Despite rice becoming an important grain and a basic food crop in Madagascar, West, East, Central and Southern Africa, rice production in Africa is still the lowest in the world and cannot satisfy the increasing requirement for rice in many African countries (Balasubramanian *et al*., 2007). Variability in crop growth generally depends on various factors that can either be time-independent (e.g. substrate, topography, soil type and depth) or time-dependent (e.g. irregularities in weather conditions, planting and emergence, weed developments etc.) (Bégué *et al*., 2008; Kumhálová and Matějková, 2017). Spatial variability in yield consists of both permanent and transitory components. The permanent patterns are usually regulated by native soil properties or endogenous factors, while the transient patterns are influenced by exogenous factors such as climate, pests and disease (Simmonds *et al*., 2013).

Some yield variability studies in rice systems have studied a single mechanism hypothesized to drive variability in in-field yield, such as land-level or water temperature, and/or a set of soil attributes assumed to be involved in yield variabilities. In addition, several of the studies have been performed in fields ranging from 0.5 to 3.6 ha (Yanai *et al*., 2001; Dobermann, 1994; Casanova *et al*., 1999), while fewer studies have been conducted in larger fields containing multiple basins. In West Africa, irrigated rice yields in the wet season were projected to

change by 21 or +7% (without / without adaptation). Without adaptation, irrigated rice yields in dry season in West Africa would drop by 45 percent, while they would drop significantly less (15%) with adaptation. Most farmers recognize spatial variability in yield after harvesting. Variability in crop yields can result in crop production fluctuations, crop price instability and, in turn, a higher market risk. Government agricultural policies and risk management are closely related to unpredictable crop price and market risk (Kim, 2009).

One of the steps toward achieving the self-sufficiency goal for rice in most developed countries is to encourage yield-enhancing technologies such as remote sensing. Remote sensing has played a variety of roles in assessing the cause of spatial and temporal variability of crops and soils and is one of the instruments that has demonstrated its ability to assist in crop management and, more precisely, in the study of variability within the field (Kumhálová and Matějková, 2017). It also provides yield monitoring and mapping technology capable of measuring, georeferencing and recording grain yields, enabling a spatial accuracy of meters to document the location and magnitude of yield variability. Therefore, this method provides a viable alternative for evaluating the status of crops due to its potential to simultaneously capture large areas (Chapman *et al*., 2014).

2.2 Urea deep placement (UDP)

The International Fertilizer Development Centre (IFDC) developed the UDP technology while working with farmers for several years in Bangladesh (Rahman and Barmon 2015). This technique has been used over the years to tackle yield

variability in rice by decreasing losses up to 40% and increasing urea efficiency to 50%. It also increases yield by 25% with an average decrease of urea use by 25% (Meybeck *et al*., 2012). With the introduction of innovative soil management techniques like the urea deep placement notwithstanding, yield variability remains a challenge. This is because modern management in sustainable agriculture needs immediate information on the condition of cultivated plants and quick response to unwanted phenomena such as pest presence and crop growth monitoring (Berner and Chojnacki, 2017).

Nitrogen (N) plays a key role in the production of rice, and is required in large quantities. It is also limited in rice production and suffers from heavy system losses when applied to puddle field as inorganic sources (Rahman and Barmon, 2015). Few studies have assessed the N loss of UDP in fields of paddy rice, especially by volatilization of NH_3. Ammonium is the dominant form of available N, in flooded and saturated anaerobic soils. Most of the nitrogen fertilizer losses occur through ammonia volatilization immediately after application into the floodwater. Urea Deep Placement (UDP) has already been found to be an important and effective plant nutrient management practice for rice (Gregory *et al*., 2010; Bandaogo *et al*., 2015). Traditional N-fertilizer surface broadcasting suggested for rice production is often ineffective (Mohanty *et al*., 1999; Nkebiwe *et al*., 2016), whiles simplified one-time deep urea placement (UDP) (5–15 cm deep) may be a promising approach to resolving the trade-off between reducing N-loss whilst also improving crop output (Savant and Stangel, 1990; Afroz *et al*., 2014; Huda *et al*., 2016; Nkebiwe *et al*., 2016).

There are growing interests in UDP compared to broadcasting due to benefits such as reducing the NH4 + concentration of floodwater (Kapoor *et al*., 2008; Afroz *et al*., 2014; Huda *et al*., 2016). Studies have identified this technology 's potential for an increase in productivity. For example, studies in Nigeria (Tarfa and Kiger, 2013; Liverpool-Tasie *et al*., 2015) show that the use of deep-placement urea technology increased rice productivity by 20-30%, with nitrogen use efficiency rising by about 40% over conventional broadcasting methods. Pasandaran *et al*. (1998), reported that UDP showed a 25% savings in N fertilizer rates leading to an average 400 kg/ha increase in rice yield in Indonesia. Bulbule *et al*. (2002), announced that the USG briquette applied at a rate of 56 kg N / ha yielded 25 per cent higher than the recommended dose of 100 kg N / ha using traditional urea in Indian rice crops. Tarfa and Kiger (2013), recorded that in Niger State, Nigeria, UDP technology increased N consumption output by 40% and irrigated rice yield by 20-30% in 2012.

2.3 Remote sensing technology

Remote sensing is the art and science of measuring the earth by means of sensors on aircraft or satellites (aerial photo). These sensors capture image data and have advanced capabilities to interpret, analyze, and visualize those images (Eliceiri *et al*., 2012). In remote sensing, electromagnetic radiation from an object is measured and translated into information about the object or into processes related to the object in the case of earth observation. Remote sensing systems are designed to distinguish specific wavelengths of the electromagnetic spectrum referred to as a

"band" or "channel". The various combinations between these channels are known as vegetation indices. Each instrument is distinguished by a particular number and range of wavelengths detected; some instruments detect distinct bands, while others detect fairly small wavelengths or wider bands (multispectral, visible and near-infrared wavelengths, microwaves, thermal sensing systems) (Shaw *et al*., 2003). Remote sensing is capable of recognizing spectral signatures of all objects and surfaces. Sensors may detect targets with a limited spatial resolution of image data identified by the smallest sampled or viewed spatial area. Digital images are composed of pixels, each of which is distinguished by different spectral and spatial attributes (Shia *et al*., 2014), as the reflectance strength or emittance measured by a sensor (Jawak *et al*., 2015). Spatial resolution refers to the area of space of each pixel reflected or printed. Remote sensing plays a unique and essential role, provided that remote sensing measurements can be reliably and operationally related to biophysical and biochemical parameters on Earth's surfaces. Nevertheless, the relationship between surface measurement and satellite data is highly dependent on the study region and the reflectance acquisition's experimental conditions.

Remote sensing systems used in applying the technology include satellites, unmanned aerial vehicles (UAVs), aircraft, balloons and a range of sensors such as optical and near-infrared, and RADAR (Radio Detection and Ranging). Diagnostic information extracted from images obtained from these on-board sensors, such as biomass, the Leaf Area Index (LAI), disease, water stress and plant lodging, can assist in crop management, yield forecasting and environmental protection. The

latest drone design, also known as Unmanned Aerial Vehicles (UAV), is divided into drones with electric drives, where electric batteries are the source of energy, and drones powered by the use of internal combustion engines. Depending on the programmed path, they are operated remotely by the operator using a transmitter, or independently.

2.4 History of remote sensing

The invention of photography started with remote sensing. Photograph is derived from the two Greek words 'photo' meaning 'light' and 'graphing' meaning 'writing'. The term, "remote sensing," was first introduced in the 1950's by Evelyn L. Pruitt of the U.S. Office of Naval Research. In his early work in 1666, Newton discovered that a prism transmitted light into a spectrum of red, orange, yellow, green, blue, indigo and violet and recombined the spectrum into white light. In 1800, for the first time in the world, Sir William Herschel explored thermal infrared electromagnetic radiation by measuring the temperature of light that a prism had split into the visible color spectrum (Zhu *et al*., 2018). Aerial photography began to develop in the 1950s out of the research started during World War II and the Korean War. Color-infrared became important in identifying various types of vegetation and in detecting diseased and damaged vegetation. In 1975, 1978, 1982 and 1984, Landsat 2, 3, 4 and 5 were launched respectively. European Radar Satellite ERS-1 was launched in 1991, this was the first satellite with an altimeter capable of measuring the earth's surface to within 5 cm. India created IRS (Indian Remote Sensing) in 1995. That same year there was the launch of OrbView-1, the

first commercial imaging satellite in the world, ERS-2, Radarsat1 and Ofeq-3 crashed the same year.

In agriculture, Yamaha developed the first UAV model (Giles and Billing, 2015). Unmanned Yamaha RMAX helicopter was introduced for use in agricultural pest control and crop monitoring. RapidEye was released in 2008. It is a constellation of five high resolution interlinked satellites (Tyc *et al*., 2005). RISAT 1 and SPOT 6 was launched in 2012. Landsat 8 was launched in 2013 by NASA - USA. Sentinel -1A, SPOT 7 and WorldView-3 were launched in 2014. ESA launched Sentinel-2 in 2014.

2.5 Remote sensing platforms

A platform is a vehicle, from which a sensor can be operated (Lillesand *et al*., 2015). There are three main remote sensing platforms: airborne (aerial), ground based, and space borne. Ground based platforms are those that are used on the ground although they need support. These platforms can be close to the ground or a few meters above ground and includes hand held cameras, tripods, towers, cranes etc. They are mostly used to study properties of a single plant or a small patch of grass (Imam, 2019), have a higher resolution since small areas are captured, and requires multiple photographs if a large area is to be studied. Non-imaging portable sensors such as CropScan, and Greenseeker are used on ground based platforms (Peteinatos *et al*., 2014).

Airborne platforms, also known as aerial platforms, are primarily operated at higher altitudes. They include helicopters, aerial cameras mounted on aircrafts, drones etc.

Generally, aircrafts are used to collect very detailed images while helicopters are used to pinpoint locations due to vibration and lack of stability. These provide a larger area coverage than ground based platforms and can be categorized into low (drones) and high (aeroplanes) altitude aircrafts (Imam, 2019). Some of the applications of airborne remote sensing platforms include aerial surveys, reconnaissance surveys etc.

Space borne platforms include satellites and shuttles and operate at a much higher altitude than ground based and airborne platforms. Space-borne vehicles, such as satellites, can occupy far more ground than aircraft, and can track areas regularly (Imam, 2019). Space based remote sensing can classify individual vegetation types and plant species through the use of high spectral and spatial resolution imagery (Fuller, 2005; He *et al*., 2011). While spatially borne hyperspectral and high spatial resolution visible sensors (QuickBird and WorldView-2) have a number of important uses in specific regions, the Landsat series of satellites appear to be the most suitable for assessing global spatial vegetation classifications (Gillespie *et al*., 2015). Space borne platforms are the most stable carrier compared to airborne and ground based platforms (Zhu *et al*., 2018) though it faces considerable number of challenges including prevention of data collection by clouds, reflectance value distortion by the atmosphere, and a probable long revisit time. Data captured using space borne platforms have been applied in climate, agriculture, weather studies etc.

2.6 Satellite remote sensing Vs UAV

Satellites may be classified based on altitude, orbital geometry (geostationary, equatorial and sun synchronous) and timing. The first remote sensing satellite emerged in 1960 for meteorological purposes (Alvino and Marino, 2017).

UAVs are compact and made of a wireframe-like carbon body, which is difficult to see in distances of more than 200 meters. This is also why fixed wing UAVs are more effective to operate because they are visible further away, e.g. > 1.5 km, and therefore cover much greater areas in one flight mission.

In the recent past, satellites were distinguished by low spatial resolution and used over large geographic areas for many purposes, but were unable to determine variability in crop yield within a field (Lee *et al*., 2010). Spatial resolution of the satellite data is measured in pixels; this is the smallest measuring unit on the ground which the sensor covers. Some satellite sensors are available which record data at or below meter level. Higher spatial resolution, however, ultimately imposes more costs in regards to data collection and image processing (Stow *et al*., 2004).

Satellite missions, labelled Sentinel 1 - 5, were set up for monitoring the environmental (van der Werff and van der Meer, 2015). Sentinel-2 's arrival in 2015 kicked off a new age in remote sensing. The mission guarantees continuity of previous missions (Landsat and SPOT) and produces geochemical and physical variables, maps of land cover and maps for land change detection. Its spatial resolution (from 60 m to 10 m) enables several small water bodies to be monitored as reported by Toming *et al*. (2016), and Sentinel-2 was able to map the water quality. It may also track chlorophyll as an indicator of phytoplankton,

chromophoric (or colored) dissolved organic materials and concentrations of dissolved organic materials. A recent research on Sentinel-2 shows that band 5 and band 3 are the most effective algorithms for obtaining the highest reflectance from dissolved organic matter (DOMs). Bands 4 and 5 were used to build a model for detecting chlorophyll with low-mean square error.

Sentinel-2 has several advantages including the following: (1) a wide area coverage, approximately 290 km (20.6° field-of-view from an altitude of 786 km) (Malenovský *et al*., 2012); (2) a high resolution of up to 10 m; (3) three red-edge bands that have special applications for vegetation analysis (4) short revisit frequency which permits a global coverage every five days; and (5) free data accessibility. Sentinel 2A has 13 spectral bands that span from the visible (VIS) and the near infrared (NIR) to the short-wave infrared (SWIR) (433–2190 nm) as shown in Table 2.1.

Table 2.1: Bands and image resolution for Sentinel 2A Satellite

Setinel-2 Bands	Central Wavelength (µm)	Resolution (m)
Band 1-Coastal Aerosol	0.443	60
Band 2-Blue	0.490	10
Band 3-Green	0.560	10
Band 4-Red	0.665	10
Band 5-Near infrared	0.705	20
Band 6-Near infrared	0.740	20
Band 7-Near infrared	0.783	20
Band 8-Near infrared	0.842	10
Band 8A-Near infrared	0.865	20
Band 9-Water vapour	0.945	60
Band 10-shortwave infrared (Cirrus)	1.375	60
Band 11-shortwave infrared	1.610	20
Band 12-shortwave infrared	2.190	20

However, when it comes to precision agricultural applications, there are two main problems with these platforms, which are related to per pixel resolution and orbit time. The second problem is the average 16-day re-visitation time, which makes its agricultural applications somewhat difficult, particularly those related to water and nutrient management.

Over the last five years, UAV platforms have become almost abundant due to inexpensive aircraft with camera payloads ranging from visible, near and thermal infrared to 3D LIDAR, the combination of which is known as Unmanned Aerial System (UAS) (Xue and Su, 2017). Developed countries have already begun using UAV's in their precision farming.

UAV Remote Sensing has very high resolution. It gives fast and low cost data, and cloud cover does not prevent acquisition, making it a useful aircraft tool for monitoring and managing crops in the growing season (Zhang and Kovacs, 2012; Nebiker *et al*., 2008). A major advantage over satellite imagery is cloud independence and revisit time and quick real-time data acquisition capability (Berni *et al*., 2009; Eisenbeiss, 2009). Additionally, high temporal resolution is achieved by high data acquisition versatility (Shahbazi *et al*., 2016). These features make UAVs highly suitable for many agricultural applications (Jensen, 2009; Swain and Zaman, 2012). In addition, UAVs outdo manned aircraft in terms of flexibility and expense, and even sharper spatial resolutions (Matese *et al*., 2015). Fine-resolution digital elevation models (DEMS) are also derived with UAVs, through post-processing stereo imagery and the ability to follow a very precise flight path (using

a programmable autopilot), allowing simple repeatability, low noise and low carbon footprint.

2.6.1 UAV platforms: fixed wings and rotary wings (advantages and disadvantages)

The UAVs can be divided into two key top-level, fixed-wing, and rotary-wing configurations. These styles pose different advantages and challenges regarding the system of control and guidance. (Alvarenga *et al*., 2015). The fixed-wing UAV features rigid wings with an airfoil allowing for flying based on the lift provided by the forward airspeed. Regulation of navigation is obtained by means of control surfaces in wings (aileron, elevator and rudder). The Aerodynamics help longer endurance and loitering flights, and also enable high-speed movement. Similar to rotary-wing aircraft, these aircraft can carry heavier payloads, too. These platforms however require a runway for taking off and landing (Kanellakis and Nikolakopoulos, 2017).

The rotary-wing presents maneuverability advantages. Such platforms are capable of accomplishing vertical take-off and landing (VTOL), low-altitude flights, and tasks of hovering. The use of rotary blades produces aerodynamic thrust forces and requires no relative speed (Alvarenga *et al*., 2015). It can also be classified into single-rotor (helicopter) and multi-rotor (quadcopter and hexacopter). Quadcopters with 4 rotors are most commonly used. Various designs are available with 3, 4, 6, 8 and even more rotors and various rotor configurations. Quadcopters have definitely increased the popularity of multicopters, and their required flight control

electronics make it very easy to maneuver them in a very short time, often within half a day (Mayr, 2015). Multi-rotors are fast and agile platforms, capable of executing demanding maneuvers. Also, they are able to hover or travel along a target. These platforms however have limited pay load capacity and endurance. Mechanical and electrical complexity is fairly small as these elements are abstracted within the flight and motor controls (Kanellakis and Nikolakopoulos 2017). A quadrotor UAV can be highly maneuverable, can hover, take off, fly, and land in small areas and can have simple control mechanisms (Altug *et al*., 2002; Pounds *et al*., 2002). A quadrotor can also fly closer to an obstacle than traditional configurations of a helicopter that have a large single rotor without fear of a rotor strike (Pounds *et al*., 2002). The dynamics of the vehicle are good for agility, and its four rotors can permit increased payload (Altug *et al*., 2002). But quadrotor dynamics will make it difficult to control the vehicle (Altug *et al*.,2002). For a small, low cost quadrotor, the task of controlling the vehicle can be even more difficult (Pounds *et al*., 2002).

The single-rotor has two rotors, the primary navigation rotor and the tail one for heading control. Usually these vehicles can take off and land vertically, and do not require airflow over the blades to move forward. Instead, the blades create the required airflow themselves. A single motor enables even longer flights with endurance compared to multi-rotors This type of vehicle can also carry high payloads in outdoor missions, such as sensors and manipulators while performing hovering tasks and long-term flights These platforms are however mechanically complex and costly (Kanellakis and Nikolakopoulos 2017).

Rotary wing UAVs have the upper hand of learning how to operate them easily. Their vertical ability to take off and land makes them perfect for narrow ways of the environment, e.g. urban. Their flight controllers are experienced and they are easy to fly and take off, it's no problem to land as well as to fly autonomously. They don't need a landing strip which is a huge advantage in the field, forests or urban environments. Their copter design also makes them suitable for tasks of inspection and observation. Because of their property of having to operate many motors to stay in the air, their energy consumption is considerably higher than that of UAVs with fixed wings. Thus, the result could be shorter travel times (about 20 to 30 minutes) and more frequent changes in battery power. Because multi-copters have to actively create their lift during the entire flight, their stamina and operating speed are restricted. Generally speaking, they have a flight time of 12 min-30 min, which means they can reach only small areas (Eisenbeiss, 2009; Cai *et al*., 2014) and have poor wind endurance.

2.7 Solar radiation and Spectral Bands

Reflected light measurements have often been used in the natural vegetation or agricultural plants for remote assessments of green biomass or physiological stress (Fernandez *et al*., 1994; Peñuelas *et al*., 1994). Red light is absorbed into photosynthetically active tissue by the green chlorophyll pigments, and thus the proportion reflected varies inversely with the amount of plant material or biomass present. However, the intensity of reflected red light in the field will depend not only on the absorbed proportion but also on its incident intensity, which varies

depending on location and time of day. Research has shown that the use of red and near infrared sensor channels on board satellites is particularly apt for vegetation study. Such bands are usually found on meteorological and earth observation satellites and frequently comprise more than 90% of vegetation information (Baret *et al*., 1989).

The spectral distribution of extraterrestrial radiation is such that the visible part of the electromagnetic spectrum accounts for about half of that. Spectral complexity defines the number of spectral bands for each pixel of information collected. Many sections are in the Near-Infrared and UV ranges. This spectral range is changed as the radiation goes downwards into the atmosphere; changes are primarily due to gases and aerosols (Wald, 2007). Light that has a relatively narrow range of wavelengths appears colored whiles the normal sunlight that contains the entire spectrum is usually described as white light.

From an eco-physiological point of view, visible radiation between the wavelengths of 400 and 700 nm is the most important type, since it relates to photosynthetically active radiation (PAR). The plant uses just 50 percent of the incident radiation to conduct photosynthesis (Varlet-Grancher *et al*., 1995). The amount of radiation intercepted by the plant cover is influenced by a number of factors such as the leaf angle, the properties of the leaf surface affecting light reflection, the thickness and chlorophyll concentration affecting the transmission of light, the size and shape of the leaf phyllotaxis and vertical stratification, the elevation of the sun and the distribution of direct and diffuse solar radiation. Of the 100 % total energy that the leaf receives, just 5% is later transformed into carbohydrates for biomass

processing (Campillo *et al*., 2012). Essentially the whole visible light is able to encourage photosynthesis, but the regions between 400 and 500 and 600 to 700 nm are the most successful. Moreover, pure chlorophyll has very weak absorption, between 500 and 600 nm wavelength. Accessory pigments complement light absorption in this area, contributing to the chlorophylls, 620-700 nm (red): Higher chlorophyll absorption ranges: 510-620 nm (orange, yellow-green); low photosynthetic activity: 380-510 nm (purple, blue and green) is the most energetic, strong chlorophyll absorption: < 380 nm (ultraviolet) and germicidal effects, even lethal < 260 nm (Campillo *et al*., 2012). Leaf is the key photosynthetic functional unit and its effectiveness in absorbing and using solar energy defines the productivity of vegetables. The region and foliage structure (the design of the canopy), assess the reception of solar radiation (LI) by a crop and the distribution of irradiance between individual leaves (Connor *et al*., 2011). Leaf area and arrangement change over the course of a crop life and, by leaf movement, even over a single day. Maximum production of crops requires complete capture of incident solar radiation which can only be accomplished by supporting water and nutrient levels (Connor *et al*., 2011). Most production strategies are geared to maximizing solar radiation interception. In the case of crops, this implies adapting agricultural practices in such a way that full canopy cover is obtained as soon as possible. Water and nutrient input deficiencies may reduce leaf growth rates, reducing yields below optimum levels due to insufficient energy capture (Gardner *et al*., 1985). The performance of canopy interception corresponds to the plant population 's ability to

intercept the incident solar radiation, which is the key factor affecting the photosynthesis and transpiration processes (Leuning *et al*., 1995).

2.8 Electromagnetic radiation

The source of remote sensing is electromagnetic radiation which travels in vacuum in the form of waves of different lengths at the speed of light. The most useful wavelengths in remote sensing cover visible light (VIS), and extend to thermal infrared (TIR) and microwave bands through the near (NIR) and shortwave (SWIR) infrared. We restrict ourselves in remote sensing to the use of electromagnetic radiation as a characteristic of numerous physical processes. All products with a temperature above $0^{o}K$ have the electromagnetic capacity to emit. Objects on or near the surface of the earth are capable of reflecting or dispersing incident electromagnetic radiation emitted by a source that may be artificial, such as flash light, laser or microwave radiation, or natural, such as sun. Solar radiation reflected by objects at the Earth's surface is measured in the visible, near-infrared (NIR) and middle-infrared (MIR) portion of the electromagnetic spectrum.

In the region of thermal-infrared (TIR), especially in the atmospheric window, measurements are taken on the surface of the earth by objects emitting radiation, be it that this radiation originates from the sun. Vegetation shows a reflectance curve which is very characteristic. There is hardly any absorption in the NIR region, and the amount of transitions between cell walls and air vacuoles in the leaf tissue determines the reflectance. As a result, green vegetation NIR reflectance is high, and a steep slope occurs at about 700 nm in the curve, the so-called red-edge area

(Clevers and Jongschaap, 2002). The cells in the plant leaves are very effective in light dispersal due to the high contrast in the refraction index between the water-rich cell content and the intercellular air spaces. The reflectance of light spectra from plants is well known to vary with plant size, tissue water content, and other intrinsic factors.

The various vegetative coverings can be differentiated in relation to overall ground elements according to their particular spectral behavior (Tucker, 1979). Visible red radiation (630-690 nm) is absorbed by chlorophyll while the near infrared radiation (760-900 nm) is strongly reflected by the cellular structures of the leaves.

2.9 Vegetation indices and their importance

An index is a number which counts the strength of a phenomenon that is too complex to be broken down into known parameters. While the portion of impact of several variables can be calculated when in a well-documented and well-controlled environment, this decomposition is generally difficult for signals detected on remote sensing images. The concept of vegetation index is well adapted to qualify vegetation over large areas, e.g. over areas that cover many pixels of an image (Bannari *et al.*, 1995). Healthy crops are characterized by strong red energy absorption and strong NIR energy reflection. The extreme contrast of red and near-infrared band absorption and scattering can be integrated into various quantitative indices of vegetation conditions. Those quantitative mathematical combinations are called vegetation indices.

The creation and use of different remote sensed vegetation indices was based on the basic assumption that certain algebraic combinations of remote sensed spectral bands can reveal useful information such as vegetation structure, vegetation cover status, photosynthetic ability, leaf density and distribution, leaf water content, mineral deficiencies and parasitic shocks or attacks (Liang, 2005). They demonstrate greater ability to detect biomass than individual spectral bands (Asrar *et al*., 1984). When studying the general vegetation reflectance curve, a feature, sensitive to the presence of green vegetation is the difference found between the red and near infrared. The spectral response of the vegetation in the red is strongly correlated with the concentration of chlorophyll while the spectral response in the near infrared is influenced by the index of the leaf area and the density of green vegetation (Major *et al*., 1990). The combination of these two spectral domains allows for the separation of vegetation from soil and the determination of photosynthetically active biomass by vegetative density cover. Various factors such as the number of leaves, their biochemical composition, the canopy structure at a particular growth phase, illumination conditions (state of atmosphere and solar angle), and background (soil) reflectance generate a reflectance signal of a canopy (Zou *et al*., 2018), therefore a strong vegetation index should be less prone to the above factors.

Vegetation indices have seen a more common use because of their computational ease. Spectral vegetation indices are statistical combinations of various spectral bands mainly in the visible and near infrared regions of the electromagnetic spectrum by combining low reflectivity in the visible portion of the spectrum with

high reflectivity in the near-infrared (Rondeaux *et al*., 1996). These numerical transformations have shown widespread variability not only with the seasonal variability of green foliage but also across space, making them suitable for detecting spatial variability within the field. Spectral vegetation indices are an easy and convenient way of extracting information from remotely sensed data, due to their ease of use, which facilitates the processing and analysis of large volumes of data collected by satellite platforms (Govaerts *et al*., 1999; Myneni *et al*., 1995).

Vegetation indices (VIs), simple reflectance functions in two or more spectral bands (Zou *et al*., 2014; Zou and Mõttus 2015) are designed to amplify the effect of specific vegetation properties while minimizing soil background and solar angle properties (Huete *et al*., 2002). In terms of their development rationale, all these indices, whether in ratio-based or in the form of a linear combination, were formulated on the basis of the strong contrast between the near infrared (NIR) and red (R) bands as vegetation strongly reflects the incident radiation in the NIR band while strongly absorbing in the R band (Tucker, 1979; Gitelson, 2004). Vegetation indices are also designed to provide a measure of the overall amount and quality of photosynthetic material in the vegetation, which is essential for many purposes to understand the state of the vegetation.

2.9.1 Types of vegetation indices

Pearson (1972), is a pioneer of vegetation indices literature. The first, two indices were developed in the form of ratios: the "Ratio Vegetation Index" (RVI) and the "Vegetation Index Number" (VIN) for vegetative cover estimation and monitoring.

$$RVI = R/NIR$$

$$VIN = NIR/R$$

Where R is the mean red channel reflectance, whiles NIR is the mean near infrared channel reflectance. Since then, a lot of vegetative indices have been developed including the Normalized Difference Vegetation Index (NDVI) (Rouse *et al*., 1974), the Soil Adjusted Vegetation Index (SAVI) (Huete, 1988), Normalized Difference Red Edge (NDRE), Optimized Soil Adjusted Vegetation Index (OSAVI), the Green Normalized Difference Vegetation Index (GNDVI) (Gitelson *et al*., 1996) and the Chlorophyll Index green (CIg).

2.9.1.1 Normalized Difference Vegetation Index (NDVI)

The most widely used and well-known vegetation index is the Normalized Difference Vegetation Index (NDVI), developed by Rouse *et al*. (1974). The idea behind NDVI is that the chlorophyll of a plant absorbs sunlight, which is captured by the electromagnetic spectrum's red-light region, while the spongy mesophyll leaf structure of a plant produces significant reflection in the spectrum's near-infrared area (Tucker, 1979; Jackson *et al*., 1983). Greener and denser vegetation thus has low red-light reflectance and high near-infrared reflectance, and thus high NDVI values. NDVI is the ratio between the near-infrared band (NIR) and the red band (R) and the sum of these two bands (Rouse *et al*., 1974) (Equation 1).

$$NDVI = \frac{NIR-Red}{NIR+Red}$$

where NIR is reflectance in the near-infrared band and RED is reflectance in the visible red band. The spectrum of the obtained values is between −1 and +1. Only

positive values equate with vegetated zones; the higher the index, the greater the target's chlorophyll content. Near zero and negative values show unvegetated surface characteristics such as rock, soil, water, ice and clouds.

The NDVI algorithm exploits the fact that green vegetation reflects less visible light and more NIR, while scattered or less green vegetation represents a greater portion of the visible and less NIR. NDVI incorporates these reflectance characteristics in a ratio so it's a photosynthetic capacity-related index. Despite its intensive use, NDVI saturates on a thick and multi-layered canopy and shows a non-linear relationship with biophysical parameters like LAI (Baret and Guyot, 1991; Lillesaeter, 1982).

2.9.1.2 Adjusted-soil vegetation index (SAVI)

NDVI 's sensitivity to soil context and atmospheric effects has created a growing interest in the creation of new indices, including SAVI, transformed soil-adjusted vegetation index (TSAVI), atmospherically resistant vegetation index (ARVI), optimized soil-adjusted vegetation index (OSAVI), etc., which are less sensitive to these external effects. These indices are potentially more accurate than NDVI, but not yet commonly used with data derived from satellites (Rondeaux *et al*., 1996).

Richardson and Wieg (1997), originally suggested the distinction of vegetation from the soil context by examining the soil line, which can be viewed as a linear relationship between the NIR and R on the 2D plane of the soil spectral reflectance values. It can therefore be seen as a detailed description of a vast amount of soil

spectral knowledge from a variety of environments (Baret *et al*., 1993). SAVI is calculated as;

$$\text{SAVI} = \frac{\text{NIR}-\text{Red}}{(\text{NIR}+\text{Red}+\text{L})} * (1 + L)$$

where NIR represents reflectance values in the near-infrared band and red represents reflectance values from the red band. The L value is a function of vegetation density. This can either be early growth stage (0.1) or mid growth stage (0.25) (Huete, 1988). Qi *et al*. (1994), noted the reduction of the dynamic range of SAVI after the adjustment factor (L) was added, which makes it unfavorable for studying in sparsely vegetated areas.

2.9.1.3 Green normalized vegetation index (GNDVI)

Instead of using the NIR and red bands which are the traditional NDVI extraction band combination, the NIR and the green band may be used to derive the Green Normalized Vegetation Difference Index (GNDVI). There is no substantial dispersion of shorter wavelength light at lower altitudes and therefore the green band performs equally well (Agribotix 2018). GNDVI is calculated with the formula below:

$$\text{GNDVI} = \frac{\text{NIR}-\text{Green}}{\text{NIR}+\text{Green}}$$

Where NIR represents Near-infrared band reflectance values and G represents green band reflectance values. The variances in the reflectance properties of the NIR and green bands allow for an assessment of vegetation density and intensity using solar radiation reflectivity. GNDVI is an indicator of chlorophyll concentration in the vegetation. Gitelson and Merzlyak, (1994), recommended the

use of the reflectance in the green range (540 to 570 nm) of the spectrum for an assessment of chlorophyll concentration.

2.9.1.4 Normalized difference red edge index (NDRE)

NDRE is very similar to NDVI index, but instead of the near infrared, it uses the red edge band. The formulae for calculating NDRE is;

$$\text{NDRE} = \frac{\text{NIR}-\text{Red Edge}}{\text{NIR}+\text{Red Edge}}$$

Since the reflectance of the red edge band is related to the content of chlorophyll and nitrogen, this index is used to estimate the content of chlorophyll in the vegetation, whereas the NDVI is more appropriate for estimating biomass. Nonetheless, accumulation over dense vegetation does not affect NDRE and can thus detect broader variations in the forest cover or health. Like the NDVI, NDRE ranges from -1 to +1, but commonly observed vegetation values range from 0 to 0.75(Wang *et al*., 2005).

2.9.1.5 Optimized soil adjustment vegetation index (OSAVI)

OSAVI is another form of the soil adjustment vegetation index. The advantage of OSAVI over the other SAVI is that knowledge on soil line parameters is not required to calculate the former (Rondeaux *et al*., 1996). OSAVI is calculated as:

$$\text{OSAVI} = \frac{\text{NIR}-\text{Red}}{\text{NIR}+\text{Red}+0.16}$$

where NIR represents reflectance values in the near-infrared band and red represents reflectance values from the red band. The 0.16 represents a canopy

background adjustment factor to account for visible soil during survey. Like NDVI it also varies from -1 to +1 (Rondeaux *et al*., 1996).

2.10 Use of UAS to assess crop performance

Analyzing their applicability in agricultural operations such as crop monitoring (Bendig *et al*., 2012), crop height estimates (Anthony *et al*., 2014), pesticide spraying (Huang *et al*., 2009) and soil and field analysis (Primicerio *et al*., 2012) is important in the use of UAVs in precision agriculture. The positive relationships between UAS imagery and leaf greenness and crop canopy status has shown the possibility to use crop canopy and leaves remotely sensed reflectance measurements to assess crop nitrogen needs (Shanahan *et al*., 2008). Borhan *et al*. (2004), in a controlled setting, employed numerous spectral and color imaging techniques to assess the nitrate and chlorophyll content of potato leaves, and recorded a linear correlation of 0.84 between multi-spectral band features and nitrate. Jongschaap and Booij (2004), measured potato nitrogen content in the canopy through remote sensing. The authors reported an exponential relationship with a strong correlation of 0.82 between the organic nitrogen content in canopy and the red edge location derived from reflection.

Depending on the crop phenology and crop type the spectral response from a crop can be well controlled using different spectral and spatial resolution. Several experiments have shown that plant safety can be measured very well by using bands of near infrared and red wavelengths. Scientists around the world use Vegetation Indices, namely GNDVI and ENDVI, to assess the status of healthy vegetation and

to differentiate between land use shifts. Crop growth and final yield estimate can be achieved by studying the change in land cover that occurs during and throughout the growing season. Seasonal change in crop growth provides information on agricultural management, and the annual changes provide information on crop area or land cover change (Mookherjee, 2016).

UAVs use cameras to capture images and sensors to compile a collection of data to help track and take on-farm decision-making. Multispectral cameras used on UAVs allow farmers to identify crop health, mitigate risk, and even identify soil health, whereas the new hyperspectral cameras may be used in the future to identify different types of vegetation. Airborne cameras are capable of taking multispectral pictures, and capturing infrared and visual spectrum data. Both can be combined to provide descriptions of plants that are safe and distressed.

Sugiura *et al*. (2005), flew over a sugar beet field and a corn field using an unmanned helicopter. They implemented a real-time kinematic global positioning system, an inertial sensor (INS) and a geomagnetic direction sensor (GDS) to obtain the index of the leaf region (LAI). Jannoura *et al*. (2015), conducted study to assess the productivity of crops over a field of peas and oats. A remote-operated hexacopter was connected to an RGB digital camera. The Normalized Green-Red Difference Index (NGRDI) was determined on the basis of the aerial pictures captured and was related to the above ground biomass and Leaf Area Index (LAI). UAV-mounted multispectral and hyperspectral cameras have been commonly used to track plant growth and biochemical indicators for many vegetation indices options (Zhou *et al*., 2017).

CHAPTER THREE

3.0 MATERIALS AND METHODS

3.1 Study site

This project was conducted during the 2018 growing season at the Tono irrigation scheme (TIS) located on latitude 10º 52'N and longitude 1º 11'W in the Kassena-Nankana District of the Upper East Region (Figure 3.1). The TIS is a government of Ghana executed project that is run through the Irrigation Company of the Upper Region (ICOUR). It is a reservoir or storage-based, gravity fed irrigation scheme with a total capacity of 93 million m^3 and a catchment area of 650 km^2. It currently supplies irrigation to 2490 ha out of a possible 3840 ha of irrigable land which is devoted primarily to rice production. There are 4,000 smallholder farmers who farm under the reservoir with allocated plot sizes between 0.2 and 0.6 ha. (Kemeze *et al*., 2016)

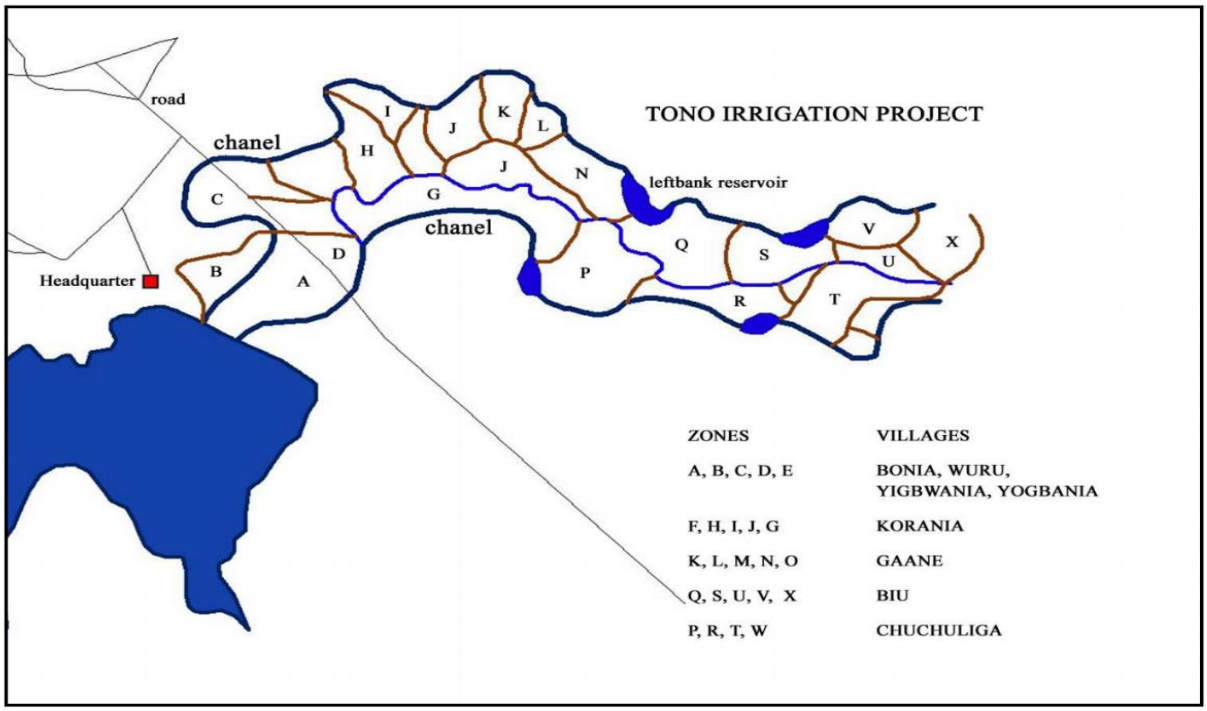

Figure 3. 1: Schematic View of the Tono Irrigation Project (Source: ICOUR UER, 2012).

3.2 Field sizes and management

With the objective to study comparative impacts of UDP and non-UDP N management systems, farmer volunteers were identified in three zones (H, I, and J) out of the 24 zones in the TIS. Farmer volunteers from zones H, I, and J (Figure 3) were selected based on their preferences for N management systems. The first group, referred to as UDP farmers was willing to test the emerging UDP technology. A second group, non-UDP volunteers, was an independent group of farmers who had plots within the perimeter but did not adopt the UDP technology.

Farmer farm sizes were determined through a ground survey in which boundary coordinates of rice fields were determined with hand held Garmin SDSMAP 64sc global positioning system (GPS).

To estimate the field size from the GPS data firstly, the longitude values were given a column header labeled x and latitude values given a column header y in an excel spreadsheet. The add XY data tool was then used after setting the geographic coordinate system of the data frame to the desired coordinate system. The excel spreadsheet was used as the input table and the longitude and latitude columns named x and y respectively were used as the x and y fields in the tool. The resulting point shapefile was an outline of the field. Then the feature to polygon tool was used to convert the point shapefile to a polygon shapefile. Area of the field was calculated using the measure tool to trace the boundary of the field while using the area setting of the tool. These field size estimates were compared to those estimated by the ATT project.

Field plots were prepared mechanically through a pay-for- service arrangement with ICOUR. In the interim, farmers raised seedlings in field nurseries on the TIS which they transplanted after a period of 2 - 4 weeks. Farmers transplanted an average of 2 seedlings per hill in the paddies. Half of the farmers in the study did no thinning out after transplanting. ICOUR provided counsel and inputs with regards to other soil amendments, weed and pest control and harvesting of the rice crop at the end of the season.

3.3 Remote Sensing using Unmanned Aerial Systems technology

Fields were flown on a fixed wing platform using the eBee Ag manufactured by senseFly corporation (Sensefly, 2016). The three zones of intervention were flown as individual units for this study

Figure 3. 2: The eBee fixed winged unmanned aerial vehicle

3.4 Data collection

The process began by importing zone boundary coordinates obtained from ground survey into emotion (sensefly, 2016). Fields were flown using the multispectral sequoia (Figure 3.3) and the Sensor Optimized for Drone Applications (SODA) (Figure 3.4) cameras. The sequoia camera consists of five different wavelength bands; NIR, Red edge, RGB, Red and Green. The sequoia was flown at 127.4 m

altitude giving a ground resolution of 12.0 cm/pixel with 60% forelap and 80% sidelap. The SODA camera was flown at 69 m altitude to obtain 1.6 cm/pixel ground resolution with image 65% forelap and 70% side lap. Images were captured during the period of May 16 – 20, 2018, close to booting of the rice crop. Drone flights were done in the mornings when the sky was clear to when the sun begins to intensify which was normally around noon. Flights begin again once temperature becomes more favorable.

Figure 3. 3: Multispectral sequoia camera

Figure 3. 4: Sensor Optimized for Drone Applications (SODA) camera

The cameras were calibrated prior to each flight. Images captured were stored on a scandisk and eventually downloaded onto the hard drive of the desktop computer for analysis.

3.5 Image Processing

Images were processed through eMotion 3 software. This software aligned, georeferenced and stitched the images together. Images were then transferred into Pix4D, another senseFly product, which generated high resolution seamless orthomosaics. Using the standard Ag Multispectral processing options in Pix4D, four vegetation indices, NDVI, NDRE, GNDVI and OSAVI were generated (Table 3.1) After the index was generated, zone boundaries were drawn by using the regions tool to generate the index values for only areas within the zone of study

Table 3. 1: Vegetation indices

Vegetation Index	Ratio	Reference
Normalized Difference Vegetation Index (NDVI)	$NDVI = \frac{NIR-Red}{NIR+Red}$	Rouse *et al*. 1974
Normalized Difference Red Edge Index (NDRE)	$NDRE = \frac{NIR-Red\ Edge}{NIR+Red\ Edge}$	Barnes *et al*. 2000
Green Normalized Difference Vegetation Index (GNDVI)	$GNDVI = \frac{NIR-Green}{NIR+Green}$	Gitelson *et al*. 1996
Optimized Soil Adjusted Vegetation Index (OSAVI)**	$OSAVI = \frac{NIR-Red}{NIR+Red+0.16}$	Rondeaux *et al*. 1996

3.6 Mapping of yield assessment sites based on NDVI

The process begun with isolation of each individual field based on the coordinates collected during the ground survey in zones H, I and J as shown in Figures 3.5, 3.6 and 3.7 respectively.

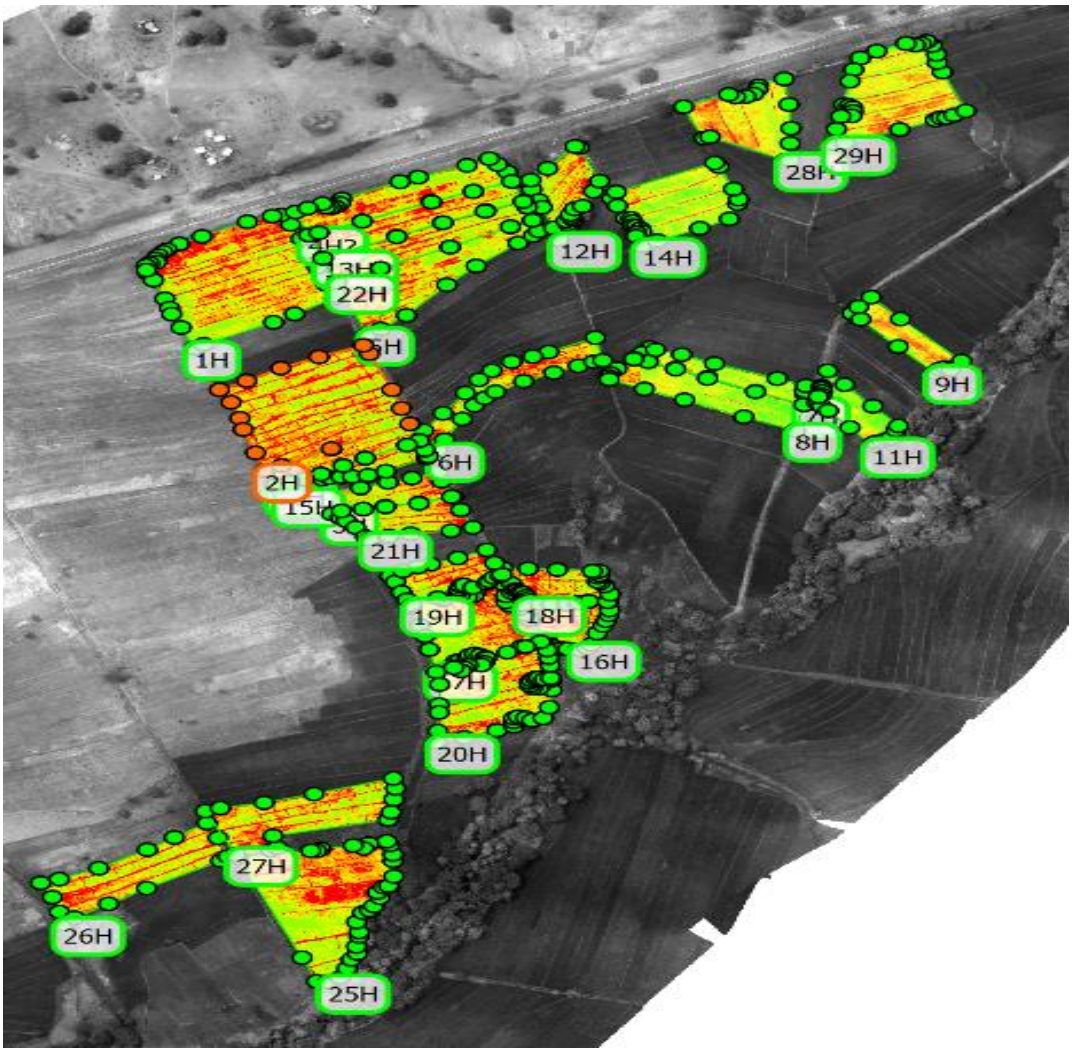

Figure 3. 6: Individual farmer fields showing ID's and boundaries in zone I.

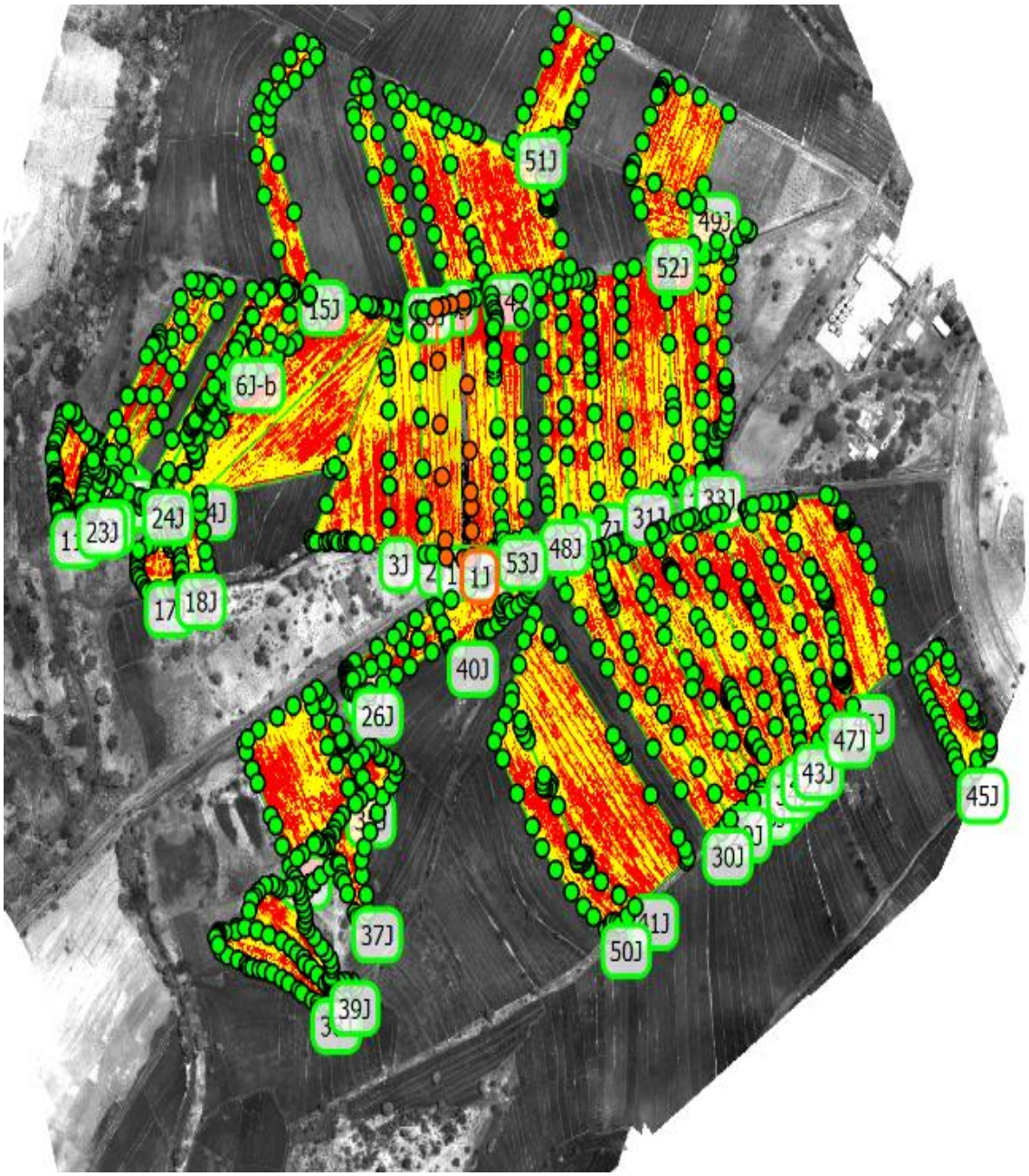

Figure 3. 7: Individual farmer fields showing ID's and boundaries in zone J.

The rational behind isolating each plot was to generate a single NDVI map across all fields in the same zone and identifying sampling locations can confound the analysis due to several factors, critical among whom is the N management effect

which is being investigated in this study. It was therefore decided to isolate individual farmer fields and analyze them separately within their own boundaries. This step was followed by the use of a classification method in Pix4D which permitted the grouping of contiguous pixels to identify areas of "high", "medium" and "low" health in each field based on NDVI values. The different health areas were mapped on the NDVI maps by recording coordinates of four corners of the high, medium and low health regions in each farmer's field.

3.7 Rice grain yield assessment in the field

A hand held GPS device was used to navigate to the midpoint of each of the three health areas identified on the NDVI maps. A net plot of 2 m x 2 m around this central point was delineated in the field and flagged as the sampling area for the health grouping. Using a hand held sickle, rice paddy in this 4 m^2 area was quantitatively harvested and put into jute sacks. Paddy was threshed by hand and winnowed and the grain was weighed. The grain was air dried for about a day and grain moisture content was determined using the M3G^{TM} (Dickey-john) mositure meter. Grain yield/ha was determined using the following formula;

$$\text{Grain yield (kg/ha)} = \frac{\text{(Grain yield (kg/net plot)*(10000 /net plot)*(100- measured grain mc\%)}}{\text{(100 - 14\% standard grain mc)}}$$

3.8 Evaluation of the soil resource

3.8.1 Soil sampling

Disturbed soil samples for laboratory analysis were taken at a depth of 0 – 25cm from all net plots from which yield data was also collected. The samples were air dried and sieved through a 2 mm sieve.

3.8.2 Laboratory analysis

Physical and chemical analyses of 2mm sieved disturbed soil samples was done in the soil and plant analysis laboratory of the department of the agronomy at Iowa State University.

3.8.3 Particle size distribution

This was determined by the pipette method (Walter *et al*., 1978).

3.8.4 Soil pH

This was measured in water extractions with a glass electrode at a soil to water ratio of 1:1.

3.8.5 Organic matter and total nitrogen

These were determined by dry combustion using a Leco Truspec CN analyser. (Combs and Nathan 1998).

3.8.6 Soil phosphorous (P)

This was extracted by a solution consisting of 0.025 normal HCl and 0.03 normal NH_4F (Bray-1 extractant) and measured by Hach DR 3900 spectrophotometer (Frank *et al*., 1998)

3.8.7 Cation Exchange Capacity and Exchangeable cations (Ca, Mg, K, Na)

These were extracted with ammonium acetate (NH_4OAc) solution (Warncke and Brown, 1998) and measured by ICP – AES (Spectro Ciros CCRD).

3.9 Statistical analysis

Analysis of variance (ANOVA) was used to test differences in yields using the SAS software as a function of treatment (SAS Institute, Cary, NC 2018). All tests of significance were assessed using an alpha of 0.05. The STATISTIX software was used to correlate yield to OSAVI.

CHAPTER FOUR

4.0 RESULTS

4.1 Farmer volunteers and field sizes

A total of 50 volunteers participated in the study, 25 each in non-UDP and UDP N management systems (Table 4.1). Zone J had 28 participants (12 non-UDP and 16 UDP), and there were 13 and 9 volunteers from zones H and I, respectively. Farm sizes range from 0.17 to 2.8 hectares among zones (Table 4.1). Zone J recorded the highest mean farm size of 8.9 ha, followed by Mean farm sizes for the three zones were 0.82 ha for zone J, 0.53 ha for zone I and 0.36 ha for zone H. Average farm sizes for non-UDP and UDP fields are 0.53 ha and 0.83 ha, respectively. The total number of farmer fields for the entire study was 85 with 44 UDP fields and 41 Non-UDP fields (Table 4.2).

Table 4.1 Farmer volunteers and average land holdings in zones H, I, and J

Zone	Number of farmer volunteers	Farm size (hectares)	Number of farmers volunteers	Farm size (hectares)
	Non-UDP		**UDP**	
H	9	3.2	4	1.5
I	4	1.6	5	3.2
J	12	8.9	16	15.7
Study area	**25**	**13.7**	**25**	**20.4**

Table 4.2: Sizes of farms in the three zones and in non-UDP and UDP fields

Zone/N-Management	Number of farmer fields	Minimum	Maximum	Mean
		Field size (ha)		
		Zones		
H	19	0.17	1.02	0.36
I	14	0.21	1.16	0.53
J	52	0.22	2.8	0.82
Total	85	0.17	2.8	0.66
		N-Management system		
Non-UDP	41	0.17	1.34	0.53
UDP	44	0.17	2.8	0.83

4.2 Physicochemical properties of the soil

The soils in the entire study site at a depth of 0 to 25 cm were light textured, predominantly sandy loams. Zone H had the highest clay content of 18.5 %, followed by zone J with 14.2 % and 13% in zone I (Table 4.3). Silt content in the soil is in the order zone J >zone H>zone I. The highest sand content of 70.30 % was obtained in zone I, 55.30 % in zone H and 57.2 % in zone J. The UDP fields had the highest clay and sand contents. However, non-UDP fields had the highest silt content of 28.05 % while UDP had the lowest (21.45 %). The study also found that areas of high crop health had the highest clay (17.07 %) and silt (25.40 %) contents while low health areas recorded the highest sand content (63.28 %). Clay and silt contents in medium health areas were higher than those in low health areas (Table 4.3).

The pH of the soil's ranges from 5.4 to 5.7 in the three zones. Zone H has the lowest pH of 5.4 whiles zone I had the highest of 5.7. Zone H recorded the highest value for bray P (0.14 mg kg^{-1}), OM (1.92 %), K (2.4 cmol(+) kg^{-1}), Ca (6.0 cmol(+) kg^{-1}), Mg (2.4 cmol(+) kg^{-1}) and CEC (12.11 cmol(+) kg^{-1}) whiles zone J recorded the least for all except bray P (12 mg kg^{-1}). Zone J had the highest value of total N (0.08 %) with zone I and H recording 0.07 % and 0.06 % respectively.

The pH for both Non-UDP and UDP fields was the same (5.6). Fields under Non-UDP N- management practice recorded slightly higher values for all chemical properties except pH, than those under the UDP management practice. However, there were no significant differences among them.

High crop health areas had the lowest pH (5.4). However, these areas had the highest organic matter content (1.57 %) and CEC (9.70 mg kg^{-1}). Some chemical properties including OM, pH, CEC, K, Mg and Ca, were high in high crop health areas but decreased in the medium and low crop health areas. Total N was same in the high and low health areas (0.9 %) but differed from medium health areas (0.8 %) whiles phosphorous levels were higher in low health areas (5.08 $mgkg^{-1}$) than high (4.82 $mgkg^{-1}$) and medium areas (4.44 $mgkg^{-1}$) (Table 4.3).

Table 4.3: Physiochemical properties of soil in the site of study (0 – 25 cm)

Zone	Sand	Silt	Clay	Textural class	OM	Total N	pH	Bray P	CEC	NH_4OAc Extractable		
									CEC	K	Mg	Ca
	%				%			(mg/kg)	(cmol (+) kg)			
H	55.3	26.2	18.5	Sandy loam	1.92	0.06	5.4	14	12.11	2.4	2.4	6.0
I	70.30	16.40	13.3	Sandy loam	1.22	0.07	5.7	10	7.98	1.6	1.6	4.5
J	57.2	28.6	14.2	Sandy loam	1.18	0.08	5.6	12	7.61	1.3	1.3	4.3
N-management systems												
Non-UDP	54.73	28.05	12.22	Sandy loam	1.56	0.08	5.6	13	10.22	2.0	2.0	5.4
UDP	64.98	21.45	13.57	Sandy loam	1.32	0.06	5.6	11	8.25	1.5	1.5	4.4
Crop health												
H (high)	56.4	25.40	17.07	Sandy loam	1.57	0.09	5.4	4.82	9.70	0.13	1.82	4.92
M (medium)	58.5	25.09	16.16	Sandy loam	1.42	0.08	5.6	4.44	9.48	0.12	1.82	5.07
L (low)	63.28	22.5	14.25	Sandy loam	1.29	0.09	5.7	5.08	8.27	0.12	1.66	4.60

4.3 Correlation between physicochemical properties of the soil and rice grain yield

Pearson correlation was run among the physicochemical properties and grain yield (Table 4.4). BrayP was the only soil property that showed a high correlation with grain yield (r = 0.63). Organic matter correlated highly with CEC (r = 0.79), K (r = 0.68), Mg (r = 0.57), Ca (r = 0.62) and N (r = 0.61). Clay content showed a high correlation with OM (r = 0.77), CEC (r = 0.90), K (r = 0.88), Mg (r = 0.87), and Ca (r = 0.91). The CEC of the soil also correlated highly with K (r = 0.82), Mg (r = 0.91) and Ca (r = 0.91). The three basic cations K, Ca and Mg, correlated highly with each other.

Table 4.4: Pearson correlation matrix of physicochemical properties of the soil and grain yield

	Sand	Clay	Silt	OM	BrayP	pH	CEC	K	Mg	Ca	N	Yield
Sand	1.00	-0.78	-0.89	-0.65	0.29	-0.13	-0.76	-0.71	-0.71	-0.71	-0.47	0.10
		<.0001	<.0001	0.00	0.17	0.54	<.0001	<.0001	0.00	0.00	0.02	0.65
Clay	-0.78	1.00	0.41	0.77	-0.37	0.27	0.90	0.88	0.87	0.91	0.47	-0.21
	<.0001		0.05	<.0001	0.08	0.21	<.0001	<.0001	<.0001	<.0001	0.02	0.32
Silt	-0.89	0.41	1.00	0.38	-0.15	0.00	0.44	0.39	0.40	0.36	0.34	0.01
	<.0001	0.05		0.07	0.47	0.99	0.03	0.06	0.06	0.08	0.10	0.95
OM	-0.65	0.77	0.38	1.00	-0.13	-0.23	0.79	0.68	0.57	0.62	0.61	-0.06
	0.00	<.0001	0.07		0.53	0.29	<.0001	0.00	0.00	0.00	0.00	0.79
BrayP	0.29	-0.37	-0.15	-0.13	1.00	-0.09	-0.46	-0.18	-0.51	-0.39	-0.16	0.63
	0.17	0.08	0.47	0.53		0.67	0.02	0.39	0.01	0.06	0.44	0.00
pH	-0.13	0.27	0.00	-0.23	-0.09	1.00	0.14	0.40	0.45	0.49	-0.26	-0.04
	0.54	0.21	0.99	0.29	0.67		0.52	0.05	0.03	0.02	0.21	0.84
CEC	-0.76	0.90	0.44	0.79	-0.46	0.14	1.00	0.82	0.91	0.91	0.48	-0.12
	<.0001	<.0001	0.03	<.0001	0.02	0.52		<.0001	<.0001	<.0001	0.02	0.56
K	-0.71	0.88	0.39	0.68	-0.18	0.40	0.82	1.00	0.81	0.90	0.42	0.00
	<.0001	<.0001	0.06	0.00	0.39	0.05	<.0001		<.0001	<.0001	0.04	1.00
Mg	-0.71	0.87	0.40	0.57	-0.51	0.45	0.91	0.81	1.00	0.95	0.29	-0.19
	0.00	<.0001	0.06	0.00	0.01	0.03	<.0001	<.0001		<.0001	0.17	0.38
Ca	-0.71	0.91	0.36	0.62	-0.39	0.49	0.91	0.90	0.95	1.00	0.33	-0.12
	0.00	<.0001	0.08	0.00	0.06	0.02	<.0001	<.0001	<.0001		0.12	0.59
N	-0.47	0.47	0.34	0.61	-0.16	-0.26	0.48	0.42	0.29	0.33	1.00	-0.04
	0.02	0.02	0.10	0.00	0.44	0.21	0.02	0.04	0.17	0.12		0.87
Yield	0.10	-0.21	0.01	-0.06	0.63	-0.04	-0.12	0.00	-0.19	-0.12	-0.04	1.00
	0.65	0.32	0.95	0.79	0.00	0.84	0.56	1.00	0.38	0.59	0.87	

4.4 Remote sensing imagery

The RGB images captured using the SODA camera were orthorectified and stitched together to produce high resolution orthomosaics of natural color images of the rice crop as shown in Figures 4.1, 4.2, and 4.3.

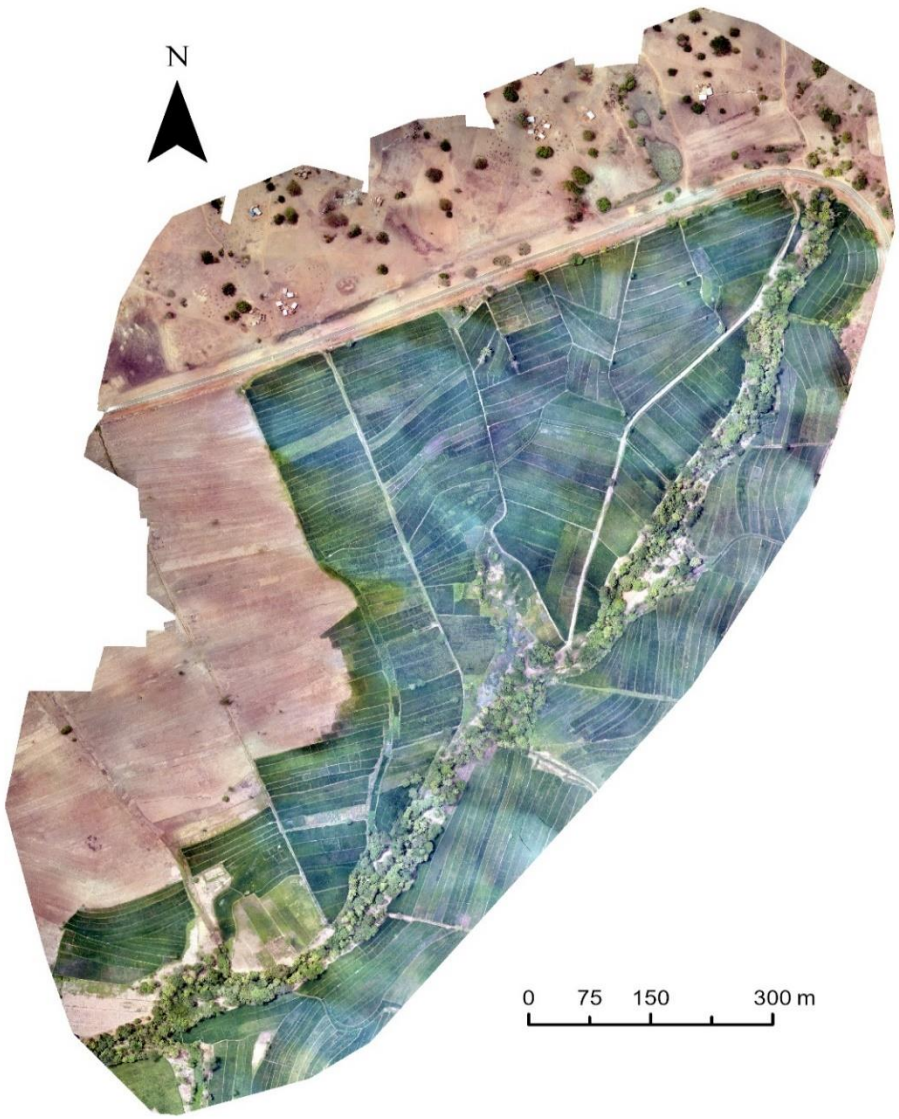

Figure 4. 1: Orthomosaic RGB images of zone H at heading stage of the rice crop.

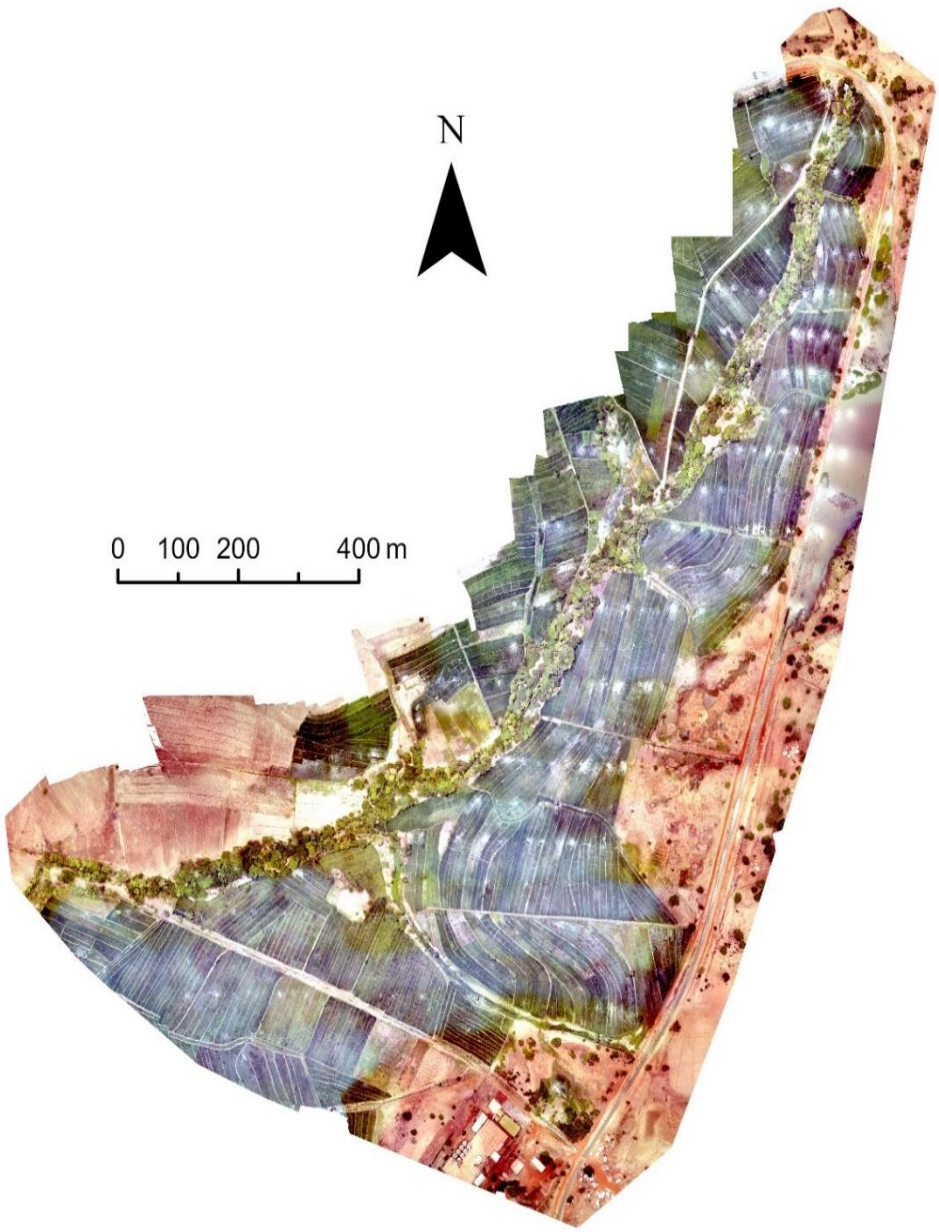

Figure 4. 2: Orthomosaic RGB images of zone I at heading stage of the rice crop.

Figure 4. 3: Orthomosaic RGB images of zone H at heading stage of the rice crop.

These orthomosaiced images represent the spatial natural color expression of the health of the rice crop at the stage at which images were captured. These images provide information on crop health

at the moment in time and provide a basis to compare and contrast crop health status of individual fields within each zone and between zones. Brown areas in the images show noncultivated or bare areas, while the green areas show the direct natural color expression of the health of the rice. Bunds which serve as boundaries between fields in most cases, are clearly discernible in the othomosaics. These bunds also show delineations in fields for water and nutrient management.

4.5 Vegetation Indices

Four vegetation indices, NDVI, NDRE, OSAVI and GNDVI, were generated from images captured on May 16, and May 18, 2018. Mean and ranges of these indices are presented in Table 4.5.

Table 4.5: Ranges of vegetation indices on the different dates of drone flight

Index	Mean	SD	SE Mean	Minimum	Maximum
			16-May		
NDVI	0.8787	0.0497	4.14E-03	0.654	0.941
NDRE	0.3271	0.052	4.33E-03	0.155	0.442
GNDVI	0.7494	0.0598	4.98E-03	0.551	0.846
OSAVI	0.6412	0.0656	5.47E-03	0.413	0.871
			18-May		
NDVI	0.8529	0.0777	6.47E-03	0.518	0.934
NDRE	0.3185	0.0689	5.74E-03	0.146	0.555
GNDVI	0.7225	0.0702	5.85E-03	0.426	0.818
OSAVI	0.6192	0.0796	6.63E-03	0.314	0.74
			May 22		
NDVI from Sentinel 2A data	0.4028	0.0300	2.498E-03	0.328	0.482

It is generally observed that images collected on May 16, 2018 produced higher vegetation index values and trailed off on May 18. It was therefore decided to use May 16 data as a basis for any comparative crop health assessment in this study.

To compare the efficacy of remote sensing platforms to characterize rice growth and performance, Sentinel 2A data of the same study area were obtained from the United States Geological Survey (USGS) Earth Explorer website at (https://earthexplorer.usgs.gov/). Due to the limitation with long revisit times of the satellite, imagery obtained on May 22, 2018 from sentinel 2A, 2018 was the closest date to the UAV flight of May 16. The false color infrared (bands 8, 4, and 3) is shown in Figure 4.4. Compared to the UAV imagery, the satellite image has a bigger footprint, and pixels completely included the boundaries of TIR, including the Tono reservoir.

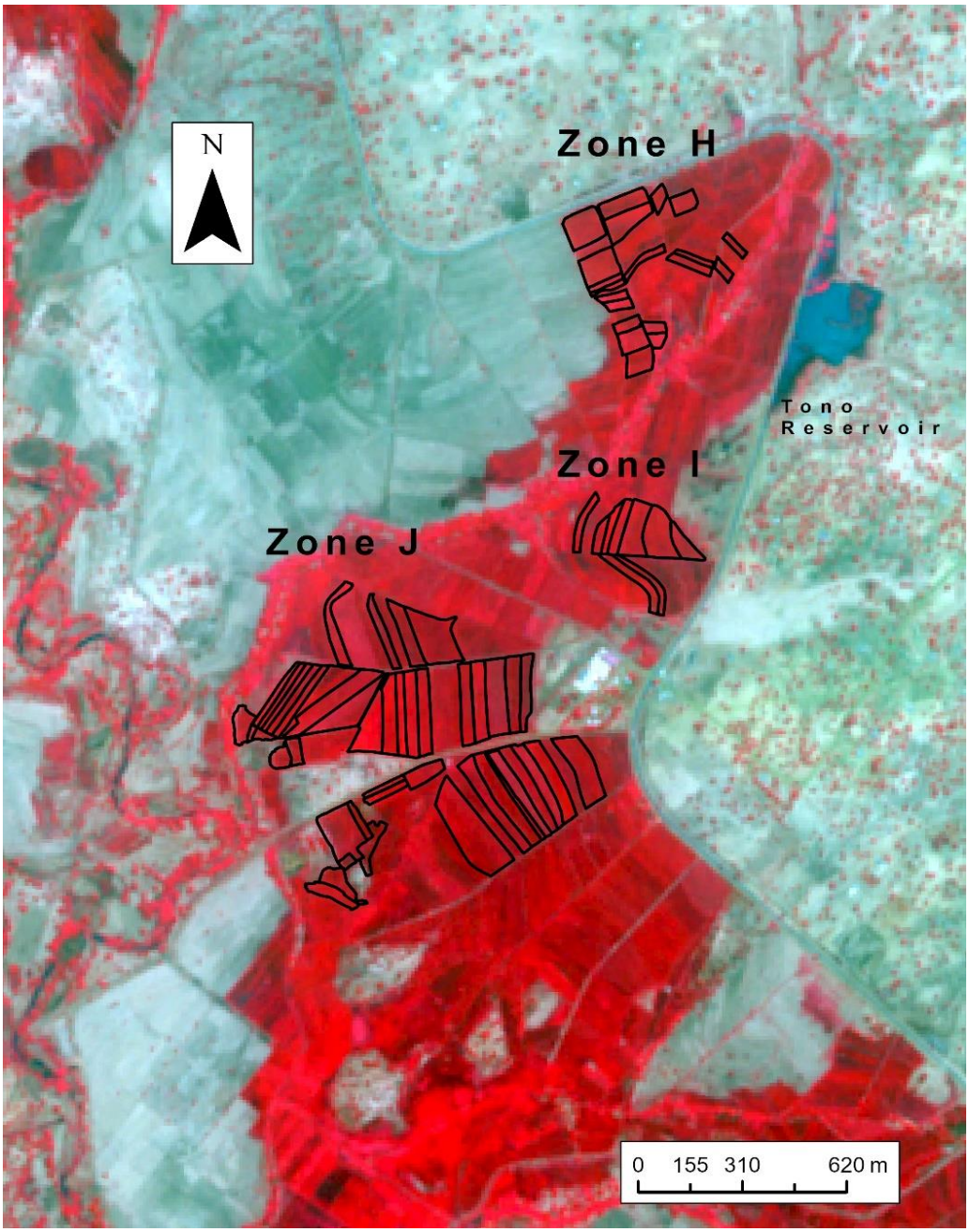

Figure 4.4: False color infrared (bands 8,4, and 3) of the full extent of Tono Irrigation Scheme captured by the Sentinel 2A satellite on May 22, 2018.

However, the resolution of the satellite imagery is far lower than that of the UAS as shown in Figure 4.4.

Using the same spatial band ratios, NDVI map was generated from the Sentinel 2A data as was done with the UAV-captured imagery (Table.4.5). Again, the low resolution of the satellite imagery resulted in NDVI values that are almost half of what was obtained from the UAS-generated imagery.

4.6 Comparative assessment of non-UDP vs. UDP using UAS technology

The goal of this section of the thesis is to use UAS technology to evaluate the impact of N management on rice grain yield. Specifically, this study compares the effect of UDP technology with any other N placement technologies used by farmers in the Tono Irrigation Scheme. The null hypothesis (H_0) is that there is no difference in rice grain yields when farmers use the UDP technology compared to any other form of N management. Alternatively, it is hypothesized that there are significant differences in rice grain yields under UDP and non-UDP N management systems (H_1). These hypotheses were tested using plot and spatial scale yield assessment methodologies.

4.6.1 Plot Scale Assessment

Rice grain yields were estimated from three 2m x 2m plots in each participating farmer field as stated earlier. These plots were generated from UAS imagery in low, medium, and high health areas. Ranges of NDVI values used in delineating the three health zones of the entire study are presented in Table 4.6. Figures 4.5 to 4.7 show the spatial distribution of relative grain yields on plots identified using crop health assessment in non-UDP and UDP fields in zones H, I, J, respectively. Rice grain yield data were tested for normality using the Shapiro-Wilk test with a threshold of 0.05. The W and P values of the test were 0.9934 and 0.7663, respectively.

Table 4.6: Ranges of NDVI used for assigning crop health categories

Health	n*	Mean	Minimum	Maximum
High	45	0.906	0.847	0.934
Medium	48	0.868	0.584	0.910
Low	45	0.586	0.586	0.881

*n – number of observations

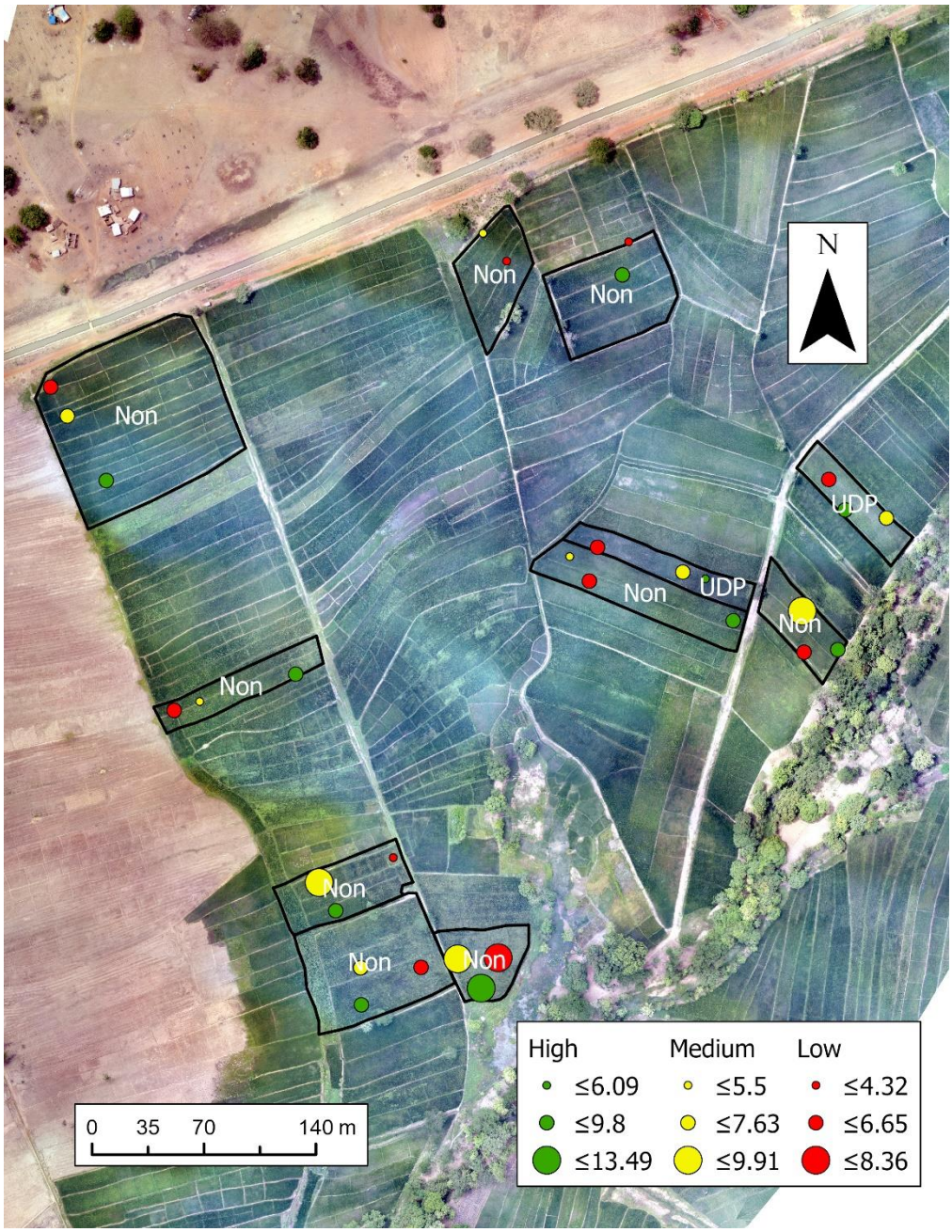

Figure 4.5: Spatial distribution of relative grain yields based on crop health classified plots in non-UDP and UDP in zone H. Green, yellow and red colors represent high, medium and low health areas, respectively

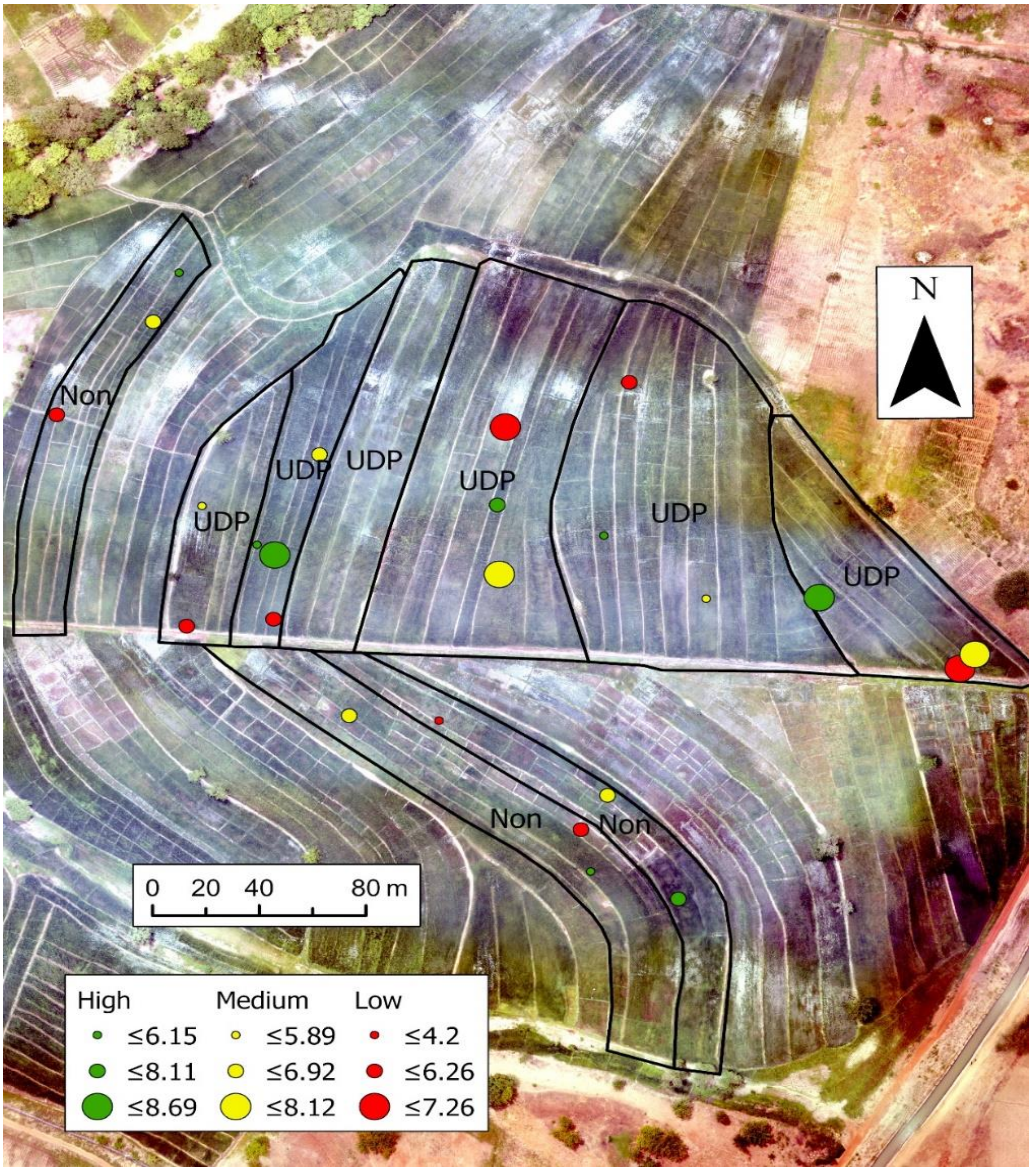

Figure 4.6: Spatial distribution of relative grain yields based on crop health classified plots in non-UDP and UDP in zone I. Green, yellow and red colors represent high, medium and low health areas, respectively

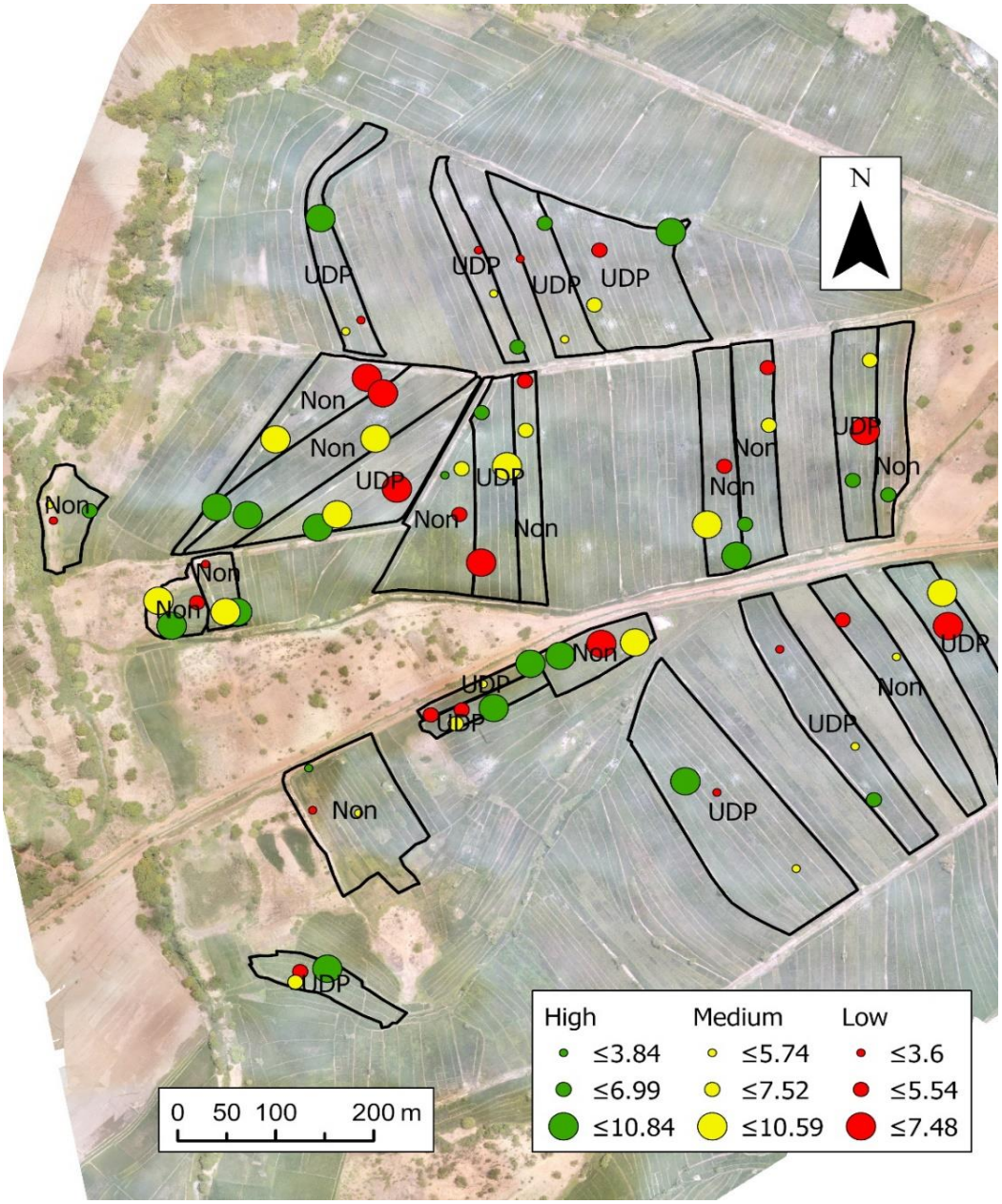

Figure 4.7: Spatial distribution of relative grain yields based on crop health classified plots in non-UDP and UDP in zone J. Green, yellow and red colors represent high, medium and low health areas, respectively

The p - value is significantly higher than the threshold of 0.05. This led to the rejection of the alternative hypothesis, H_1 and acceptance the null hypothesis, Ho, that our sample is normally distributed. Analysis of variance of the data showed significant effects of N management (P= 0.04) and midseason crop health on end of season rice grain yield. Zone and treatment x zone interaction did not influence grain yield with p values of 0.30 and 0.65, respectively.

Figure 4.8 shows the relationship between midseason crop health and end of season grain yields for the entire study area. Rice grain yield in the delineated high zone area was found to be higher, but not statistically different, from those in the medium zone. However, these two zones produced significantly higher rice grain yields compared to the low health area. The same relationships were obtained when data was analyzed as a function of non-UDP vs. UDP fields in the study area (Figure 4.9).

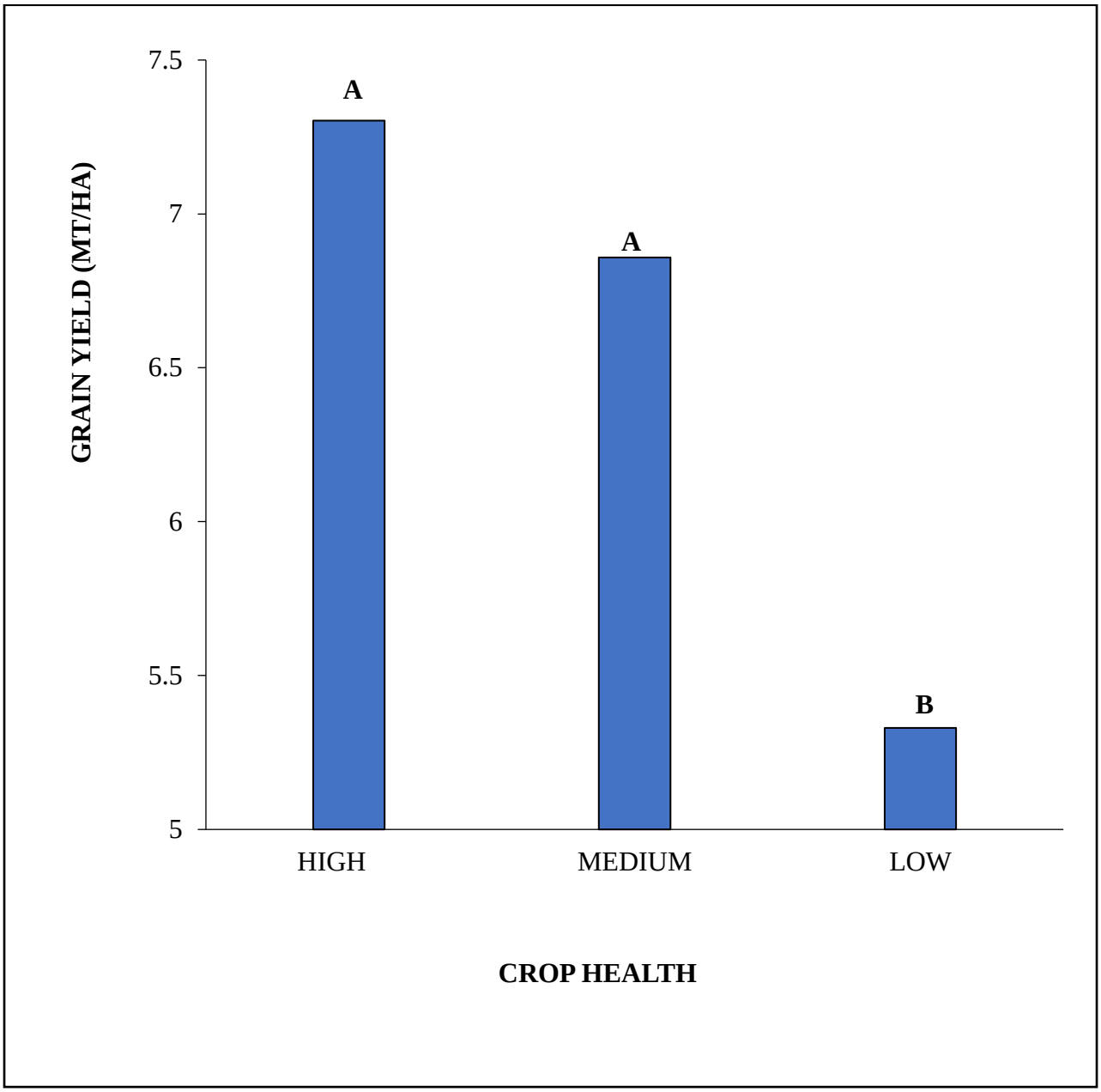

Figure 4.8: Average rice grain yield in high, medium and low zones in entire study area

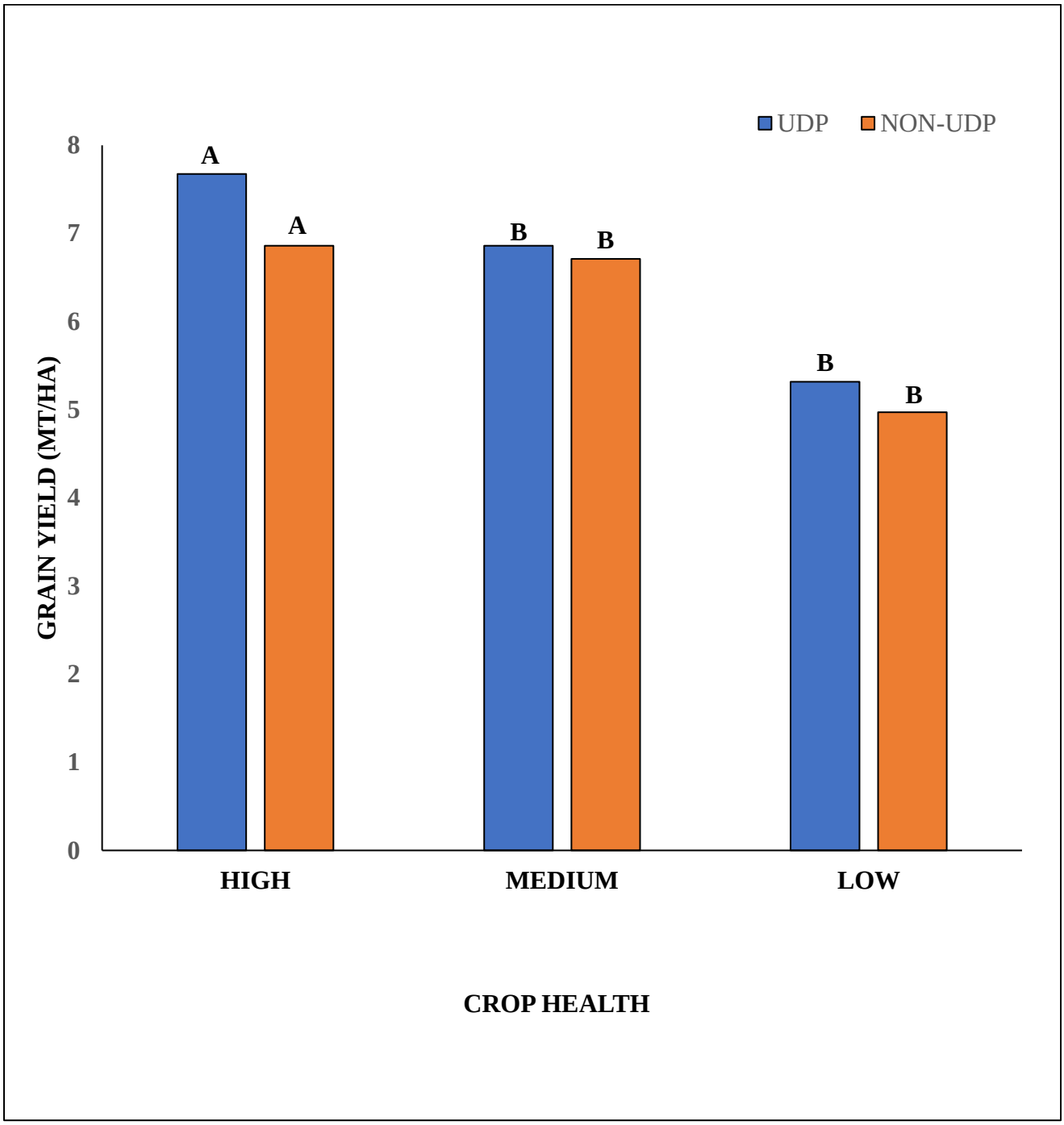

Figure 4.9: Average rice grain yield in high, medium and low zones as a function of N management technology

4.6.1.1 Grain yield in UDP and Non-UDP fields

In testing the null hypothesis of no difference in yields irrespective of N management system used by farmers, a comparative assessment of average grain yield under UDP and non-UDP was carried out. This began with the assessment of yield variability using the Box-Whisker plot in Figure 4.10.

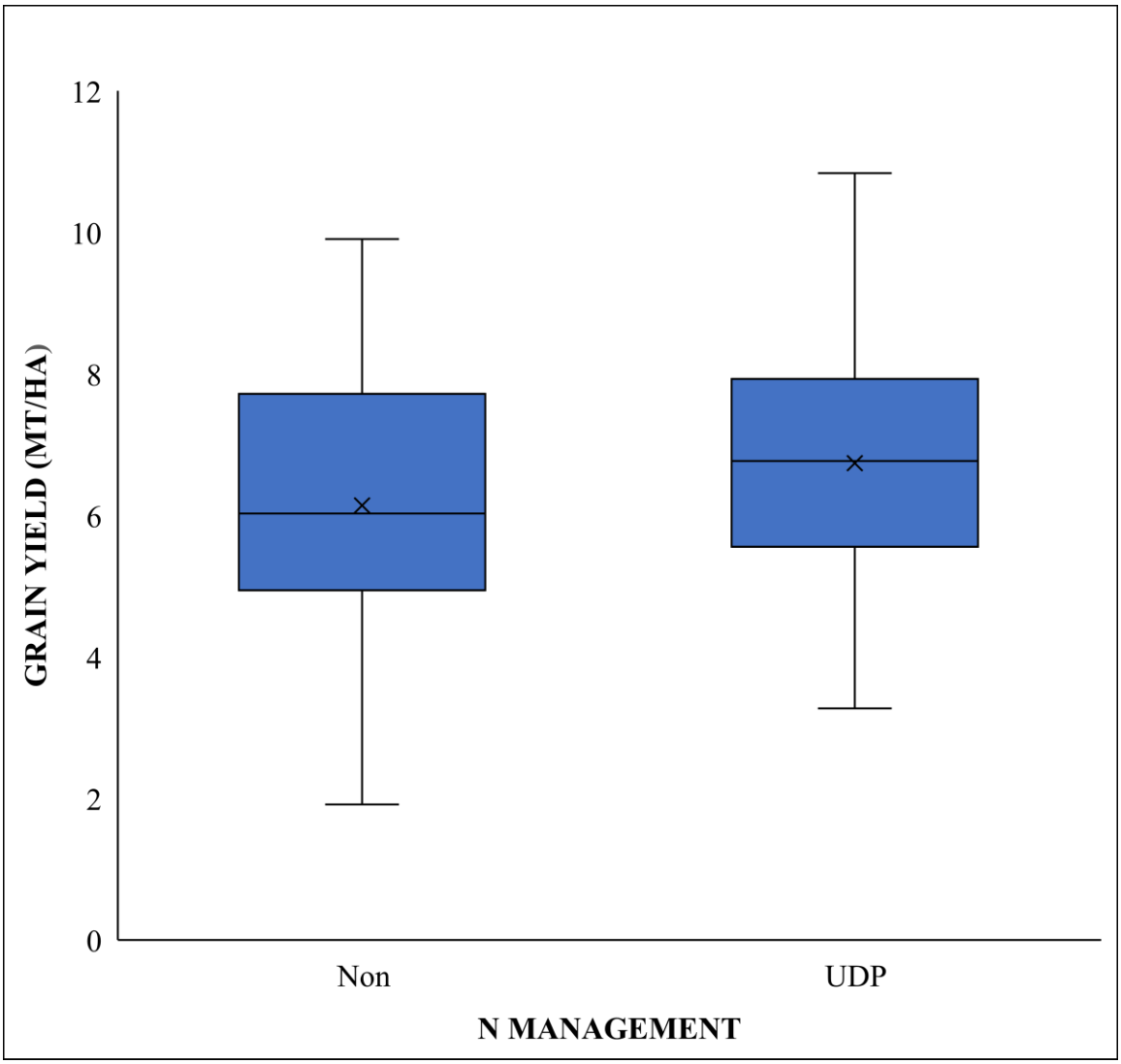

Figure 4.10: Box and whisker plot of average grain yield for the entire study site.

There was more variation in yield in non-UDP system compared to UDP. Rice grain yields varied from 1.92 – 9.91 MT/ha in non-UDP fields compared to 3.37 – 10.84 MT/ha in UDP. Median yields in non-UDP and UDP are 6.03 and 6.77 MT/ha, respectively. The middle 50% of the yield in non-UDP is between 4.98 and 7.84 MT/ha with a difference of 2.86 MT/ha. The UDP fields has a narrower middle 50% yield range of 2.36 MT/ha. This could partially account for the yield disparity between non-UDP and UDP. Average yield in UDP fields is 6.81 MT/ha compared to 6.19 MT/ha in non-UDP fields (Figure 4.11).

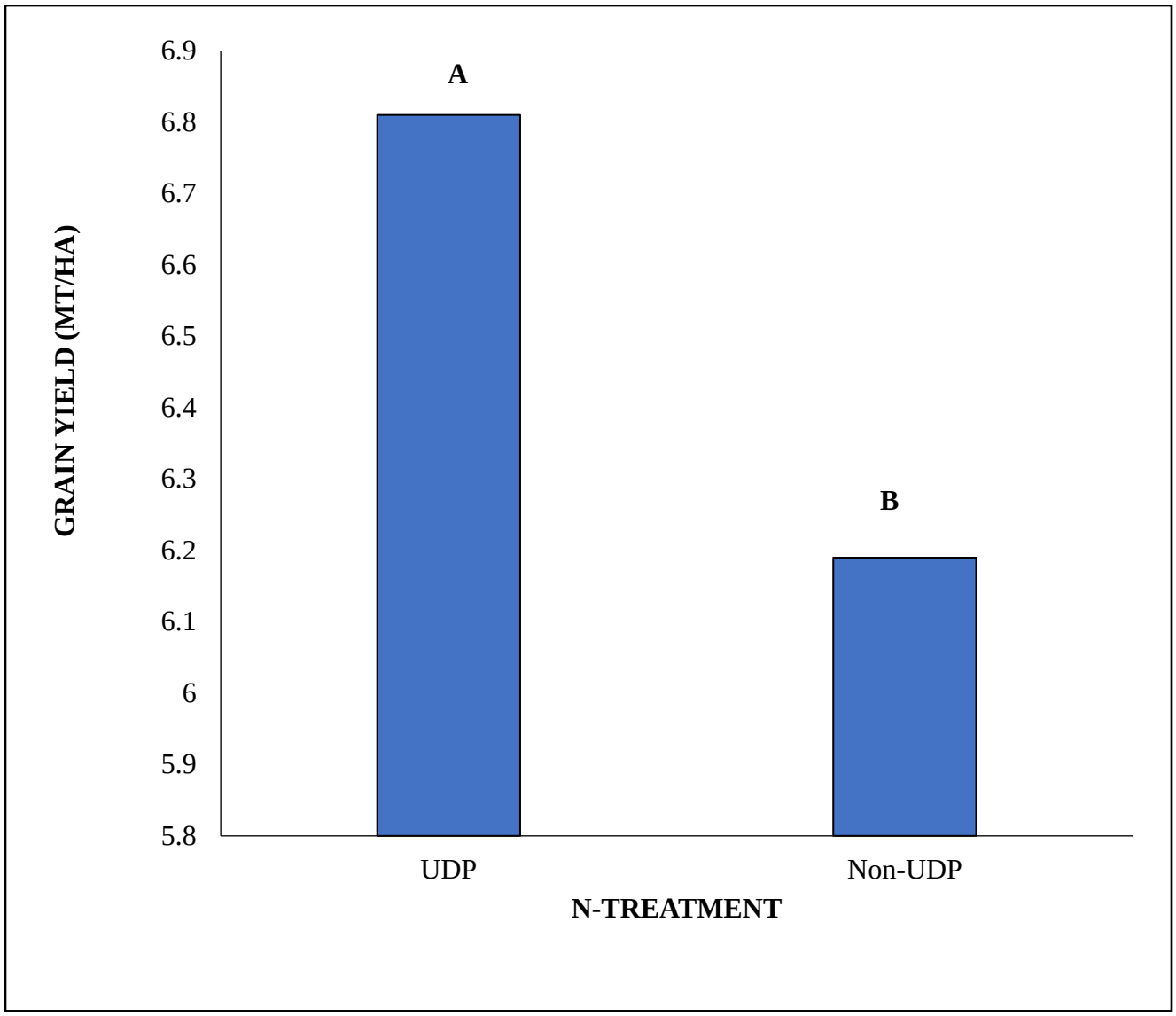

Figure 4.11: Grain yield in non-UDP and UDP fields

4.7 In-field midseason geospatial spectral variability and end of season grain yield

The purpose of this section is to use UAV data collected midseason to estimate end of season rice grain yields as a function of N management. This process began with identification of the best predictive spectral index by creating a correlation matrix of plot scale estimated grain yields and VI's. (Table 4.7).

Table 4.7: Correlation matrix of rice grain yield and vegetation indices

Vegetation Index	Grain Yield
NDVI	0.48
NDRE	0.46
GNDVI	0.50
OSAVI	0.50

All correlations are significant at $p<0.05$

Although GNDVI and OSAVI had the strongest correlation with grain yield, it was decided to use OSAVI as the optimal spectral index on a spatial scale. Developed by Rondeaux *et al*. (1996), OSAVI has a soil adjustment coefficient (0.16) which was introduced to minimize variations in soil background. This index does not also have the problem of saturation at high reflectance like NDVI. Field maps using OSAVI were generated for each zone at booting of rice crop (Figure 4.12,4.13 and 4.14).

Rice grain data collected from crop health (high, medium and low) were partitioned into two groups as a function of the two N management systems, UDP and non-UDP.

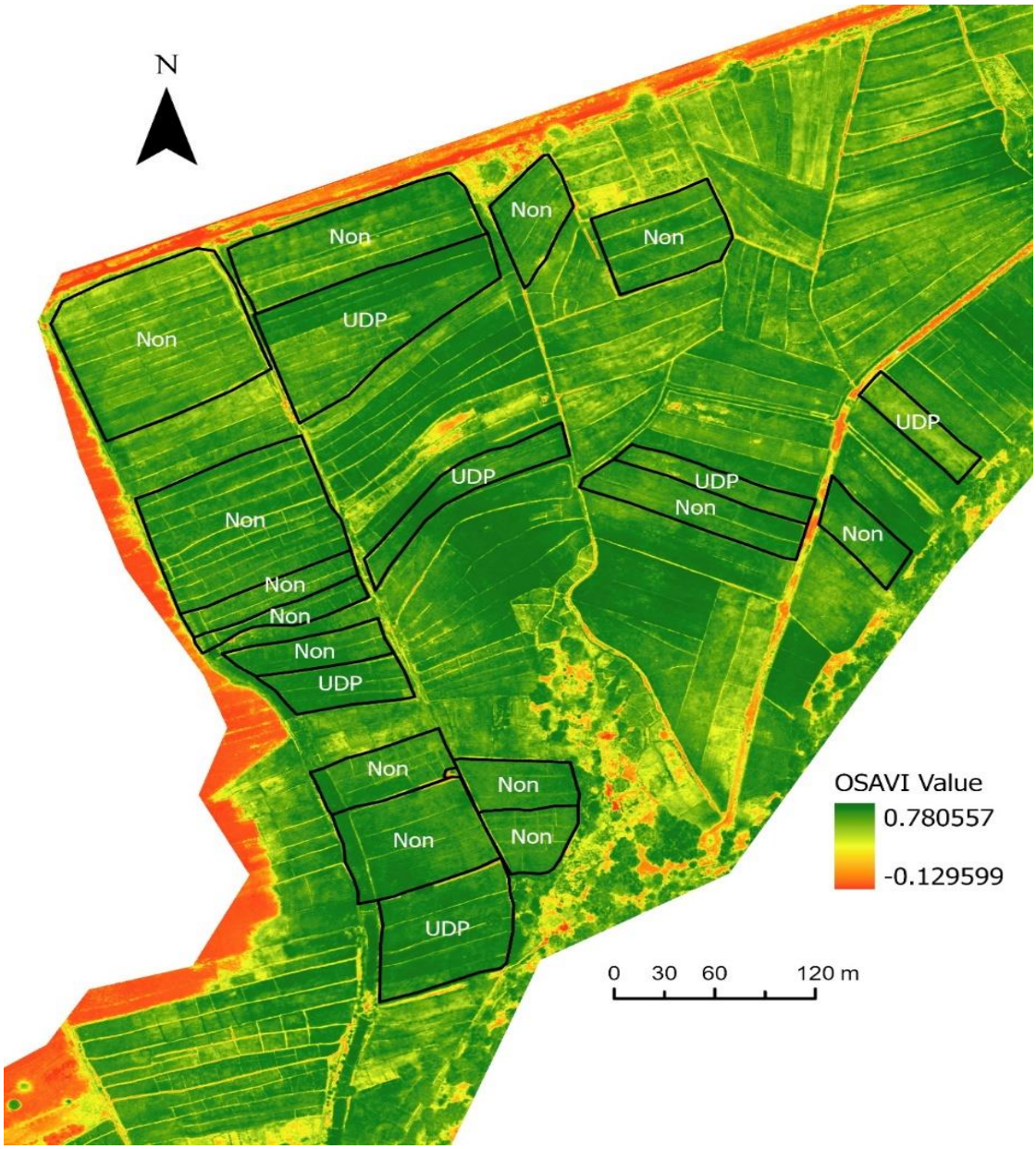

Figure 4.12: OSAVI map of zone H at booting of rice crop

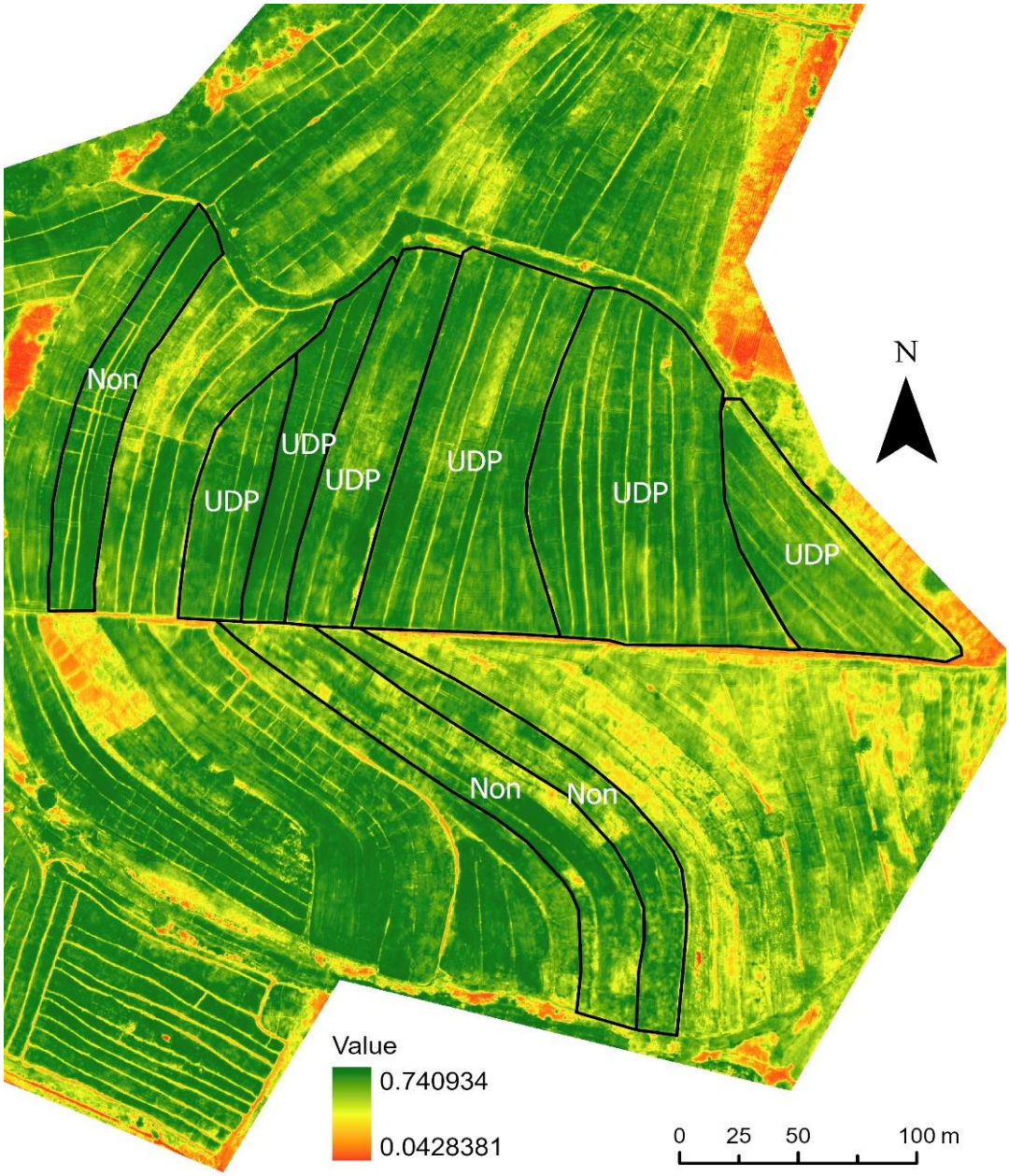

Figure 4.13: OSAVI map of zone I at booting of rice crop

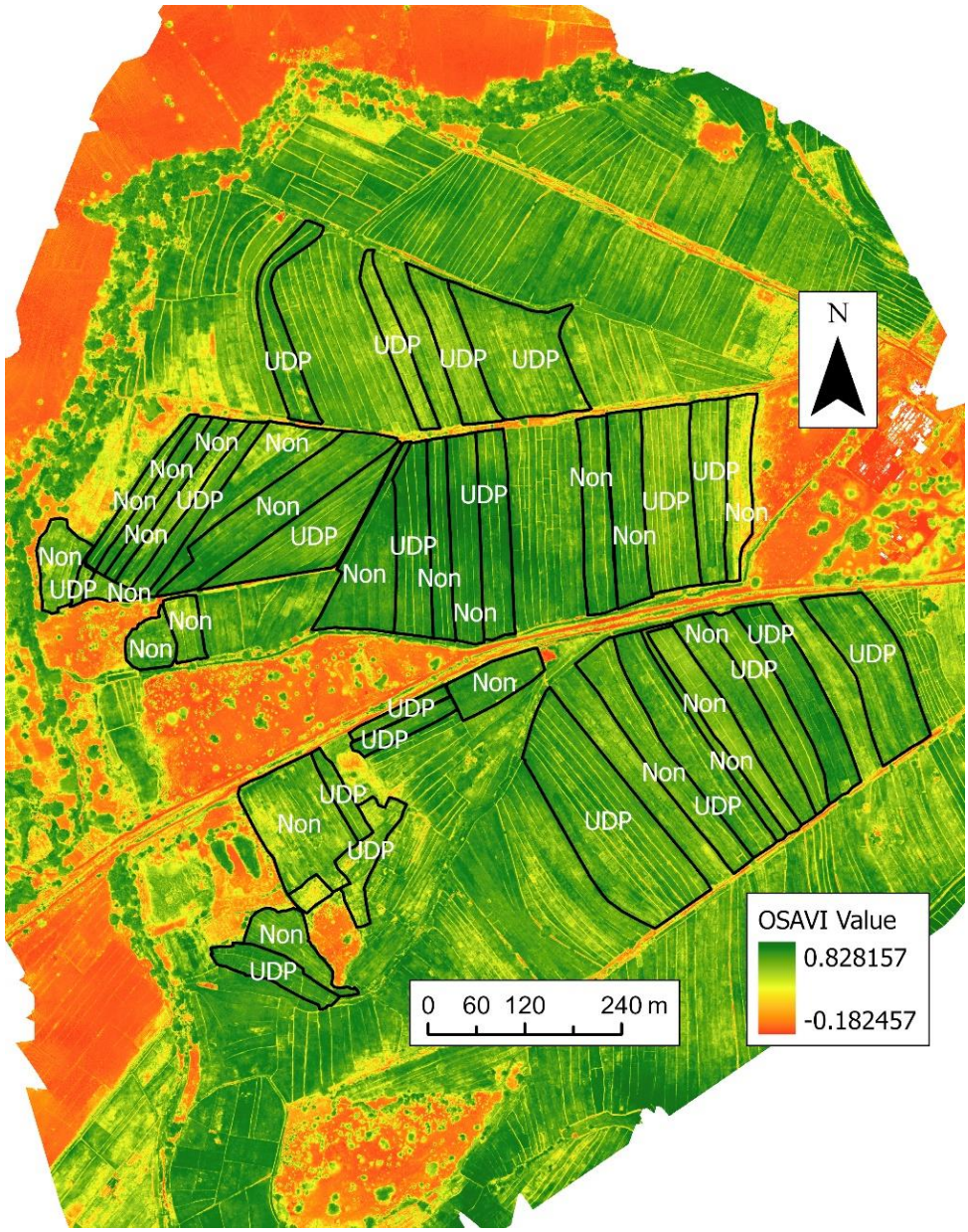

Figure 4.14: OSAVI map of zone J at booting of rice crop

In each of these groups, empirical relationships were established between OSAVI and rice grain yields through linear regressions as shown in Figures 4.15 and 4.16.

The OSAVI vs. rice grain yield prediction equation for the UDP group is:

Grain yield = 14.278*OSAVI with an R^2 value of 0.3633.

For the non-UDP group, the prediction equation is:

Grain yield = 14.004*OSAVI – 2.5994 and R^2 is 0.3254.

Accompanying the prediction curves are prediction intervals which express the uncertainty in the forecasts when using these prediction curves. A 95% prediction interval was used for both curves which indicates that one has a 95% chance that any new observation is actually contained within the lower and upper prediction bounds of 5 and 95%.

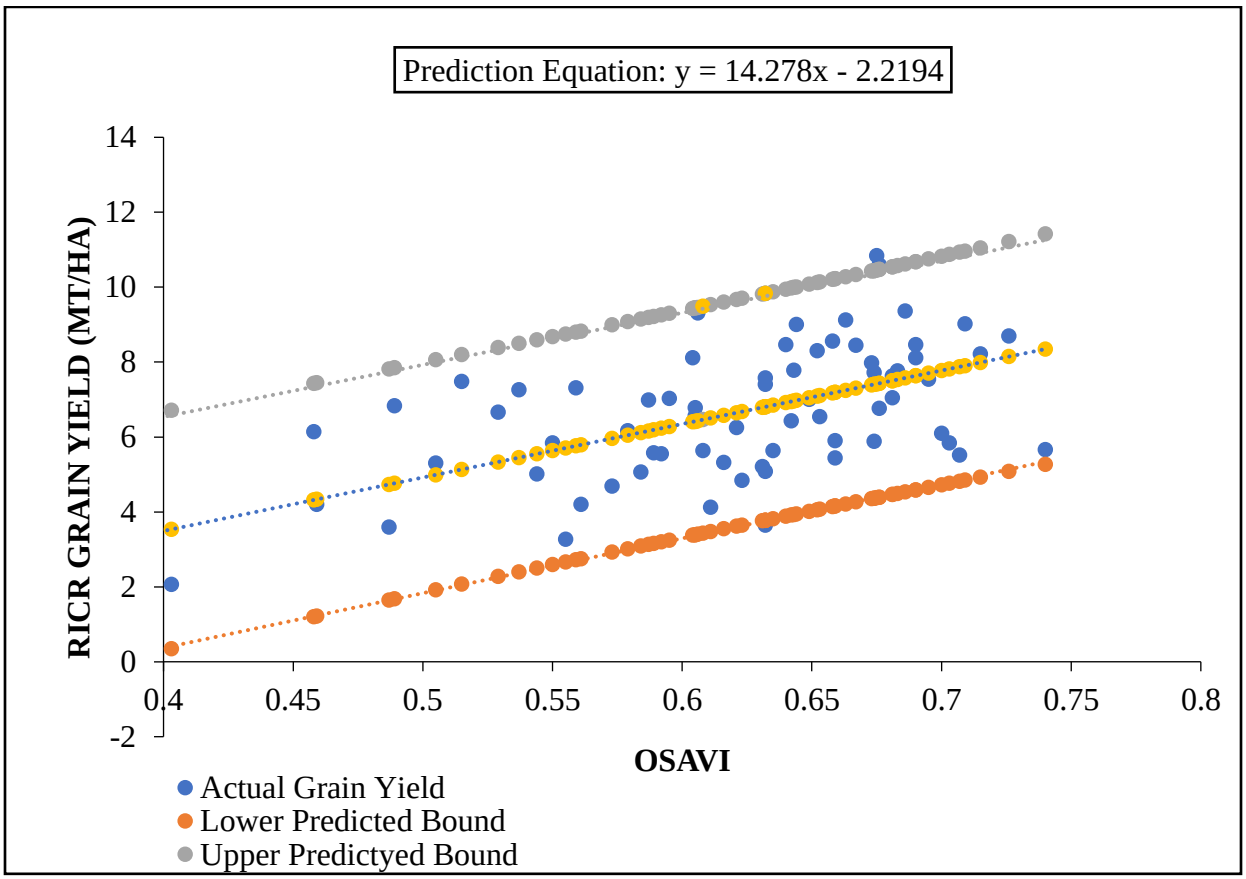

Figure 4.15: Rice grain yield as a function of OSAVI: UDP

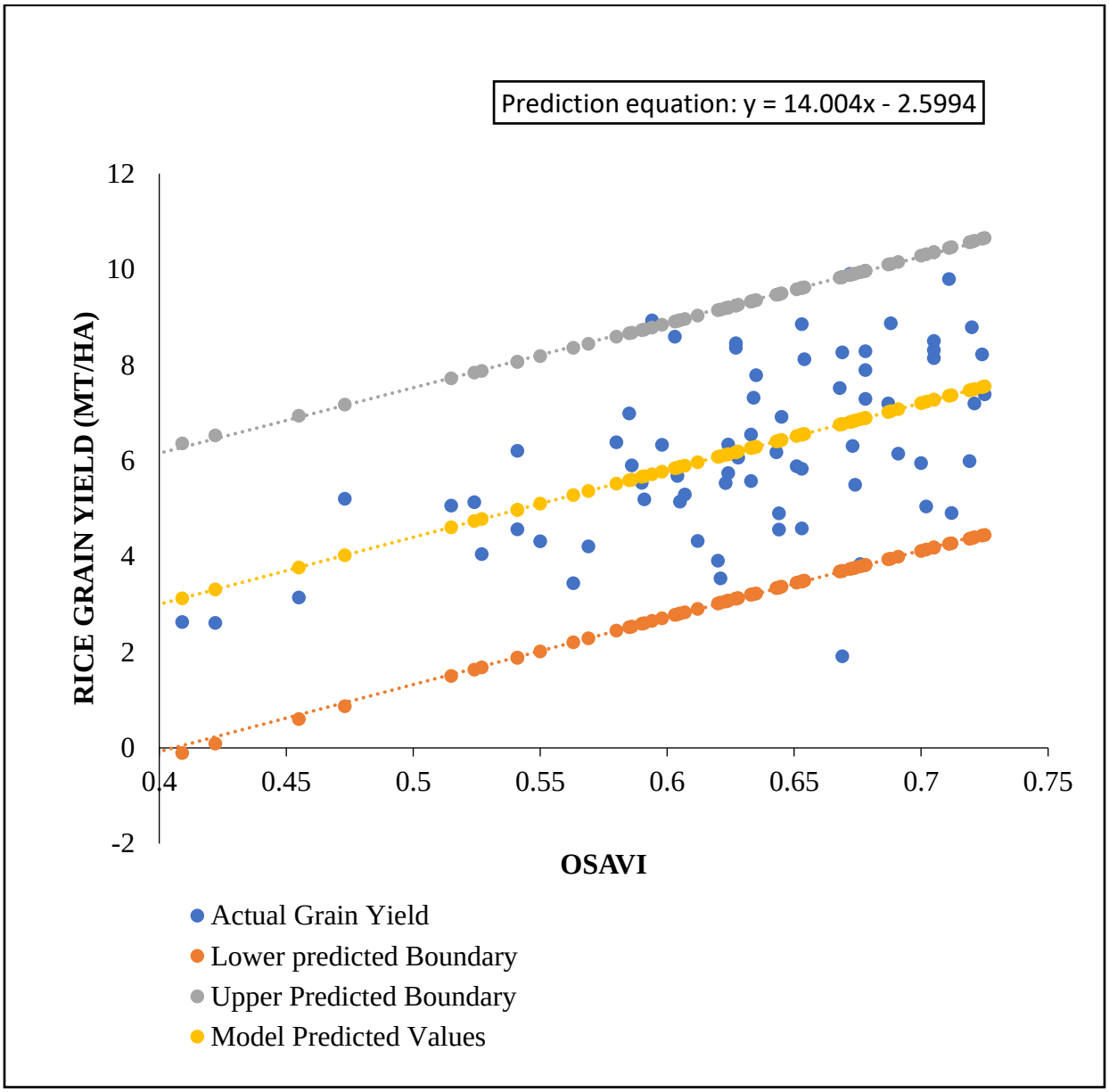

Figure 4.16: Rice grain yield as a function of OSAVI: Non-UDP

The predicted values have low "unusualness" for both non-UDP and UDP volunteers suggesting that the independent data points generated are close to the rest of the data.

4.8 Jenks Classification and estimation of whole field yields

4.8.1 Jenks classification of OSAVI imagery

The Jenks natural breaks algorithm was used as a standard method to divide the OSAVI developed imagery for each farmer's field into 4 homogenous classes using ArcGIS. Examples of Jenk's classified field are presented in Figures 4.17 (high yielding field) and 4.18 (low yielding field). The outputs of this classification include the minimum, maximum and mean OSAVI values for different classes. Examples of these parameters are presented in Tables 4.8 (high yielding field) and 4.9 (low yielding field). It also gives the area coverage of each group (in hectares) and the percent of the total area field occupied by the class.

Mean OSAVI values of each class were used to estimate grain yield in kg/ha from the OSAVI-grain yield plots for both the non- UDP and UDP groups. The predicted value was multiplied by the number of hectares in that particular group to estimate the number of kilograms of rice grain (Table 4.10). The sum of kilograms of rice grain in a field divided by the total number hectares gives the estimate per ha rice grain for the field. Crop yield maps were developed for each zone as a function of N management system generated from Jenks classified OSAVI (Figure 4.19, 4.20 and 4.21).

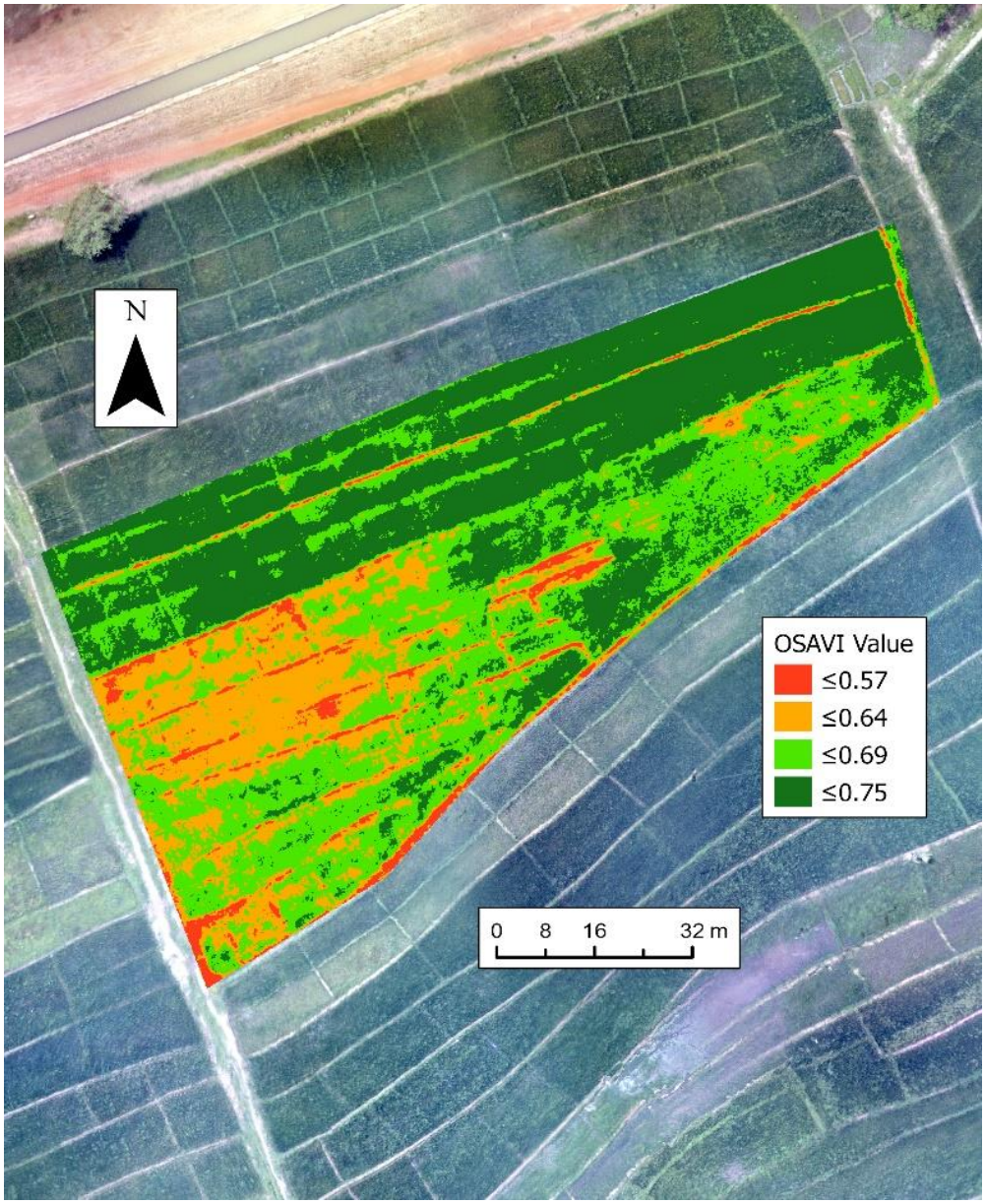

Figure 4.17: Jenks classified OSAVI image of field 2 of zone H (considered high yielding)

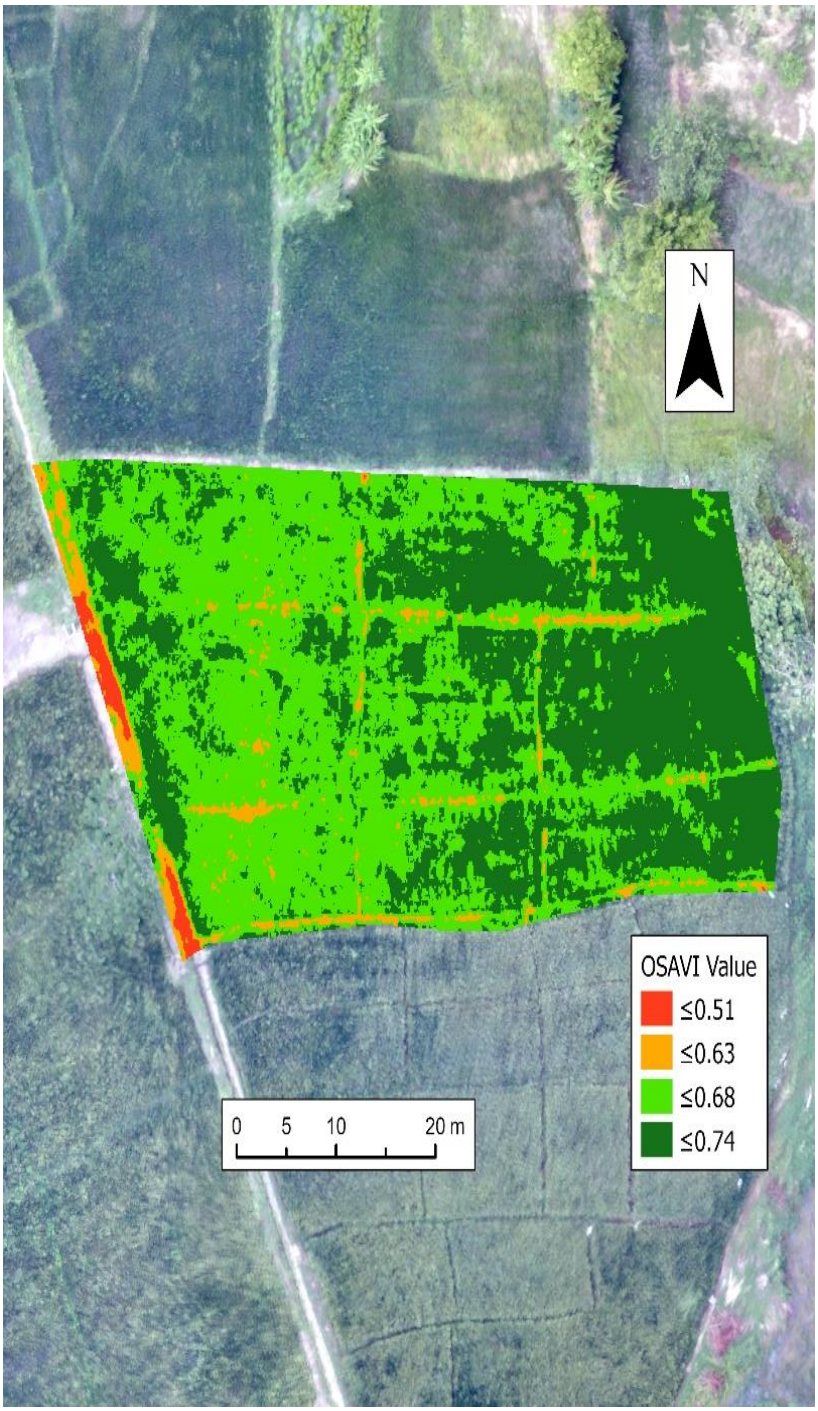

Figure 4.18: Jenks classified OSAVI image of field 18 of zone H (observed as low yielding)

Table 4.8: Parameters of classified OSAVI image of field 2 of zone H (considered high yielding)

Minimum	Maximum	Mean	Area (Ha)	Area (%)
0.63	0.71	0.75	0.42	45.61
0.57	0.63	0.69	0.37	40.54
0.52	0.57	0.64	0.09	9.44
0.46	0.52	0.57	0.04	4.42

Table 4.9: Parameters of classified OSAVI image of field 18 of zone H (considered low yielding)

Minimum	Maximum	Mean	Area (Ha)	Area (%)
0.63	0.71	0.67	0.05	22.5
0.58	0.63	0.605	0.13	65.13
0.53	0.58	0.555	0.02	10.34
0.46	0.53	0.495	0	2.02

Table 4.10: Jenks classification of non-UDP and UDP fields under the different management zones.

	non-UDP			UDP		
Zone	Field size (ha)	Total grain yield (kg)	Grain yield (kg/ha)	Field size (ha)	Total grain yield (kg)	Grain yield (kg/ha)
H	4.3	25.17	5.95	2.62	17.42	6.63
I	2.60	14.77	5.68	2.64	16.45	6.32
J	14.57	94.24	6.47	44.44	188.52	7.42

.

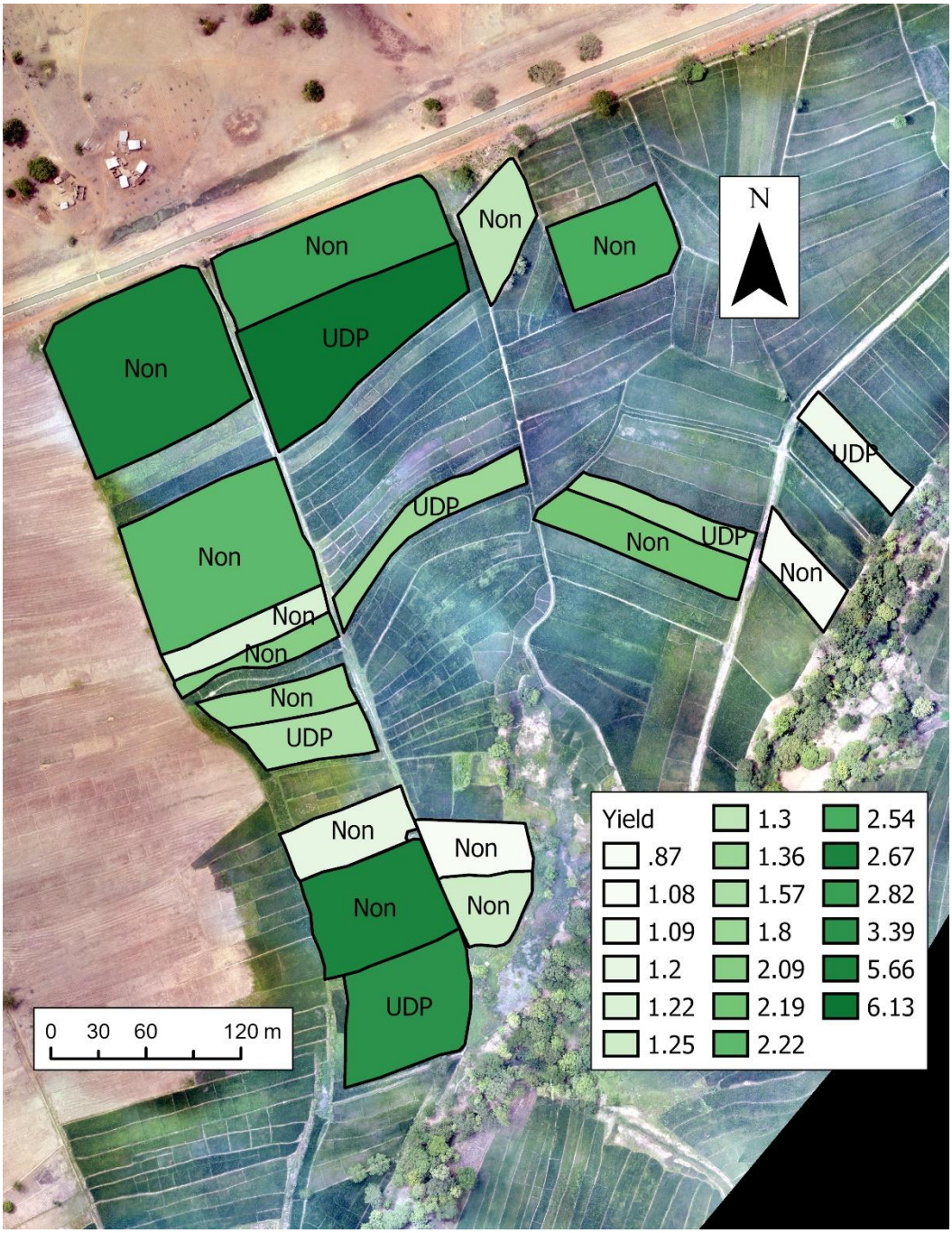

Figure 4.19: Total grain yields in producer fields of Zone H as a function of N management system generated from Jenk's classified OSAVI

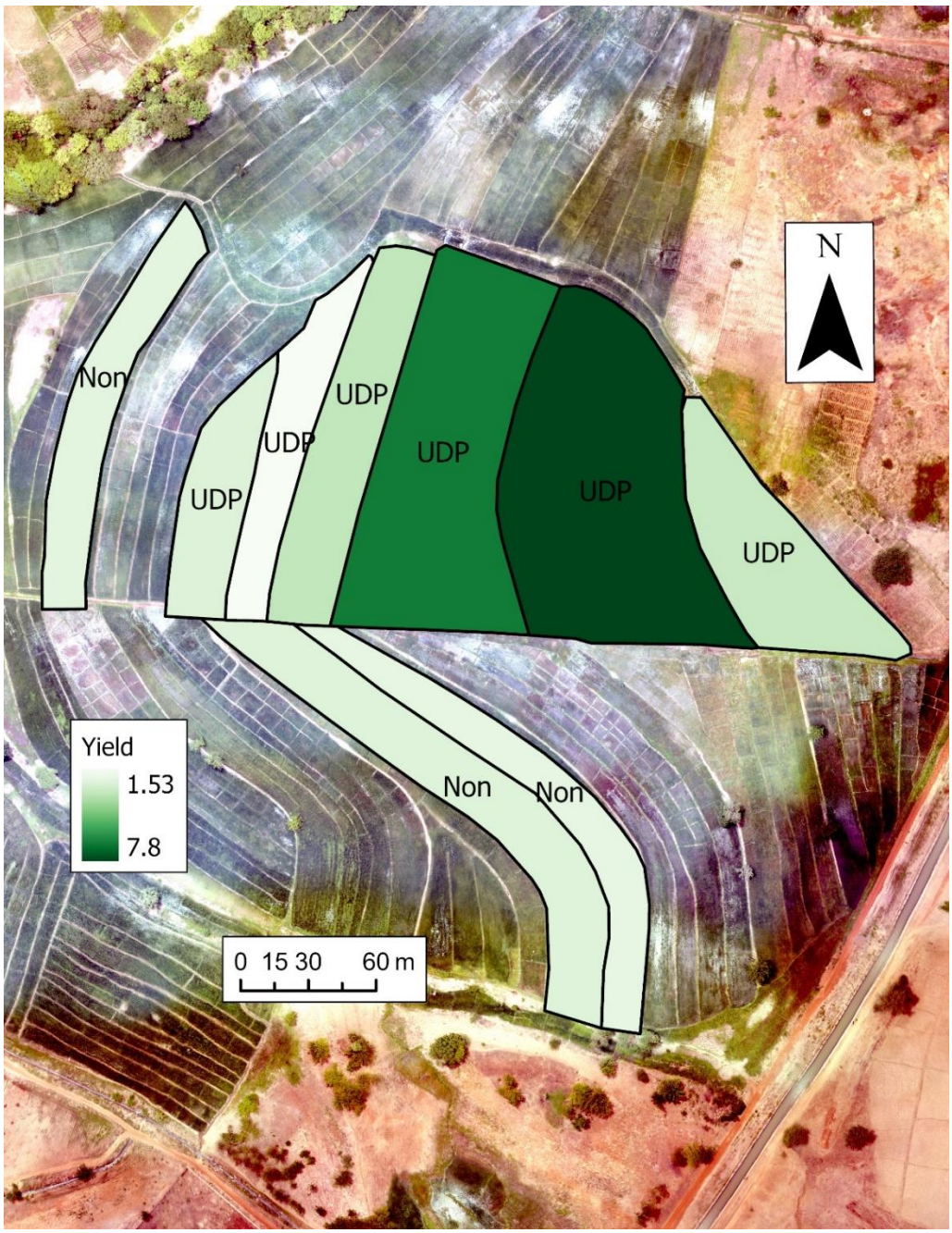

Figure 4.20: Total grain yields in producer fields of Zone I as a function of N management system generated from Jenk's classified OSAVI

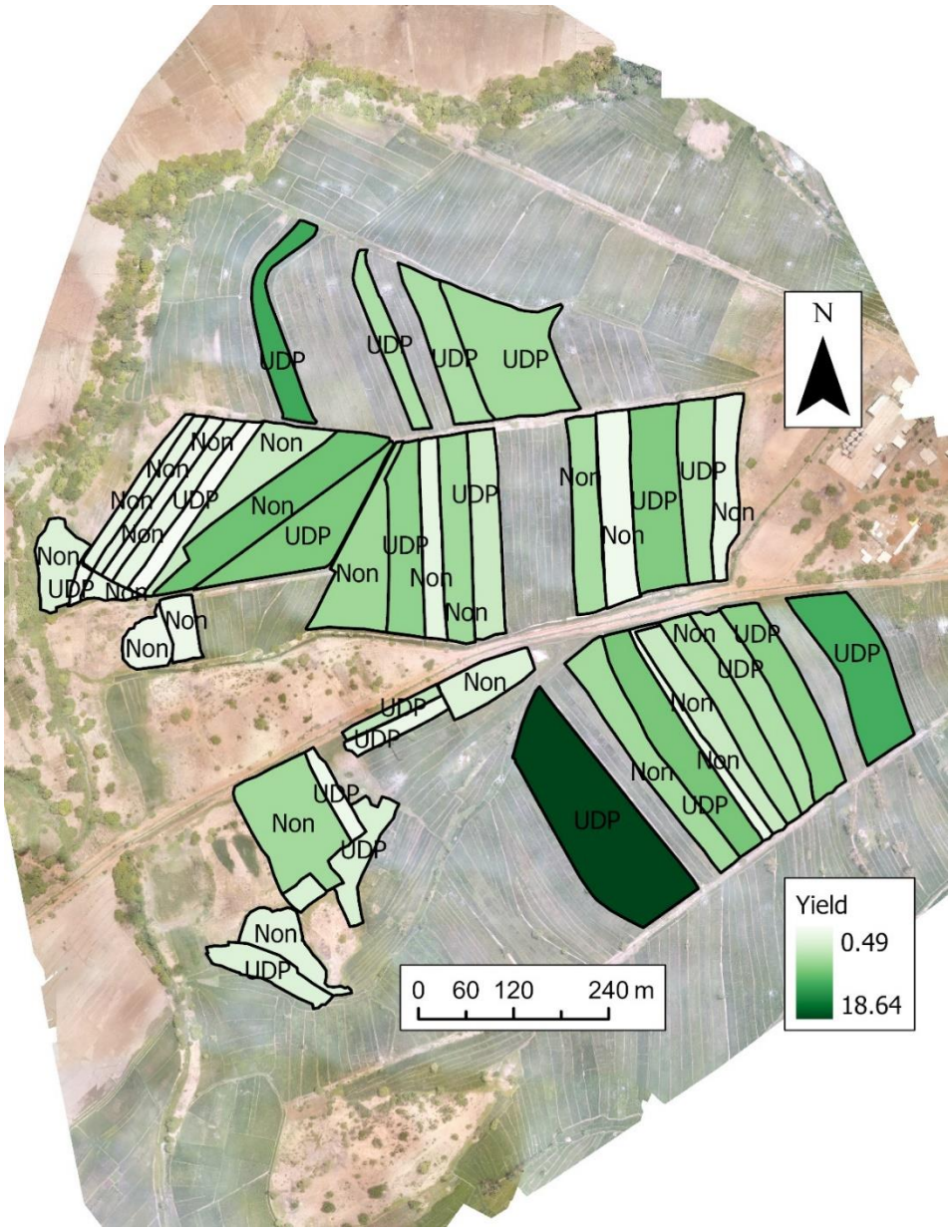

Figure 4.21: Total grain yields in producer fields of Zone j as a function of N management system generated from Jenk's classified OSAVI

4.9 Transplanting Dates

Figure 4.22 represents the dates on which farmers transplanted seedling from nurseries and the number of collaborating farmers for each day for non-UDP farmers whiles Figure 4.23 represents those for UDP farmers. Majority of non-UDP farmers transplanted as early as February 18, 2018 with just three (3) farmers transplanting on March 27, 2018. Few of the UDP farmers started transplanting as early as February 16th with majority transplanting on the 4th of March. Transplanting ended on March 22nd on UDP farms, five days earlier than their non-UDP counterparts.

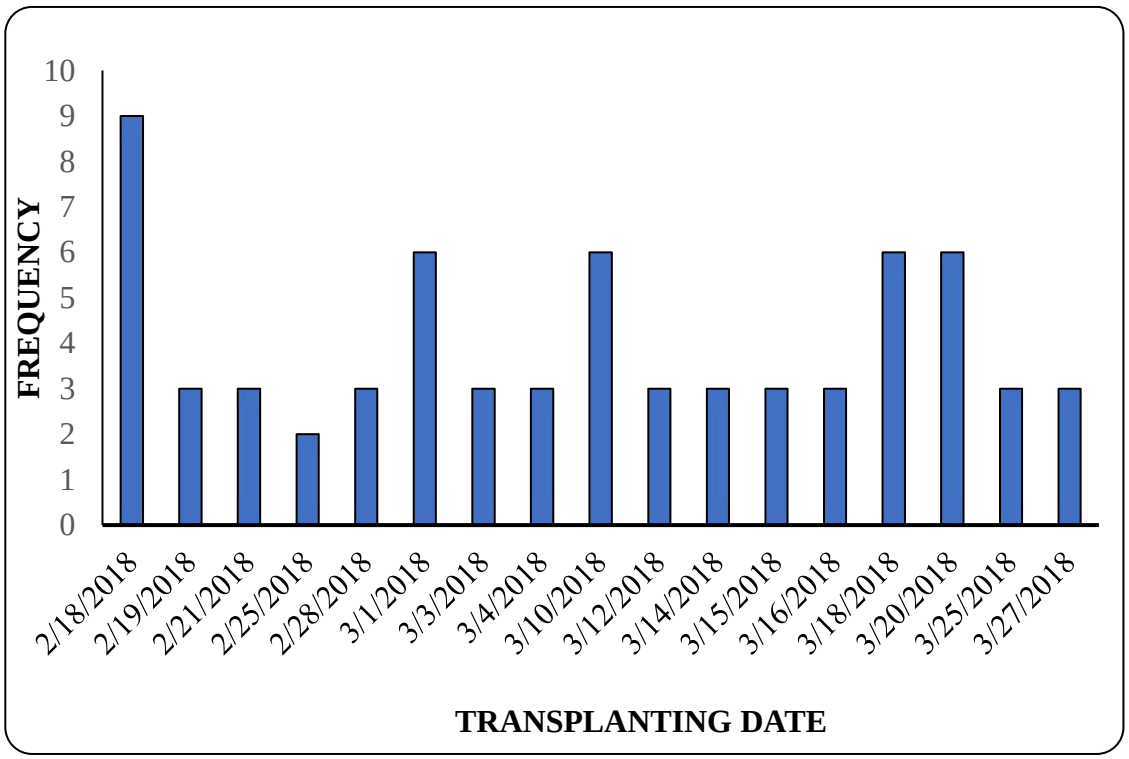

Figure 4.22: Date and number of non-UDP farmers who transplanted on those dates

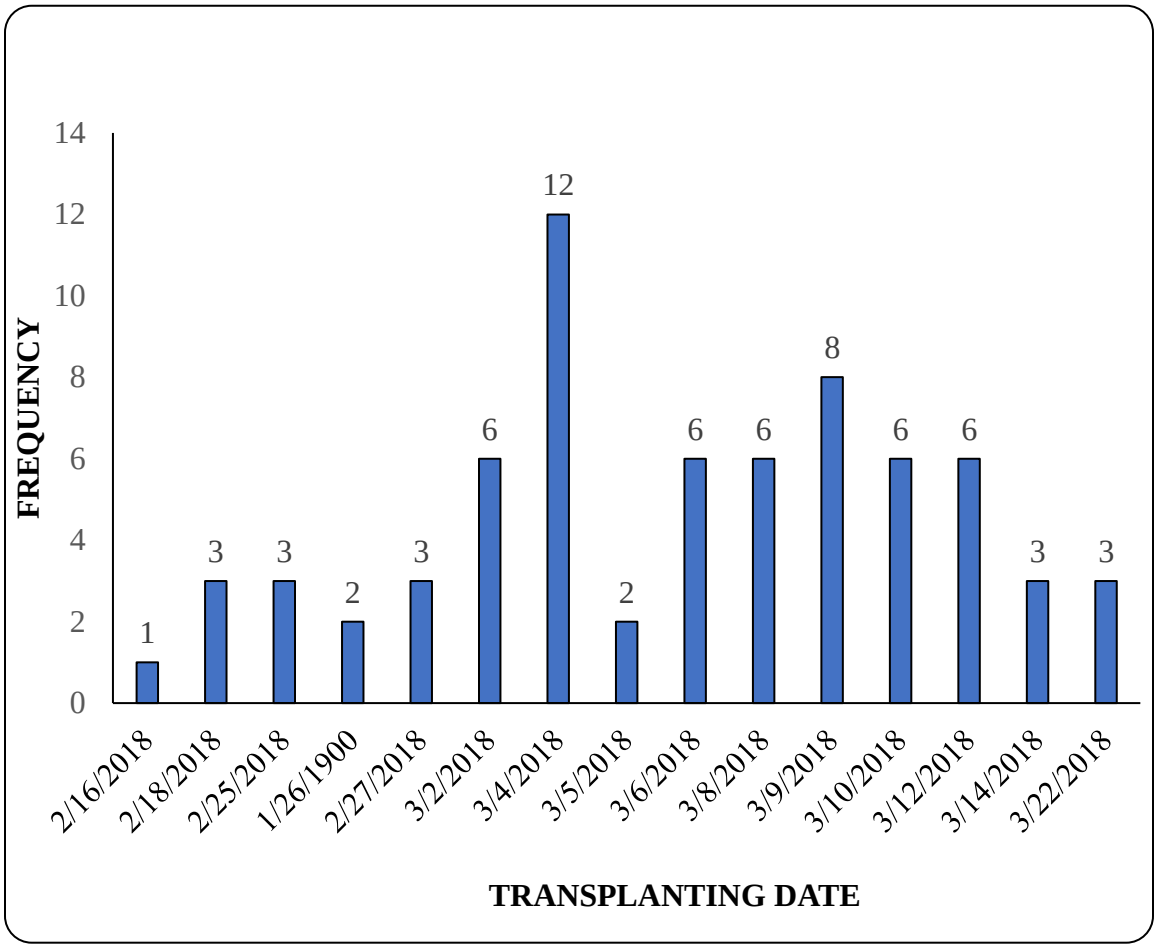

Figure 4.23 Date and number of non-UDP farmers who transplanted on those dates

4.10 Test for normality

Data generated from the spatial yield evaluation were tested for normality by applying the Shapiro-Wilk test to the residuals of the linear regression analysis. The normal probability plot as well as the W statistic of 0.9776 suggest that the data are normally distributed.

Results of subsequent analysis of variance of estimated rice grain yield suggest that N management and zone, both with P<0.0001, significantly impact rice grain yield. With respect to zone, the highest yield of 6.7 MT/ha was obtained in zone J which was significantly higher than the 6.33 and 6.02 MT/ha in zones H and I respectively (Figure 4.24).

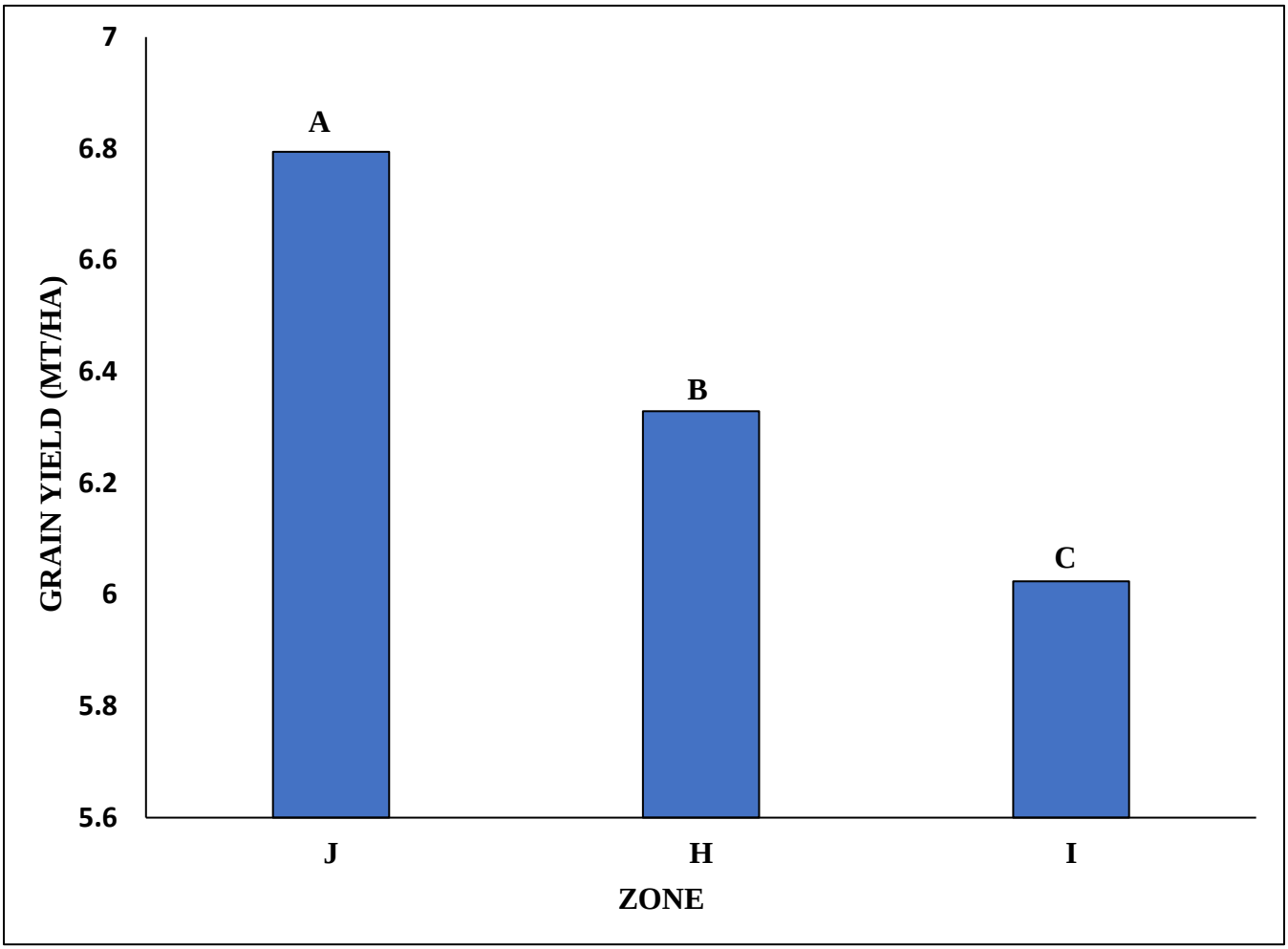

Fig 4.24: Grain yield in the different zones

The box and whisker plot of grain yields as a function of N management technology is presented in Figure 4.25. In the non-UDP fields, rice grain yield varied from 5.30 to 7.56 MT/ha with a mean of 6.20 MT/ha. In the UDP fields, grain yield varied from 4.85 – 8.00 MT/ha and the mean yield was 6.89 MT/ha. Median yields for the two management systems were 6.08 and 6.92 MT for non-UDP and UDP fields, respectively. The UDP field yields had a higher variance of 0.46 compared to 0.37 for non-UDP. The middle 50% of the yield in non-UDP management system ranged from 5.50 – 7.51 MT/ha and it ranges from 5.63 -8.00 MT/ha for UDP. Overall, the UDP fields out yielded the non UDP fields by 0.64 MT/ha and this difference is statistically significant (Figure 4.26).

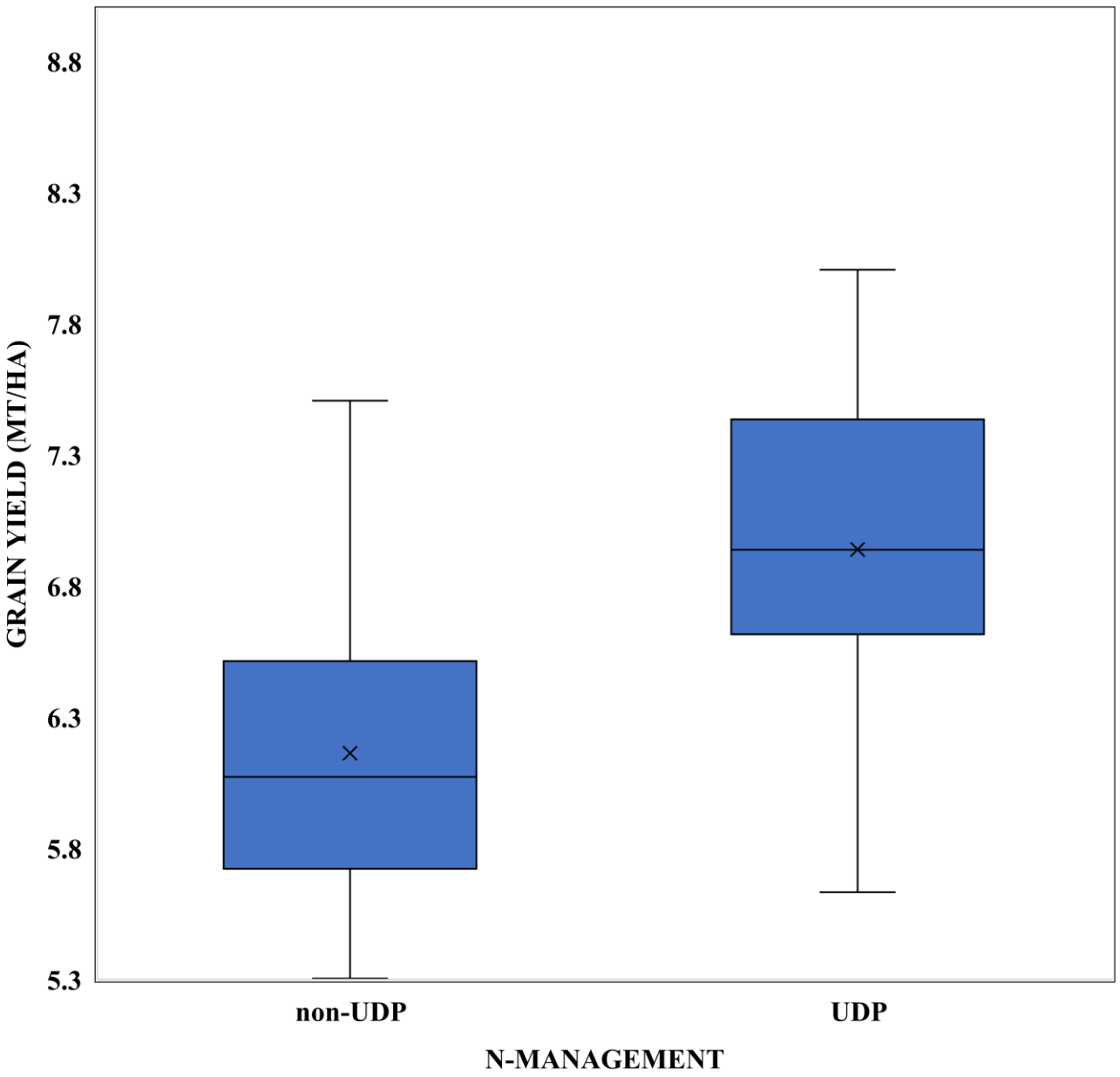

Figure 4.25: Box whisker plot of rice grain yields in study zone

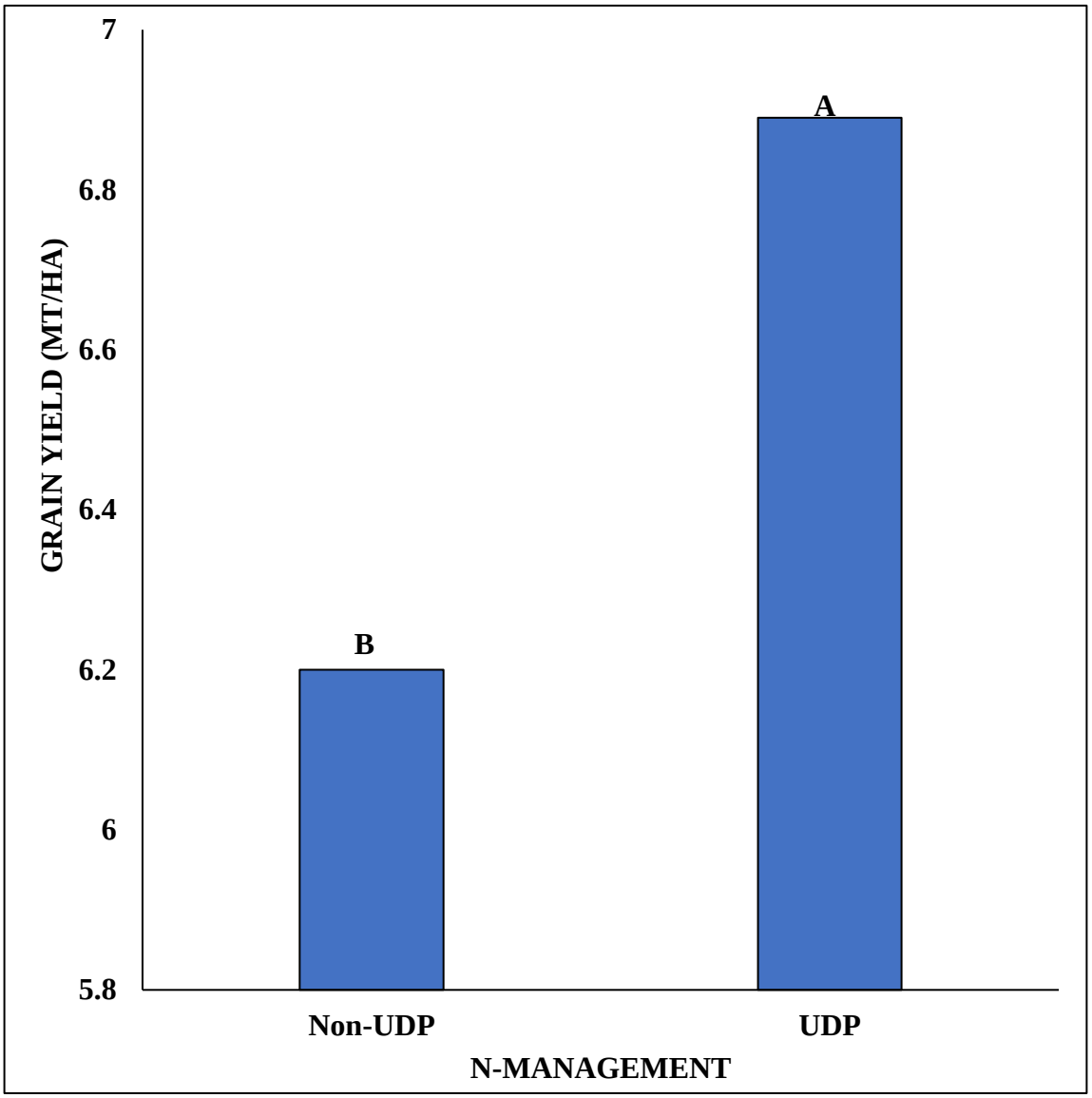

Figure 4.26: Rice grain yield estimated on a spatial basis as a function N-management

4.11 Plot Scale vs. Spatial Scale Assessment

A comparative assessment of results of two approaches of yield assessment is presented in Table 4.11.

Table 4.11: Descriptive statistics of results from plot and spatial based assessments of rice grain yield

Statistic	Plot Scale		Spatial Scale	
	Non-UDP	UDP	Non-UDP	UDP
N	72	68	40	42
			MT/ha	
Mean	6.19	6. 81	6.20	6.89**
Range	1.92 – 9.07	3.27 – 10.84	5.3.0- 7.75	4.85 – 8.00
Median	6.03	6.77	6.08	6.92
Middle 50% Yield	2.86	2.37	0.79	0.82
Variance	3.30	2.72	0.37	0.46

** Significant differences in yields between non-UDP and UDP

Essentially there are no significant differences in a lot of the yield descriptive statistics when using one approach or the other. However, the table clearly shows a clear difference in the two approaches in the variance of yields estimated. Using the spatially-based approach clearly decreases variance in estimated yields. This could be a good reason to adopt the spatial

assessment of yields when operating on wide territorial or regional scales. In the plot scale yield estimation was limited to 4m^2 areas and results can be influenced by conditions of the close environment. On the other hand, areas of yield estimation in this study varied from 0.07 – 2.7 ha. This helps spread any errors over wider areas, thus reducing the variability in results.

CHAPTER FIVE

5.0 DISCUSSION

5.1 Physicochemical properties of the soil

Physical properties

In terms of Zones, H recorded the highest clay content whiles zone I had the highest sand content. There are larger pore spaces between sand particles which leads to high drainage and less holding capacity for both water and nutrients. The low yields in zone I could be attributed to its high sand content. Dou *et al*. (2016), reported higher rice yields in clay soils as compared to sandy soils. He attributed the lower rice yield to the larger pore spaces and low water retaining capacity of sandy soils.

Chemical properties

The lowest pH of 5.4 was recorded in zone H and can be termed as strongly acidic whiles the pH of zone I and J were moderately acidic. However, yields were low in zone H compared to zone J. Rice is reported to tolerate a pH range of 4 to 8, and pH changes within this range does not appear to influence yield (Fan *et al*., 2016). Zone H recorded the highest value of organic matter but not the highest yield. Although high CEC (Lal, 2014) and OM could indicate good soils with corresponding high yields, lower yields were recorded in zone H as compared to zone J. In general, increases in OM are seen by many farmers as beneficial, because higher rates are seen as directly linked to better plant nutrition, improved water retention capacity, enhanced porosity etc. (Carter and Stewart, 1996; Lal, 2002). Janzen *et al*. (1992), found out that the relationship between soil quality indicators (e.g. organic soil carbon (SOC)) and soil functions does not always lead to an increasingly linear simple relationship with the magnitude of the indicator and that therefore higher values of these soil quality indicators does not necessarily mean higher yields. Baldock and

Skjemstad (1999) and Skjemstad (2002) have noted that total SOC might not be a reasonable predictor of how well a specific soil feature is likely to perform; primarily because the different pools that make up the bulk SOC differ greatly in their physical and chemical properties. Although zone I had the highest sand content its total nitrogen was higher than that of zone H. This shows that low values of N cannot always be attributed to high sand content as reported by (Ge *et al*., 2013). Bray P was the only soil chemical property that had a significant influence on rice yield. Available P is the most limiting nutrient in the lowland soils of Ghana, but under hydromorphic conditions P utilization and availability is enhanced (Buri *et al*., 2012). Similarly, Cao *et al*. (2004), reported an increase in available P in paddy rice fields.

Although not statistically significant, Non-UDP fields had higher values for all chemical properties of the soil but had the lowest yield. This could be that, the broadcast of fertilizer (Non-UDP practice) does not allow the crop to make good use of N, as some are readily dissolved and leached beyond plant roots whiles others are lost through volatilization (Urea fertilizer) unlike the UDP technology in which nutrients takes time to dissolve (Poggi-Varaldo and Estrada-Vazquez, 1997). In terms of crop health zones, there was a general decline in most chemical properties (OM, pH, CEC, K, Mg and Ca) as crop health declined, and this is reflected in grain yield. This observed relationship reflects the importance of soil nutrients to crop health.

5.2 Best date image selection for the study

Vegetative indices peaked on May 16th (mid-season) indicating crops attained maximum greenery on this date. The indices obtained on this date also correlated with yield and showed the potential of mid-season VIs to predict yield with reasonable precision. The importance of mid-season vegetative index in predicting grain yield has been underscored by other studies. Panda *et al*.

(2010), stated that mid cropping season of corn best correlated with grain yield. Similarly, Ali *et al*. (2019), also stated that, the peak greenness stage has the best correlation coefficient for yield prediction models. Similarly, studies which used mid-season crop information for N management, (Cammarano *et al*., 2014), water management, weed and other problems (Mckinnon, 2016), was also used to predict end of season grain yield.

5.3 Comparative assessment of crop health zones under plot scale assessment

There was significant difference between high and low crop health status which reflected in the average yield at the end of the study in both UDP and Non-UDP fields. This means that mid-season crop health status can be used to predict end of season crop yield. Yields in medium and high health areas were not significantly different from each other across all zones but both were significantly different from the low health areas as identified using NDVI. High mid-season NDVI values imply healthier denser vegetation whiles low values indicate areas with less vigor. These findings are similar to the findings of Brummel (2019), who also established a relationship between mid-season health of maize and grain yield.

5.4 Yield comparison between UDP and NON-UDP fields under plot scale assessment

The difference in yield between UDP and Non-UDP of 0.62 MT/ha was statistically significant which shows the UDP technology is better for maximum rice growth yields. The difference in yield can be attributed to the fact that the UDP technology allows N to be released slowly into the soil for plant uptake unlike the Non-UDP technology where N could be readily dissolved for plant use. The rate of leaching is low under the UDP technology, with its slow release of nutrients and thus ensuring the continuous supply of N to plants which increases N-use efficiency (Cao *et al*., 1984).

This corroborates previous findings that UDP technology significantly increases rice yields over other N management practices used in flooded rice production systems (Savant and Stangel, 1990). Furthermore, (Mazid *et al*., 2016) also recorded significant increase (22 %) in yield with deep placement of urea briquettes compared to prilled urea in their research to prove that fertilizer deep placement increases rice production in southern Bangladesh. Increase in yield with UDP have also been documented by several researchers (Alam *et al*., 2013; Bandaogo *et al*., 2015; Gregory *et al*., 2010; Mohanty *et al*., 1999).

5.5 In-field midseason geospatial spectral variability and end of season grain yield

Remote sensing has been used to predict crop yields mainly based on the relationship between yield and vegetation indices (Wójtowicz *et al*., 2016). Even the relation between yield and VIs are affected by spatial and temporal constraints, as reported by many researchers (Schwalbert *et al*., 2018) but it could be used for identifying management zones (Blackmore (2003); Patil *et al*., 2014), evaluating within-field variability and subsequently, the need for precision agriculture practices. As highlighted by Yang *et al*. (2012), utilization of in-season remote sensing imagery has a tremendous potential to produce an "on-the-go" impact on the farming operation. In this study, OSAVI showed the highest correlation with yield which is in contrast with the findings of Rey *et al*. (2013), who recorded a correlation coefficient of 0.50 between NDVI and yield and 0.44 for OSAVI, indicating that NDVI is the best vegetation index to use for yield forecasting. Additionally, the results from this study is in contrast to the finding of Kayad *et al*. (2019), who reported the GNDVI as the most correlated VI with corn grain yield at the field scale. The OSAVI performed better because it has a soil correction factor taking into account bare land and water bodies whiles the other vegetation indices do not. Also, NDVI has saturation problem (Gao *et al*.,

2000) whiles OSAVI does not. This is mostly because the amount of red-light absorption by leaves reaches a peak when canopy cover is 100% (Tucker, 1977) with NIR reflectance increasing since addition of leaf number results in multiple scattering. This imbalance results in a slight change in the NDVI ratio which then correlates poorly with biomass.

5.6 Effects of transplanting date on yield

The results showed the decrease in yield as transplanting of seedlings delayed among both UDP and Non-UDP farmers. Several investigations have been done on the importance of transplanting date in rice growth and yield (Islam *et al*., 2015; Mahmood *et al*., 1995). Decrease in yield with delayed transplanting date could be that seedlings which stay longer in nursery beds tend to have their primary tillers degenerated which lead to reduced growth and tiller production (Mobasser *et al*., 2007). Aghamolki *et al*. (2015), reported in his research that rice crop transplanted on the 21st of May recorded higher number of effective tillers and grain yield as compared to those transplanted on the 10th of June. Islam *et al*. (2015), also recorded highest grain yield in seedlings transplanted on the 20th of January followed by those transplanted on the 1st of February and lastly 20th February. This might be because seedlings transplanted earlier have full time to reach maturity under favorable weather conditions (Chaudhary *et al*., 2011) whiles the delayed transplanted seedlings may have been affected by harsh temperatures during the growing period (Mahajan *et al*., 2009). This also follows the findings of Mahmood *et al*. (1995), who reported a gradual decrease in plant height, flag leaf area, days to maturity, number of filled grains per panicle, weight of 1000 paddy and yield of paddy per hill with delayed transplantation date. Vishwakarma *et al*. (2016), recorded a reduction of grain yield by 7.82% in hybrid rice planted on 7th July as compared to those transplanted on 27th June. This show how essential the date of seedling transplant is crucial to rice growth and yield.

CHAPTER SIX:

6.0 CONCLUSION AND RECOMMENDATION

6.1 Conclusion

Results from this study indicate the following findings:

1 The UAS technology using the eBee platform proved to be a useful tool in capturing multispectral images used in producing vegetative indices that correlate end of season crop yields.

2 Rice crop health values were not different in high and medium zones however, both zones significantly out yielded the low health zones under both non-UDP and UDP N-management systems.

3 Yield assessment on the spatial scale also confirmed the superiority of UDP technology over non-UDP in enhancing rice productivity as observed using plot scale analysis.

4 The study also showed that OSAVI is the best predictive spectral index to use in estimating end of season rice grain yields as a function of N management.

5 The Jenks natural breaks algorithm proved a useful tool to be used as a standard method to divide farmer's field into homogenous classes using ArcGIS.

6 In terms of in-field spatial variation, yield in fields under the non-UDP N-management system showed greater variations compared to UDP system.

7 The UDP technology proved to be the best N-management system under this study.

6.2 Recommendation

The study recommends that, the OSAVI vegetation index should be frequently used as it proved to be a better vegetation index than the most commonly used vegetation index (NDVI). The use of the urea deep placement technology should also be encouraged in order to achieve higher rice yields.

Also, the local and national administrations should explore the use of the UAS technology as a decision support tool for early detection and management of problems associated with crop production.

REFERENCES

Abdullahi, H. S., Mahieddine, F., and Sheriff, R. E. (2015). Technology impact on agricultural productivity: A review of precision agriculture using unmanned aerial vehicles. In *International conference on wireless and satellite systems*, 388-400. Springer, Cham.

Acevedo-Opazo, C., Tisseyre, B., Guillaume, S., and Ojeda, H. (2008). The potential of high spatial resolution information to define within-vineyard zones related to vine water status. *Precision Agriculture*, 9(5): 285-302

Adu-Gyamfi, A. (2012). An overview of compulsory land acquisition in Ghana: Examining its applicability and effects. *Environmental Management and Sustainable Development*, 1(2): 187-203

Afroz, H., and Islam, M. R. (2014). Floodwater nitrogen, rice yield and N use efficiency as influenced by deep placement of nitrogenous fertilizers. *Journal of Environmental Science and Natural Resources*, 7(1): 207-213.

Aghamolki, M. T. K., Yusop, M. K., Jaafar, H. Z., Kharidah, S., Musa, M. H., and Zandi, P. (2015). Preliminary Analysis of Growth and Yield Parameters in Rice Cultivars When Exposed to Different Transplanting Dates. *Electronic Journal of Biology*, 11(4): 147–153.

Agribotix. Colorado: Agribotix. 2018. Available online: https://agribotix.com/blog/2017/04/30/comparing-rgb-based-vegetation-indices-with-ndvi-for-agricultural-drone-imagery/ (accessed on 7th January 2020).

Aker, J. C., Block, S., Ramachandran, V., and Timmer, C. P. (2010). West African experience with the world rice crisis, 2007–2008. *The rice crisis: markets, policies and food security*, 143-162.

Alam, M. M., Karim, M. R., and Ladha, J. K. (2013). Integrating best management practices for

rice with farmers' crop management techniques: A potential option for minimizing rice yield gap. *Field Crops Research*, 144: 62–68. https://doi.org/10.1016/j.fcr.2013.01.010.

Al-hassan, S. (2012). Technical Efficiency in Smallholder Paddy Farms in Ghana: An Analysis Based on Different Farming Systems and Gender. Journal of Economics and Sustainable Development, 3(5): 91- 105

Ali, A. M., Savin, I., Poddubsky, A., Aboelghar, M., and Salem, N. (2019). Integrated Method for Rice Cultivation Monitoring Using Sentinel-2 Data and Leaf Area Index, 1-17.

Altug, E., Ostrowski, J. P., and Mahony, R. (2002). Control of a quadrotor helicopter using visual feedback. In *Proceedings 2002 IEEE International Conference on Robotics and Automation*, 1: 72-77.

Alvarenga, J., Vitzilaios, N. I., Valavanis, K. P., and Rutherford, M. J. (2015). Survey of unmanned helicopter model-based navigation and control techniques. *Journal of Intelligent and Robotic Systems*, 80(1): 87-138.

Alvino, A., and Marino, S. (2017). Remote sensing for irrigation of horticultural crops. *Horticulturae*, 3(2): 1–40. https://doi.org/10.3390/horticulturae3020040.

Anthony, D., Elbaum, S., Lorenz, A., and Detweiler, C. (2014). On crop height estimation with UAVs. In *2014 IEEE/RSJ International Conference on Intelligent Robots and Systems*, 4805-4812.

Asrar, G. Q., Fuchs, M., Kanemasu, E. T., and Hatfield, J. L. (1984). Estimating absorbed photosynthetic radiation and leaf area index from spectral reflectance in wheat 1. *Agronomy journal*, 76(2): 300-306.

Atzberger, C. (2013). Advances in remote sensing of agriculture: Context description, existing operational monitoring systems and major information needs. *Remote Sensing*, 5(2): 949–

981. https://doi.org/10.3390/rs5020949

Azumah, S. B., and Adzawla, W. (2017). Effect of urea deep placement technology adoption on the production frontier: Evidence from irrigation rice farmers in the Northern Region of Ghana. *International Journal of Biological, Biomolecular, Agricultural, Food and Biotechnological Engineering*, 11(4): 288-294

Baret, F., Guyot, G., and Major, D. J. (1989). TSAVI: a vegetation index which minimizes soil brightness effects on LAI and APAR estimation. In *12th Canadian Symposium on Remote Sensing Geoscience and Remote Sensing Symposium*, 3: 1355-1358.

Baret, F., and Guyot, G. (1991). Potentials and limits of vegetation indices for LAI and APAR assessment. *Remote sensing of environment*, 35(2-3): 161-173

Baret, F., Jacquemoud, S., and Hanocq, J. F. (1993). The soil line concept in remote sensing. *Remote Sensing Reviews*, 7(1): 65-82.

Balasubramanian, V., Sie, M., Hijmans, R. J., and Otsuka, K. (2007). Increasing Rice Production in Sub-Saharan Africa: Challenges and Opportunities. *Advances in Agronomy*, 94(06): 55–133. https://doi.org/10.1016/S0065-2113(06)94002-4.

Baluja, J., Diago, M. P., Balda, P., Zorer, R., Meggio, F., Morales, F., and Tardaguila, J. (2012). Assessment of vineyard water status variability by thermal and multispectral imagery using an unmanned aerial vehicle (UAV). *Irrigation Science*, 30(6): 511-522

Bandaogo, A., Bidjokazo, F., Youl, S., Safo, E., Abaidoo, R., and Andrews, O. (2015). Effect of fertilizer deep placement with urea supergranule on nitrogen use efficiency of irrigated rice in Sourou Valley (Burkina Faso). *Nutrient Cycling in Agroecosystems*, 102(1): 79-89.

Bannari, A., Morin, D., Bonn, F., and Huete, A. R. (1995). A review of vegetation indices. *Remote sensing reviews*, 13(1): 95-120.

Bannor, R., K. (2015). Long run and short run causality of rice consumption by urbanization and income growth in Ghana. *ACADEMICIA: An International Multidisciplinary Research Journal*, 5(2): 173-189.

Baldock, J. A., and Skjemstad, J. O. (1999). Soil organic carbon/soil organic matter. In '*Soil analysis: an interpretation manual*'. (Eds KI Peverill, LA Sparrow, DJ Reuter), 159–170.

Bendig, J., Bolten, A., and Bareth, G. (2012). Introducing a low-cost mini-UAV for thermal-and multispectral-imaging. *International Archives of the Photogrammetry. Remote Sensing and Spatial Information Sciences*, 39: 345-349.

Bégué, A., Todoroff, P., and Pater, J. (2008). Multi-time scale analysis of sugarcane within-field variability: Improved crop diagnosis using satellite time series? *Precision Agriculture*, 9(3): 161–171. https://doi.org/10.1007/s11119-008-9063-3

Berner, B., and Chojnacki, J. (2017). Use of drones in crop protection. *IX International Scientific Symposium "Farm Machinery and Processes Management in Sustainable Agriculture"*, Lublin, Poland, 2017. https://doi.org/10.24326/fmpmsa.2017.9

Berni, J. A. J., Zarco-Tejada, P. J., Suárez, L., González-Dugo, V., and Fereres, E. (2009). Remote sensing of vegetation from UAV platforms using lightweight multispectral and thermal imaging sensors. *International Archives of the Photogrammetry. Remote Sensing and Spatial Information Sciences*, 38(6): 1-6.

Blackmore, S. (2003). *The role of yield maps in precision farming* (Doctoral dissertation, Cranfield University).

Borhan, M. S., Panigrahi, S., Lorenzen, J. H., and Gu, H. (2004). Multispectral and color

imaging techniques for nitrate and chlorophyll determination of potato leaves in a controlled environment. *Transactions of the American Society of Agricultural Engineers*, 47(2): 1- 599.

Brummel, D. (2019). *Delineation of NDVI-based soil management zones: Applications of UAS technology.* Iowa state university, Iowa.

Buri, M. M., Issaka, R. N., Wakatsuki, T., and Kawano, N. (2012). Improving the productivity of lowland soils for rice cultivation in Ghana: The role of the Sawah system. *Journal of Soil Science and Environmental Management*, 3(3): 56-65.

Bulbule, A. V., Purkar, J. K., and Jogdande, N. D. (2002). Management of nitrogen for rainfed transplanted rice. *Crop Research-Hisar*, 23(3): 440-445.

Carter, M. R. and Stewart, B. A. (1996). *Structure and organic matter storage in agricultural soils* (Vol. 8), CRC Press: Boca Raton.

Cai, G., Dias, J., and Seneviratne, L. (2014). A survey of small-scale unmanned aerial vehicles: Recent advances and future development trends. *Unmanned Systems*, 2(2): 175-199.

Cammarano, D., Fitzgerald, G. J., Casa, R., and Basso, B. (2014). *Assessing the Robustness of Vegetation Indices to Estimate Wheat N in Mediterranean Environments*, 2827–2844. https://doi.org/10.3390/rs6042827

Campillo, C., Fortes, R., and Prieto, M. D. H. (2012). Solar radiation effect on crop production. *Solar radiation*, 1: 168-194.

Cao, Z. H., De Datta, S. K., and Fillery, I. R. P. (1984). Nitrogen-15 Balance and Residual Effects of Urea-N in Wetland Rice Fields as Affected by Deep Placement Techniques. *Soil Science Society of America Journal*, 48(1): 203-208.

Cao, Z. H., Huang, J. F., Zhang, C. S., and Li, A. F. (2004). Soil quality evolution after land use

change from paddy soil to vegetable land. *Environmental Geochemistry and Health*, 26(2): 97-103.

Casanova, D., Goudriaan, J., Bouma, J., and Epema, G. F. (1999). Yield gap analysis in relation to soil properties in direct-seeded flooded rice. *Geoderma*, 91(3-4): 191-216.

Chaudhary, S. K., Singh, J. P., and Jha, S. (2011). Effect of integrated nitrogen management on yield, quality and nutrient uptake of rice (Oryza sativa) under different dates of planting. *Indian Journal of Agronomy*, 56(3): 228-231.

Chapman, S. C., Merz, T., Chan, A., Jackway, P., Hrabar, S., Dreccer, M. F., ... and Jimenez-Berni, J. (2014). Pheno-copter: a low-altitude, autonomous remote-sensing robotic helicopter for high-throughput field-based phenotyping. *Agronomy*, 4(2): 279-301.

Connor, D. J., Loomis, R. S., and Cassman, K. G. (2011). *Crop ecology: productivity and management in agricultural systems*. Cambridge University Press.

Combs, S. M., Nathan, M. V., and Brown, J. R. (1998). Soil Organic Matter. p. 53-58. *Recommended Chemical Soil Test Procedures for the North Central Region*, (221).

Clevers, J. P., and Jongschaap, R. (2002). Imaging spectrometry for agricultural applications. *Imaging spectrometry*, 157-199. Springer, Dordrecht.

Chen, J., Zhu, W., Tian, Y. Q., Yu, Q., Zheng, Y., and Huang, L. (2017). Remote estimation of colored dissolved organic matter and chlorophyll-a in Lake Huron using Sentinel-2 measurements. *Journal of Applied Remote Sensing*, 11(03): 036007. https://doi.org/10.1117/1.jrs.11.036007

Cress, J. J., Sloan, J. L., and Hutt, M. E. (2011). Implementation of unmanned aircraft systems by the US Geological Survey. *Geocarto International*, 26(2): 133-140.

Dahikar, S. S., and Rode, S. V. (2014). Agricultural crop yield prediction using artificial neural

network approach. *International journal of innovative research in electrical, electronics, instrumentation and control engineering*, 2(1): 683-686.

Danquah, I. B., and Egyir, D. I. S. (2014). Factors that Influence Household Demand for Locally Produced Brown Rice in Ghana. *Computer Engineering and Intelligent Systems*, 5(7): 14–24.

Danso-Abbeam, G., Armed, M., and Baidoo, F. (2014). Determinants of Consumer Preference for Local Rice in Tamale Metropolis , Ghana. *International Journal of Education and Social Science*, 1(2): 114–122.

Defoer, T., Wopereis, M. C. S., Jones, M. P., Lançon, F., Erenstein, O., and Guei, R. G. (2004). Rice-based production systems for food security and poverty alleviation in sub-Saharan Africa. *International Rice Commission Newsletter*, 53: 85-96

Diagne, A., Alia, D. Y., Amovin-Assagba, E., Wopereis, M. C., Saito, K., and Nakelse, T. (2013). Farmer perceptions of the biophysical constraints to rice production in sub-Saharan Africa, and potential impact of research. *Realizing Africa's rice promise*, 46-68.

Dobermann, A. (1994). Factors causing field variation of direct-seeded flooded rice. *Geoderma*, 62(1-3): 125-150.

Dong, N. M., Brandt, K. K., Sørensen, J., Hung, N. N., Hach, C. Van, Tan, P. S., and Dalsgaard, T. (2012). Effects of alternating wetting and drying versus continuous flooding on fertilizer nitrogen fate in rice fields in the Mekong Delta, Vietnam. *Soil Biology and Biochemistry*, 47: 166–174. https://doi.org/10.1016/j.soilbio.2011.12.028

Dou, F., Soriano, J., Tabien, R. E., and Chen, K. (2016). Soil texture and cultivar effects on rice (Oryza sativa, L.) grain yield, yield components and water productivity in three water regimes. *PloS one*, 11(3): e0150549.

Eliceiri, K. W., Berthold, M. R., Goldberg, I. G., Ibáñez, L., Manjunath, B. S., Martone, M. E., ...

and Stuurman, N. (2012). Biological imaging software tools. *Nature methods*, 9(7): 697.

Eisenbeiss, H. (2009). UAV Photography. Doctoral dissertation, University of Technology Dresden, Dresden ,Germany. https://doi.org/10.3929/ethz-a-010782581

Fan, X., Tang, Z., Tan, Y., Zhang, Y., Luo, B., Yang, M., ... and Xu, G. (2016). Overexpression of a pH-sensitive nitrate transporter in rice increases crop yields. *Proceedings of the National Academy of Sciences*, 113(26):7118-7123.

Fernandez, S., Vidal, D., Simon, E., and SOLl3-SUGRANES, L. (1994). Radiometric characteristics of Triticum aestivum cv, Astral under water and nitrogen stress. *International Journal of Remote Sensing*, 15(9): 1867-1884.

Fernández, J. E. (2014). Plant-based sensing to monitor water stress: Applicability to commercial orchards. *Agricultural Water Management*, 142: 99–109. https://doi.org/10.1016/j.agwat.2014.04.017

Frank, K., Beegle, D., and Denning, J. (1998). Phosphorus. *JR Brown (ed.) Recommended chemical soil test procedures for the North Central region. North Central Regional Publications. 221 (revised), Missouri Agricultural Experiment Station, SB 1001, Columbia*, 21-29.

Fuller, D. O. (2005). Remote detection of invasive Melaleuca trees (Melaleuca quinquenervia) in South Florida with multispectral IKONOS imagery. *International Journal of Remote Sensing*, 26(5): 1057-1063.

Gao, X., Huete, A. R., Ni, W., and Miura, T. (2000). Optical–biophysical relationships of vegetation spectra without background contamination. *Remote sensing of environment*, 74(3): 609-620.

Gardner, F. P., Pearce, R. B., and Mitchell, R. L. (1985). Carbon fixation by crop

canopies. *Physiology of Crop Plants. Iowa State University Press*, 31-57.

Ge, S., Xu, H., Ji, M., and Jiang, Y. (2013). Characteristics of soil organic carbon, total nitrogen, and C/N ratio in Chinese apple orchards. *Open Journal of Soil Science* 3(5): 213-217.

Giles, D., and Billing, R. (2015). Deployment and Performance of a UAV for Crop Spraying. *Chemical engineering transactions*, 44: 307-312

Gillespie, T. W., Willis, K. S., and Ostermann-Kelm, S. (2015). Spaceborne remote sensing of the world's protected areas. *Progress in Physical Geography*, 39(3): 388-404.

Gitelson, A. A., Kaufman, Y. J., and Merzlyak, M. N. (1996). Use of a green channel in remote sensing of global vegetation from EOS-MODIS. *Remote sensing of Environment*, 58(3): 289-298.

Gitelson, A. A. (2004). Wide dynamic range vegetation index for remote quantification of biophysical characteristics of vegetation. *Journal of plant physiology*, 161(2): 165-173.

Gitelson, A., and Merzlyak, M. N. (1994). Spectral reflectance changes associated with autumn senescence of Aesculus hippocastanum L. and Acer platanoides L. leaves. Spectral features and relation to chlorophyll estimation. *Journal of plant physiology*, 143(3): 286-292.

Govaerts, Y. M., Verstraete, M. M., Pinty, B., and Gobron, N. (1999). Designing optimal spectral indices: A feasibility and proof of concept study. *International journal of remote sensing*, 20(9): 1853-1873.

Gregory, D. I., Haefele, S. M., Buresh, R. J., and Singh, U. (2010). Fertilizer use, markets, and management. *Rice in the global economy. Strategic research and policy issues for food security. Los Banos, Philippines: International Rice Research Institute*, 231-263.

Haboudane, D., Miller, J. R., Pattey, E., Zarco-Tejada, P. J., and Strachan, I. B. (2004).

Hyperspectral vegetation indices and novel algorithms for predicting green LAI of crop canopies: Modeling and validation in the context of precision agriculture. *Remote sensing of environment*, 90(3): 337-352.

Hall, A., Lamb, D. W., Holzapfel, B., and Louis, J. (2002). Optical remote sensing applications in viticulture - A review. *Australian Journal of Grape and Wine Research*, 8(1): 36–47. https://doi.org/10.1111/j.1755-0238.2002.tb00209.x

He, K. S., Rocchini, D., Neteler, M., and Nagendra, H. (2011). Benefits of hyperspectral remote sensing for tracking plant invasions. *Diversity and Distributions*, 17(3): 381-392.

Herwitz, S. R., Dunagan, S., Sullivan, D., Higgins, R., Johnson, L., Zheng, J., ... and Aoyagi, M. (2003). Solar-powered UAV mission for agricultural decision support. In *IGARSS 2003. 2003 IEEE International Geoscience and Remote Sensing Symposium. Proceedings (IEEE Cat. No. 03CH37477)* 3: 1692-1694.

Herwitz, S. R., Johnson, L. F., Dunagan, S. E., Higgins, R. G., Sullivan, D. V., Zheng, J., ... and Slye, R. E. (2004). Imaging from an unmanned aerial vehicle: agricultural surveillance and decision support. *Computers and electronics in agriculture*, 44(1): 49-61.

Huang, Y., Hoffmann, W. C., Lan, Y., Wu, W., and Fritz, B. K. (2009). Development of a spray system for an unmanned aerial vehicle platform. *Applied Engineering in Agriculture*, 25(6): 803-809.

Huda, A., Gaihre, Y. K., Islam, M. R., Singh, U., Islam, M. R., Sanabria, J., ... and Jahiruddin, M. (2016). Floodwater ammonium, nitrogen use efficiency and rice yields with fertilizer deep placement and alternate wetting and drying under triple rice cropping systems. *Nutrient cycling in agroecosystems*, 104(1): 53-66.

Huete, A. R. (1988). A soil-adjusted vegetation index (SAVI). Remote Sensing of Environment,

25: 295−309.

Huete, A. R., Liu, H., and van Leeuwen, W. J. (1997). The use of vegetation indices in forested regions: issues of linearity and saturation. In *IGARSS'97. 1997 IEEE International Geoscience and Remote Sensing Symposium Proceedings. Remote Sensing-A Scientific Vision for Sustainable Development*, 4: 1966-1968.

Huete, A., Didan, K., Miura, T., Rodriguez, E. P., Gao, X., and Ferreira, L. G. (2002). Overview of the radiometric and biophysical performance of the MODIS vegetation indices. *Remote sensing of environment*, 83(1-2): 195-213.

Imam, E. (2019). Remote Sensing Platforms and Sensors. 1-27.

Islam, A. S., Rahman, M. A., Rahman, A. L., Islam, M. T., and Rahman, M. I. (2015). Field performance evaluation of push type prilled urea applicator in rice cultivation. *Bangladesh Rice Journal*, 19(2): 71-81.

Jackson, R. D., Slater, P. N., and Printer, P. J. (1983). Discrimination of growth and water stress in wheat by various vegetation indices through clear and turbid atmosphere. *Remote Sensing of the Environment*, 15: 187-208.

Jannoura, R., Brinkmann, K., Uteau, D., Bruns, C., and Joergensen, R. G. (2015). Monitoring of crop biomass using true colour aerial photographs taken from a remote controlled hexacopter. *Biosystems Engineering*, 129: 341-351.

Janzen, H. H., Larney, F. J., and Olson, B. M. (1992, February). Soil quality factors of problem soils in Alberta. *Proceedings of the Alberta Soil Science Workshop*, 29: 17-28.

Jawak, S. D., Devliyal, P., and Luis, A. J. (2015). A comprehensive review on pixel oriented and

object-oriented methods for information extraction from remotely sensed satellite images with a special emphasis on cryospheric applications. *Advances in Remote Sensing*, 4(3): 177-195.

Jensen, J. R. (2009). *Remote sensing of the environment: An earth resource perspective 2/e*. Pearson Education India.

Jongschaap, R. E., and Booij, R. (2004). Spectral measurements at different spatial scales in potato: relating leaf, plant and canopy nitrogen status. *International Journal of Applied Earth Observation and Geoinformation*, 5(3): 205-218.

Kanellakis, C., and Nikolakopoulos, G. (2017). Survey on computer vision for UAVs: Current developments and trends. *Journal of Intelligent and Robotic Systems*, 87(1): 141-168.

Kapoor, V., Singh, U., Patil, S. K., Magre, H., Shrivastava, L. K., Mishra, V. N., ... and Diamond, R. (2008). Rice growth, grain yield, and floodwater nutrient dynamics as affected by nutrient placement method and rate. *Agronomy Journal*, 100(3): 526-536.

Kayad, A., Sozzi, M., Gatto, S., Marinello, F., & Pirotti, F. (2019). Monitoring within-field variability of corn yield using Sentinel-2 and machine learning techniques. *Remote Sensing*, *11*(23), 2873.

Kemeze, F. H., Miranda, M. J., Kuwornu, J., and Amin-Somuah, H. (2016). Optimal Management of Runoff Reservoir Supply: The Case of Tono Reservoir in Northern Ghana. In *2016 Annual Meeting, July 31-August 2, Boston, Massachusetts* (No. 236030). Agricultural and Applied Economics Association.

Kim, M. (2009). Climate change impact on rice yield and production risk. *Asian Journal of Rural Development*, 32(2): 17–29. https://doi.org/10.22004/ag.econ.90682

Kumhálová, J., and Matějková, Š. (2017). Yield variability prediction by remote sensing sensors

with different spatial resolution, 195–202. https://doi.org/10.1515/intag-2016-0046

Lal, R. (2002). Soil carbon dynamics in cropland and rangeland. *Environmental pollution*, 116(3): 353-362.

Lal, R. (2014). Societal value of soil carbon. *Journal of Soil and Water Conservation*, 69(6): 186A-192A.

Lamb, D. W., Weedon, M. M., and Bramley, R. G. V. (2004). Using remote sensing to predict grape phenolics and colour at harvest in a Cabernet Sauvignon vineyard: Timing observations against vine phenology and optimising image resolution. *Australian Journal of Grape and Wine Research*, 10(1): 46-54.

Lee, W. S., Alchanatis, V., Yang, C., Hirafuji, M., Moshou, D., and Li, C. (2010). Sensing technologies for precision specialty crop production. *Computers and electronics in agriculture*, 74(1): 2-33.

Leuning, R., Kelliher, F. M., De Pury, D. G. G., and Schulze, E. D. (1995). Leaf nitrogen, photosynthesis, conductance and transpiration: scaling from leaves to canopies. *Plant, Cell and Environment*, 18(10): 1183-1200

Liang, S. (2005). *Quantitative remote sensing of land surfaces* (Vol. 30). John Wiley and Sons, New York.

Lillesaeter, O. (1982). Spectral reflectance of partly transmitting leaves: laboratory measurements and mathematical modeling. *Remote sensing of Environment*, 12(3): 247-254.

Lillesand, T., Kiefer, R. W., and Chipman, J. (2015). *Remote sensing and image interpretation* (7th Edn). John Wiley and Sons, New York.

Liverpool-Tasie, L. S. O., Adjognon, S., and Kuku-Shittu, O. (2015). Productivity effects of

sustainable intensification: The case of Urea deep placement for rice production in Niger State, Nigeria. *African Journal of Agricultural and Resource Economics Volume*, 10(1): 51-63.

Mahajan, G., Bharaj, T. S., and Timsina, J. (2009). Yield and water productivity of rice as affected by time of transplanting in Punjab, India. *Agricultural Water Management*, 96(3): 525-532.

Mahmood, N., Hussain, A., and Saleem, M. (1995). Effect of transplanting date and irrigation on rice paddy yield. *Science*, 14(3): 49-52.

Major, D. J., Baret, F., and Guyot, G. (1990). A ratio vegetation index adjusted for soil brightness. *International journal of remote sensing*, 11(5): 727-740.

Malenovský, Z., Rott, H., Cihlar, J., Schaepman, M. E., García-Santos, G., Fernandes, R., and Berger, M. (2012). Sentinels for science: Potential of Sentinel-1, -2, and -3 missions for scientific observations of ocean, cryosphere, and land. *Remote Sensing of Environment*, 120: 91–101. https://doi.org/10.1016/j.rse.2011.09.026.

Martín, P., Zarco-Tejada, P. J., González, M. R., and Berjón, A. (2007). Using hyperspectral remote sensing to map grape quality in Tempranillo'vineyards affected by iron deficiency chlorosis. *Vitis-Geilweilerhof-*, 46(1): 7-14.

Mašková, Z., Zemek, F., and Kv, J. (2008). Normalized difference vegetation index (NDVI) in the management of mountain meadows. *Boreal environment research*, 13: 417–432.

Matese, A., Toscano, P., Di Gennaro, S. F., Genesio, L., Vaccari, F. P., Primicerio, J., … and Gioli, B. (2015). Intercomparison of UAV, aircraft and satellite remote sensing platforms for precision viticulture. *Remote Sensing*, 7(3): 2971–2990. https://doi.org/10.3390/rs70302971

Mayr, W. (2015). UAVs for Production. *Photogrammetric Week*, 15: 51–56.

Mazid Miah, M. A., Gaihre, Y. K., Hunter, G., Singh, U., and Hossain, S. A. (2016). Fertilizer deep placement increases rice production: evidence from farmers' fields in southern Bangladesh. *Agronomy Journal*, 108(2): 805-812.

Mckinnon, B. T. (2016). Agricultural drones: What farmers need to know. *Boulder, Colorado*.

Medcalf, K. A., Bodevin, N., Cameron, I., Webber, J., and Turton, N. (2011). Assessing the potential of using remote sensing in support of current Phytophthora work, report to The Food and Environment Research Agency.

Mobasser, H. R., Tari, D. B., Vojdani, M., Abadi, R. S., and Eftekhari, A. (2007). Effect of seedling age and planting space on yield and yield components of rice (Neda variety). *Asian Journal of Plant Sciences*, 6(2): 438–40.

Mohanty, S. K., Singh, U., Balasubramanian, V., and Jha, K. P. (1999). Nitrogen deep-placement technologies for productivity, profitability, and environmental quality of rainfed lowland rice systems. *Nutrient Cycling in Agroecosystems*, 53(1): 43-57.

Myneni, R. B., Hall, F. G., Sellers, P. J., and Marshak, A. L. (1995). The interpretation of spectral vegetation indexes. *IEEE Transactions on Geoscience and Remote Sensing*, 33(2): 481-486.

Meybeck, A., Holmgren, P., and Fao, V. G. (2012). Climate Smart Agriculture, Planet Under Pressure, New knowledge towards Solutions, London, 26-29 March.

Mookherjee, A. (2016). A Study to Determine Yield for Crop Insurance using Precision Agriculture on an Aerial Platform. Symbiosis International University, Lavale, Mulshi, Pune, Maharashtra 412115, India.

Moldenhauer, K. E. W. C., and Slaton, N. (2001). Rice growth and development. *Rice production handbook*, 192: 7-14.

Ministry of Food and Agriculture (MOFA), (2009) "Evaluation of the Ghana Rice Campaign"; A marketing campaign implemented by Engineers Without Borders and the Ghana Ministry of Food and Agriculture to stimulate the rice value chain, April 2009.

Ministry of Food and Agriculture (MoFA) Statistics, Research and Information Directorate (SRID), "Agriculture in Ghana: Facts and Figures 2010.

Mosleh, M. K., Hassan, Q. K., and Chowdhury, E. H. (2016). Development of a remote sensing-based rice yield forecasting model. *Spanish Journal of Agricultural Research*, 14(3): 1-11. https://doi.org/10.5424/sjar/2016143-8347.

Nebiker, S., Annen, A., Scherrer, M., and Oesch, D. (2008). A light-weight multispectral sensor for micro UAV—Opportunities for very high resolution airborne remote sensing. *The International Archives of the Photogrammetry, Remote Sensing and Spatial Information Sciences*, 37(6): 1193–1200.

Nicholson, S. E., and Farrar, T. J. (1994). The influence of soil type on the relationships between NDVI, rainfall, and soil moisture in semiarid Botswana. I. NDVI response to rainfall. *Remote sensing of environment*, 50(2): 107-120.

Nkebiwe, P. M., Weinmann, M., Bar-Tal, A., and Müller, T. (2016). Fertilizer placement to improve crop nutrient acquisition and yield: a review and meta-analysis. *Field crops research*, 196: 389-401.

Nwanze, K. F., Mohapatra, S., Kormawa, P., Keya, S., and Bruce-Oliver, S. (2006). *Rice development in sub-Saharan Africa*. 677: 675–677. https://doi.org/10.1002/jsfa.2415

Olaf, K., and Emmanuel, D. (2009). Global food security response: Ghana rice study. *Attachment I to the Global Food Security Response West African Rice Value Chain Analysis*.

Panda, S. S., Ames, D. P., and Panigrahi, S. (2010). Application of vegetation indices for

agricultural crop yield prediction using neural network techniques. *Remote Sensing*, 2(3): 673-696.

Pasandaran, E., Gultom, B., Adiningsih, J. S., Apsari, H., and ri Rochayati, S. (1998). Government policy support for technology promotion and adoption: a case study of urea tablet technology in Indonesia. *Nutrient cycling in Agroecosystems*, 53(1): 113-119.

Patil, V. C., Al-Gaadi, K. A., Madugundu, R., Tola, E. H., Marey, S. A., Al-Omran, A. M., ... & Al-Dosari, A. (2014). Delineation of management zones and response of spring wheat (Triticum aestivum) to irrigation and nutrient levels in Saudi Arabia. *Int. J. Agric. Biol*, *16*, 104-110.

Pearson, R. L. (1972). Remote mapping of standing crop biomass for estimation of the productivity of the shortgrass prairie. In *Eighth International Symposium on Remote Sensing of Enviroment*, 1357-1381. University of Michigan.

Peñuelas, J., Gamon, J. A., Fredeen, A. L., Merino, J., and Field, C. B. (1994). Physiological Changes in Nitrogen-and. *Remote Sensing of the Environment*, 48: 135-146.

Peteinatos, G. G., Weis, M., Andújar, D., Rueda Ayala, V., and Gerhards, R. (2014). Potential use of ground-based sensor technologies for weed detection. *Pest management science*, 70(2): 190-199

Poggi-Varaldo, H. M., and Estrada-Vazquez, C. (1997). Agricultural wastes. *Water environment research*, 69(4): 575-603.

Pounds, P., Mahony, R., Hynes, P., and Roberts, J. M. (2002). Design of a four-rotor aerial robot. In *Proceedings of the 2002 Australasian Conference on Robotics and Automation (ACRA 2002)*, 145-150. Australian Robotics and Automation Association.

Primicerio, J., Di Gennaro, S. F., Fiorillo, E., Genesio, L., Lugato, E., Matese, A., and Vaccari,

F. P. (2012). A flexible unmanned aerial vehicle for precision agriculture. *Precision Agriculture*, 13(4): 517-523.

Qi, J., Chehbouni, A., Huete, A. R., Kerr, Y. H., and Sorooshian, S. (1994). A Modified Soil Adjusted Vegetation Index", *Remote Sensing of the Environment*, 48: 119–126.

Rahman, S., and Barmon, B. K. (2015). Exploring the potential to improve energy saving and energy efficiency using fertilizer deep placement strategy in modern rice production in Bangladesh. *Energy Efficiency*, 8(6): 1241-1250.

Rahman, S., and Barmon, B. K. (2015). Productivity and efficiency impacts of Urea Deep Placement technology in modern rice production: An empirical analysis from Bangladesh. *The Journal of Developing Areas*, 119-134.

Ragasa, C., Dankyi, A., Acheampong, P., Wiredu, A. N., Chapoto, A., Asamoah, M., and Tripp, R. (2013). Patterns of adoption of improved rice technologies in Ghana. *International Food Policy Research Institute Working Paper*, 35: 6-8.

Rochette, P., Angers, D. A., Chantigny, M. H., Gasser, M.-O., MacDonald, J. D., Pelster, D. E., and Bertrand, N. (2013). Ammonia Volatilization and Nitrogen Retention: How Deep to Incorporate Urea? *Journal of Environmental Quality*, 42(6): 1635–1642. https://doi.org/10.2134/jeq2013.05.0192

Rey, C., Martín, M. P., Lobo, A., Luna, I., Diago, M. P., Millan, B., and Tardáguila, J. (2013). Multispectral imagery acquired from a UAV to assess the spatial variability of a Tempranillo vineyard. *Precision agriculture*, 13: 617-624. Wageningen Academic Publishers, Wageningen.

Richardson, A. J., and Wiegand, C. L. (1977). Distinguishing vegetation from soil background information. *Photogrammetric engineering and remote sensing*, 43(12): 1541-1552.

Rondeaux, G., Steven, M., and Baret, F. (1996). Optimization of soil-adjusted vegetation indices. *Remote sensing of environment*, 55(2): 95-107.

Rouse, J. W., Haas, R. H., Schell, J. A., and Deering, D. W. (1974). Monitoring vegetation systems in the Great Plains with ERTS. *NASA special publication*, 351-309.

Sakamoto, T., Yokozawa, M., Toritani, H., Shibayama, M., Ishitsuka, N., and Ohno, H. (2005). A crop phenology detection method using time-series MODIS data. *Remote sensing of environment*, 96(3-4): 366-374.

Sarkar, T. K., Ryu, C. S., Kang, Y. S., Kim, S. H., Jeon, S. R., Jang, S. H., ... and Kim, H. J. (2018). Integrating UAV remote sensing with GIS for predicting rice grain protein. *Journal of Biosystems Engineering*, 43(2): 148-159.

SAS Institute Inc. 2018. SAS/STAT® 15.1 User's Guide. Cary, NC: SAS Institute Inc.

Savant, N. K., and Stangel, P. J. (1990). Deep placement of urea supergranules in transplanted rice: Principles and practices. *Fertilizer Research*, 25(1): 1–83. https://doi.org/10.1007/BF01063765

Schwalbert, R. A., Amado, T. J., Nieto, L., Varela, S., Corassa, G. M., Horbe, T. A., ... & Ciampitti, I. A. (2018). Forecasting maize yield at field scale based on high-resolution satellite imagery. *Biosystems engineering*, *171*, 179-192.

Seck, P. A., Touré, A. A., Coulibaly, J. Y., Diagne, A., and Wopereis, M. C. S. (2013). Africa's rice economy before and after the 2008 rice crisis. *Realizing Africa's Rice Promise*, 24–34. https://doi.org/10.1079/9781845938123.0024.

SenseFly. (2016). eBee: senseFly SA. Retrieved from https://www.sensefly.com/drone/ebee-mapping-drone/

Shahbazi, M., Théau, J., and Ménard, P. (2016). Recent applications of unmanned aerial imagery

in natural resource management. *GISciece and Remote Sensing*, 51(4): 339–365. https://doi.org/10.1080/15481603.2014.926650

Shanahan, J. F., Kitchen, N. R., Raun, W. R., and Schepers, J. S. (2008). Responsive in-season nitrogen management for cereals. *Computers and electronics in agriculture*, 61(1): 51-62.

Shi, C., and Wang, L. (2014). Incorporating spatial information in spectral unmixing: A review. *Remote Sensing of Environment*, 149: 70-87.

Shaw, G. A., and Burke, H. K. (2003). Spectral imaging for remote sensing. *Lincoln laboratory journal*, 14(1): 3-28.

Shi, C., and Wang, L. (2014). Incorporating spatial information in spectral unmixing: A review. *Remote Sensing of Environment*, 149: 70-87.

Simmonds, M. B., Plant, R. E., Peña-Barragán, J. M., van Kessel, C., Hill, J., and Linquist, B. A. (2013). Underlying causes of yield spatial variability and potential for precision management in rice systems. *Precision Agriculture*, 14(5): 512–540. https://doi.org/10.1007/s11119-013-9313-x

Skjemstad, J. O. (2002). Importance of soil organic matter fractions to crop production, soil structure and soil resilience. *Grains Research and Development Corporation Final Report CSO, 195*.

Stow, D. A., Hope, A., McGuire, D., Verbyla, D., Gamon, J., Huemmrich, F., ... and Hinzman, L. (2004). Remote sensing of vegetation and land-cover change in Arctic Tundra Ecosystems. *Remote sensing of environment*, 89(3): 281-308.

Stroppiana, D., Migliazzi, M., Chiarabini, V., Crema, A., Musanti, M., Franchino, C., and Villa, P. (2015). Rice yield estimation using multispectral data from UAV: A preliminary experiment in northern Italy. In *2015 IEEE International Geoscience and Remote Sensing*

Symposium (IGARSS), 4664-4667, Institute of Electrical and Electronics Engineers.

Sugiura, R., Noguchi, N., and Ishii, K. (2005). Remote-sensing technology for vegetation monitoring using an unmanned helicopter. *Biosystems engineering*, 90(4): 369-379.

Swain, K. C., and Zaman, Q. U. (2012). Rice crop monitoring with unmanned helicopter remote sensing images. *Remote Sensing of Biomass-Principles and Applications*, 254-272.

Tanaka, A., Johnson, J., Senthilkumar, K., Akakpo, C., Segda, Z., Yameogo, L. P., … and Saito, K. (2017). On-farm rice yield and its association with biophysical factors in sub-Saharan Africa. *European Journal of Agronomy*, 85: 1–11. https://doi.org/10.1016/j.eja.2016.12.010

Tarfa, B., and Kiger, B. (2013). UDP and Rice production in Nigeria: The experience so far. In *Conference on Guiding Investments in Sustainable Intensification in Africa (GISAIA), organised by International Fertilizer Development Corporation (IFDC) held in Abuja, Nigeria–June18.*

Tiamiyu, S. A., Eze, J. N., Yusuf, T. M., Maji, A. T., and Bakare, S. O. (2015). *Rainfall Variability and Its Effect on Yield of Rice in Nigeria*. 49: 63–68. https://doi.org/10.18052/www.scipress.com/ILNS.49.63.

Tomlins, K., Manful, J., Gayin, J., Kudjawu, B., and Tamakloe, I. (2007). Effect of phytate and storage conditions on the development of the ‘ hard-to-cook .’ *Journal of the Science of Food and Agriculture*, 87: 1237–1243. https://doi.org/10.1002/jsfa

Toming, K., Kutser, T., Laas, A., Sepp, M., Paavel, B., and Nõges, T. (2016). First experiences in mapping lakewater quality parameters with sentinel-2 MSI imagery. *Remote Sensing*, 8(8): 1–14. https://doi.org/10.3390/rs8080640

Tucker, C. J. (1977). Spectral estimation of grass canopy variables. *Remote Sensing of Environment*, 6(1): 11-26.

Tucker, C.J. (1979) Red and photographic infrared linear combinations for monitoring vegetation. *Remote Sensing of the Environment*, 8(2):127–150

Tsujimoto, Y., Rakotoson, T., Tanaka, A., and Saito, K. (2019). Challenges and opportunities for improving N use efficiency for rice production in sub-Saharan Africa. *Plant Production Science*, 22(4): 413-427.

Tyc, G., Tulip, J., Schulten, D., Krischke, M., and Oxfort, M. (2005). The RapidEye mission design. *Acta Astronautica*, 56(1-2): 213-219.

Van der Werff, H., and van der Meer, F. (2015). Sentinel-2 for mapping iron absorption feature parameters. *Remote Sensing*, 7(10): 12635–12653. https://doi.org/10.3390/rs71012635.

Varlet-Grancher, C., Bonhomme, R., and Sinoquet, H. (1995). Crop structure and light microclimate: Characterization and applications. *Field Crops Research*, 40: 195–197. https://doi.org/10.1016/s0378-4290(95)90004-7.

Vishwakarma, A., Singh, J. K., Sen, A., Bohra, J. S., and Singh, S. (2016). Effect of transplanting date and age of seedlings on growth, yield and quality of hybrids under system of rice (Oryza sativa) intensification and their effect on soil fertility. *Indian Journal of Agricultural Sciences*, 86(5): 679-685.

Wahab, I., Hall, O., and Magnus, J. (2018). Remote Sensing of Yields : Application of UAV Imagery-Derived NDVI for Estimating Maize Vigor and Yields in Complex Farming Systems in Sub-Saharan Africa, 2(3): 1-28. https://doi.org/10.3390/drones2030028

Wald, L. (2007). Solar radiation energy (fundamentals). *Solar Energy Conversion and Photoenergy Systems, edited by Julian Blanco and Sixto Malato, in Encyclopedia of Life Support Systems (EOLSS), Developed under the Auspices of the UNESCO, Eolss Publishers, Oxford, UK,[http://www. eolss. net]*, 1: 1-10

Walter, N. F., Hallberg, G. R., and Fenton, T. S. (1978). Particle size analysis by the Iowa State University, Soil Survey Lab. *Standard procedures for evaluation of quaternary materials in Iowa. Iowa Geological Survey, Iowa City*, 61-74.

Wang, Q., Adiku, S., Tenhunen, J., and Granier, A. (2005). On the relationship of NDVI with leaf area index in a deciduous forest site. *Remote sensing of environment*, 94(2): 244-255.

Wang, F., and Liu, X. (2008). Upconversion multicolor fine-tuning: visible to near-infrared emission from lanthanide-doped NaYF4 nanoparticles. *Journal of the American Chemical Society*, 130(17): 5642-5643.

Warncke, D., and Brown, J. R. (1998). Potassium and other basic cations. *Recommended chemical soil test procedures for the North Central Region*, 1001: 31-33.

Wójtowicz, M., Wójtowicz, A., and Piekarczyk, J. (2016). *Application of remote sensing methods in agriculture*. 31–50.

Xijie, L. (2013). *Remote sensing, normalized difference vegetation index (NDVI), and crop yield forecasting*, Doctoral dissertation, M. Sc. Thesis, University of Illinois at Urbana-Champaign, IL, USA.

Xue, J., and Su, B. (2017). Significant remote sensing vegetation indices: A review of developments and applications. *Journal of Sensors*, 1-17. https://doi.org/10.1155/2017/1353691

Yanai, J., Lee, C. K., Kaho, T., Iida, M., Matsui, T., Umeda, M., and Kosaki, T. (2001). Geostatistical analysis of soil chemical properties and rice yield in a paddy field and application to the analysis of yield-determining factors. *Soil Science and Plant Nutrition*, 47(2): 291-301.

Yan, D., Zhu, Y., Wang, S., and Cao, W. (2006). A quantitative knowledge-based model for

designing suitable growth dynamics in rice. *Plant production science*, 9(2): 93-105.

Yang, C., Everitt, J. H., Du, Q., Luo, B., & Chanussot, J. (2012). Using high-resolution airborne and satellite imagery to assess crop growth and yield variability for precision agriculture. *Proceedings of the IEEE*, *101*(3), 582-592.

Yengoh, G. T., Dent, D., Olsson, L., Tengberg, A. E., and Tucker, C. J. (2015). Limits to the Use of NDVI in Land Degradation Assessment. In *Use of the Normalized Difference Vegetation Index (NDVI) to Assess Land Degradation at Multiple Scales*, 27-30. Springer, Cham.

Zarco-Tejada, P. J., Berni, J. A., Suárez, L., and Fereres, E. (2008). A new era in remote sensing of crops with unmanned robots. *SPIE Newsroom*, 2-4.

Zhang, C., and Kovacs, J. M. (2012). The application of small unmanned aerial systems for precision agriculture: a review. *Precision agriculture*, 13(6): 693-712. https://doi.org/10.1007/s11119-012-9274-5

Zhou, X., Zheng, H. B., Xu, X. Q., He, J. Y., Ge, X. K., Yao, X., ... and Tian, Y. C. (2017). Predicting grain yield in rice using multi-temporal vegetation indices from UAV-based multispectral and digital imagery. *ISPRS Journal of Photogrammetry and Remote Sensing*, 130: 246-255.

Zhu, L., Suomalainen, J., Liu, J., Hyyppä, J., Kaartinen, H., and Haggren, H. (2018). A review: remote sensing sensors. *Multi-purposeful application of geospatial data*, 19-42.

Zou, X., Mõttus, M., Tammeorg, P., Torres, C. L., Takala, T., Pisek, J., ... and Pellikka, P. (2014). Photographic measurement of leaf angles in field crops. *Agricultural and Forest Meteorology*, 184: 137-146.

Zou, X., and Mõttus, M. (2015). Retrieving crop leaf tilt angle from imaging spectroscopy data. *Agricultural and Forest Meteorology*, 205: 73-82.

Zou, X., Haikarainen, I., Haikarainen, I. P., Mäkelä, P., Mõttus, M., and Pellikka, P. (2018). Effects of crop leaf angle on LAI-sensitive narrow-band vegetation indices derived from imaging spectroscopy. *Applied sciences*, 8(9): 1435.

APPENDIX

Appendix 1: Analysis of variance of rice grain yield estimated on plot scale

Source	DF	SS	MS	F	P
Zone	2	5.74	2.872	1.22	0.298
Health	2	98.974	49.487	21.03	0.000
Treatment	1	10.16	10.165	4.32	0.039
Zone*Treatment	2	2.00	1.003	0.43	0.654
Error	132	310.67	2.353		
Total	139				

Appendix 2: Analysis of Variance of rice grin yield from spatial based estimation

Source	DF	SS	MS	F	P
N-Management	1	5.9483	5.94826	18.31	0.0001
Zone	2	7.3112	3.65562	11.25	0.0001
N-Mgt * Zone	2	0.3214	0.16069	0.49	0.6117
Error	76	24.6861	0.32482		
Total	81				

Appendix 3: Estimated rice grain yields based on Jenks classification of OSAVI imagery and extrapolation of yields per unit hectare of the fields: Zone J.

Field Number	Estimated grain yield from classified OSAVI imagery (kg)	Total Farm Size (ha)	Rice grain Yield (kg/ha)	Estimated grain yield from classified OSAVI imagery (kg)	Total Farm Size (ha)	Rice grain Yield (kg/ha)
	Zone J: Non UDP			Zone J: UDP		
1	6.68	0.93	7.19	8.01	1	8.01
2	7.34	0.98	7.51	8.99	1.26	7.13
3	9.76	1.41	6.92	6.51	0.84	7.75
4	4.86	0.69	7.05	6.48	0.93	6.97
5	1.51	0.26	5.79	4.77	0.6	7.96
6	6.76	0.95	7.12	7.13	0.92	7.75
7	3.29	0.53	6.21	12.00	1.61	7.45
8	2.62	0.40	6.55	5.23	0.68	7.69
9	1.51	0.23	6.55	0.91	0.13	7.02
10	1.64	0.26	6.31	0.49	0.07	6.94
11	1.59	0.27	5.88	2.03	0.27	7.53
12	2.67	0.40	6.70	9.33	1.31	7.12
13	2.40	0.34	7.01	8.78	6.71	6.71
14	2.35	0.36	6.51	6.32	7.21	7.21
15	2.37	0.34	6.97	1.58	6.58	6.58

Appendix 3 (continue): Estimated rice grain yields based on Jenks classification of OSAVI imagery and extrapolation of yields per unit hectare of the fields: Zone J.

Field Number	Estimated grain yield from classified OSAVI imagery (kg)	Total Farm Size (ha)	Rice grain Yield (kg/ha)	Estimated grain yield from classified OSAVI imagery (kg)	Total Farm Size (ha)	Rice grain Yield (kg/ha)
	Zone J: Non UDP			**Zone J: UDP**		
16	4.98	0.97	5.72	3.45	0.6	5.75
17	2.22	0.35	6.36	3.24	0.47	6.89
18	7.11	1.17	6.07	18.64	2.7	6.90
19	2.71	0.51	5.30	6.40	0.9	7.07
20	6.64	0.98	6.78	8.34	1.09	7.65
21	7.10	1.28	5.55	3.81	0.51	7.47
22	3.06	0.48	7.51	10.40	1.44	7.22
23	3.07	0.48	6.40	11.63	1.93	6.02
24				5.14	0.69	7.46
25				6.75	0.93	7.26
26				6.22	0.95	6.55
27				5.58	0.72	7.75
28				4.20	0.56	7.18
29				6.16	0.83	7.42
Mean	**4.10**	**0.63**	**6.52**	**6.50**	**1.53**	**7.08**

Appendix 4: Estimated rice grain yields in zone H based on Jenks classification of OSAVI imagery

Field Number	Estimated grain yield from classified OSAVI imagery (kg)	Farm Size (ha)	Rice grain yield of field (kg/ha)	Estimated grain yield from classified OSAVI imagery (kg)	Farm Size (ha)	Rice grain Yield (kg/ha)
Zone H: Non-UDP				**Zone H: UDP**		
1	5.66	1.02	5.55	6.13	0.92	6.66
2	1.36	0.21	6.48	1.80	0.26	6.91
3	2.22	0.37	6.01	1.14	0.18	6.35
4	2.82	0.50	5.65	1.09	0.18	6.08
5	2.19	0.36	6.09	3.39	0.53	6.40
6	1.22	0.20	6.09	1.57	0.23	6.82
7	1.30	0.22	5.91	2.30	0.32	7.20
8	2.54	0.43	5.90			
9	1.25	0.20	6.27			
10	2.54	0.43	5.90			
11	0.87	0.15	5.78			
12	1.20	0.21	5.72			
Mean	**2.1**	**0.36**	**5.95**	**2.49**	**0.37**	**6.63**

Appendix 5: Estimated rice grain yields based on Jenks classification of OSAVI imagery and extrapolation of yields per unit hectare of the fields: Zone I

Field Number	Estimated grain yield from classified OSAVI imagery (kg)	Farm size (ha)	Rice grain Yield (kg/ha)	Estimated grain yield from classified OSAVI imagery (kg)	Farm size (ha)	Rice grain Yield (kg/ha)
		Zone I: Non UDP			**Zone I: UDP**	
1	3.75	0.76	4.94	3.07	0.51	6.01
2	2.46	0.44	5.58	7.80	1.16	6.72
3	2.21	0.38	5.82	6.65	1.00	6.65
4	2.35	0.37	6.35	3.18	0.47	6.77
5	3.18	0.53	6.35	1.53	0.20	7.28
6	0.82	0.15	5.45	1.70	0.30	5.68
7				2.09	0.43	4.85
8				1.30	0.23	5.63
Mean	**0.433**	**2.46**	**5.75**	**0.54**	**3.42**	**6.20**